

ON DELTA MODULATION

by

David J. Greig B.Sc. B.E. (Hons.)

submitted in partial fulfilment of the requirements
for the degree of

Master of Engineering Science, in the
Faculty of Engineering

UNIVERSITY OF TASMANIA

HOBART

- MARCH 1969 -

ACKNOWLEDGEMENTS

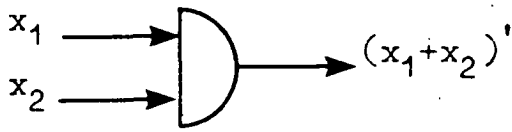
The work contained in this thesis was carried out in the Electrical Engineering department of the University of Tasmania. The author wishes to thank all the members of the above department for their assistance. In particular the author thanks Professor C.H. Miller, and Mr. P. Watt, his supervisor, for their help and encouragement.

I hereby declare that, except as stated herein, this thesis contains no material which has been accepted for the award of any other degree or diploma in any University, and that, to the best of my knowledge this thesis contains no copy of material previously published or written by another person except where due reference is made in the text of this thesis.

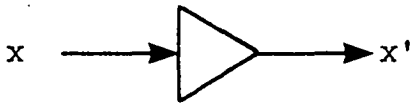
INDEX

| | |
|---|----|
| INTRODUCTION | 1 |
| 1. INVESTIGATION OF THE CONTINUOUS-CARRIER AND PULSE MODULATIONS | 3 |
| Introduction | |
| 1.1 Continuous Carrier Systems. | |
| 1.2 Pulse Modulations. | |
| 1.3 Comparison of Modulations. | |
| 1.4 Introducing Delta Modulation. | |
| 2. INVESTIGATION OF DELTA MODULATION | 14 |
| Introduction | |
| 2.1 The Principles of Delta and Delta-Sigma Modulation. | |
| 2.2 Early work by de Jager on Delta Modulation. | |
| 2.3 A Review of Zetterberg's paper "A Comparison Between Delta and Pulse Code Modulation". | |
| 2.4 Delta-Sigma Modulation. | |
| 2.5 Thermal Noise Considerations. | |
| 2.6 The Problem of Obtaining Output Spectrum of a Delta Modulator in Terms of the Input Spectrum. | |
| 2.7 Conclusions. | |
| 3. AN EXPERIMENTAL DELTA-SIGMA MODULATOR | 41 |
| Introduction | |
| 3.1 The Delta-sigma Modulation System. | |
| 3.2 Demodulator Circuitry. | |
| 3.4 Channel Simulation. | |
| 3.5 Performance of System. | |
| 3.6 Measurement of Signal-to-Noise Ratio. | |
| 3.7 Quantizing Noise on D.C. Signal. | |
| 3.8 Comparison of Theoretical and Measured Signal-to-Noise Properties | |
| 3.9 Conclusions. | |
| 4. OTHER CONSIDERATIONS OF DELTA-MODULATION | 66 |
| 4.1 Introduction | |
| 4.2 Simple Method of Improving the Performance of Existing System. | |
| 4.3 Compended Delta Modulation. | |
| 4.4 Analogue-to-Digital Converter. | |
| 4.5 Considerations in Choosing Delta Modulation. | |
| 4.6 Consideration for Delta Modulation for Telephone Systems. | |
| 4.7 Conclusions. | |
| APPENDICES | 79 |
| BIBLIOGRAPHY | 87 |

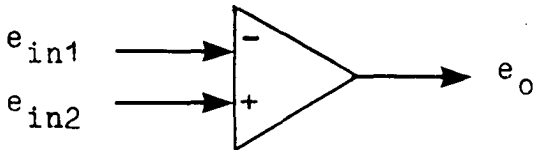
SYMBOLS USED IN BLOCK DIAGRAMS



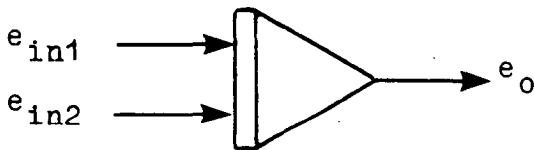
Two Input NOR Gate



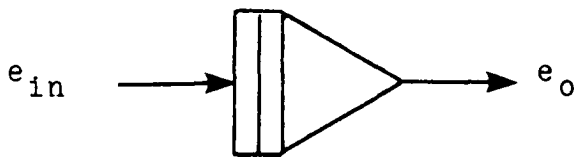
Negation Amplifier



Operational Amplifier



Integrator



Low Pass Filter



Block as labelled

INTRODUCTION

The purpose of this thesis is to introduce Delta Modulation as an alternative to the more conventional carrier and pulse modulations.

Chapter I briefly discusses the carrier and pulse modulations from the standpoint of signal - to - noise ratio, bandwidth occupancy and threshold effects. In this way, the merits of each is brought to the fore and the superiority of FM and PCM can be seen.

Chapter II introduces Delta Modulation, a pulse code modulation, giving an extensive review of much of the more prominent literature on the subject. Aspects such as channel capacity, power, spectral densities, overloading, signal - to - noise ratio and bandwidth, are discussed.

In Chapter III an experimental Delta-Sigma Modulation System is described in detail, from design to performance. Observations are made which correspond to some made in theory. The system transmits static signals and AC signals up to 20 HZ. The accuracy is good and the circuits simple.

In Chapter IV suggestions are made to improve the system's performance by simple means. Also mentioned are more elaborate means (Continuous Delta Modulation) which enhance the performance considerably but detract from the simplicity.

Much of the literature quoted in the bibliography shows and discusses how delta modulation is simple in circuitry yet has all the advantages of PCM. It is upon this theme that the prototype Delta-Sigma Modulator is designed and built. All the circuits are kept as simple as possible. With integrated circuits, delta modulation is fast becoming an economical proposition.

Delta modulation, though simple to implement, requires greater bandwidth than the conventional carrier modulations and PCM (for the same performance). At times this would make Delta Modulation uneconomical. However, there is a place for Delta Modulation alongside FM and PCM for some particular applications.

CHAPTER ONE

INVESTIGATION OF THE CONTINUOUS CARRIER AND PULSE MODULATIONS

INTRODUCTION

The earliest electronic communication systems were the telegraph and telephone. The telegraph preceded the telephone and made use of a 'pulse code' known as morse code. At the time of the telegraph, man was unable to send his own voice over a transmission line. He could only switch simple on-off signals onto the line.

The next development was the telephone. A microphone (voice to electrical signal transducer) was invented to put the human voice on the transmission line. The telegraph and telephone reduced the size of the world by making communications faster and easier. A demand was created for more telephones and greater transmission distances.

With greater distances, the cost of a single channel per transmission line becomes large. Moreover, increased interference over greater transmission distances reduces the quality of the transmitted signal.

The signal to be transmitted generally has a small finite bandwidth compared to the channel itself. It is, therefore, wasteful to transmit one signal at a time on the transmission path. In order to make full use of the transmission path, a number of messages are transmitted simultaneously by one of two accepted methods. They are, frequency division, by modulating subcarriers, and time division, which allows time sharing of the path. In either case modulation of the signals is required.

Signals are modulated for a number of reasons. Some are listed below:

- (i) To multiplex channels.
- (ii) To shift frequencies to their assigned location.
- (iii) To increase bandwidth occupancy and transmitted power.
- (iv) To increase frequency for ease of radiation.
- (v) To balance bandwidth occupancy and sensitivity to noise.
- (vi) To translate frequencies for ease in meeting transmission requirements.

1.1 CONTINUOUS CARRIER SYSTEMS

The most widely used modulations are the sinusoidal carrier modulations. The waveform

$$e(t) = A(t) \cos (\omega_c t + \phi(t))$$

has three parameters which may be varied: $A(t)$ the amplitude, gives rise to amplitude modulation (AM). By varying the phase, $\phi(t)$, gives phase modulation (PM). If the derivative of $\phi(t)$ with respect to time is allowed to vary, a variation in frequency occurs and frequency modulation (FM) is obtained.

Frequency modulation is superior to amplitude modulation, the chief reason being in the ability of FM to exchange bandwidth occupancy in the transmission medium for improved noise performance.

f_c = carrier frequency,

f_m = modulating frequency,

W = bandwidth.

The various continuous carrier and pulse systems are investigated in terms of their signal - to - noise ratios at the outputs of the detectors. For a given f_m , some systems

require a greater bandwidth than others. The systems are considered on the basis of same signal - to - noise ratio at the input to the detector. The greater the bandwidth, the greater the noise at the input. Therefore, to give the same signal - to - noise ratio at the input, different signal powers would have to be transmitted.

If S_o/N_o denotes signal - to - noise ratio at the output, and S_{in}/N_{in} denotes signal - to - noise ratio at the input, then for AM double side band (AM - DSB)⁽¹⁾,

$$S_o/N_o = 2 S_{in}/N_{in} \quad (1.1)$$

and bandwidth,

$$W = 2 f_m \quad (1.2)$$

For AM single sideband (AM - SSB)

$$S_o/N_o = S_{in}/N_{in} \quad (1.3)$$

and bandwidth

$$W = f_m \quad (1.4)$$

In both cases, the signal-to-noise ratio is independent of the bandwidth W and, therefore, cannot be improved by using a greater bandwidth.

For frequency modulation, if f_d is the maximum frequency deviation of the carrier, then

$$f_d/f_m = m_f$$

is defined as the modulation index for an FM system. A distinction is made within the FM system depending upon the value of m_f . For $m_f > 0.6$ the system is known as wide band FM (WBFM), and $m_f < 0.6$ is narrow band FM(NBFM).

Evaluation of output signal-to-noise ratio for low values of signal-to-noise ratio is quite difficult, but a simplified analysis ⁽¹⁾ for large signal-to-noise ratios gives some idea of the performance of F.M.

For WBFM,

$$S_o/N_o = 3m_f^3 S_{in}/N_{in} \quad (1.5)$$

with bandwidth

$$W \approx 2m_f f_m \quad (m_f > 5) \quad (1.6)$$

For NBFM,

$$S_o/N_o = 3m_f^2 S_{in}/N_{in} \quad (1.7)$$

with bandwidth

$$W = 2f_m \quad (1.8)$$

Equation 1.6 is an approximation, but with equation 1.5 a good indication of how bandwidth and signal-to-noise ratio can be exchanged, is obtained.

A comparison between WBFM and ΔM -DSB can be made as regards signal-to-noise ratio for two cases.

(1) Identical total transmitted power

$$\frac{(S_o/N_o)_{\text{WBFM}}}{(S_o/N_o)_{\Delta M\text{-DSB}}} = (9/2)m_f^2 \quad (1.9)$$

(2) For identical carrier powers

$$\frac{(S_o/N_o)_{\text{WBFM}}}{(S_o/N_o)_{\Delta M\text{-DSB}}} = 3m_f^2 \quad (1.10)$$

In case (2) for $m_f^2 > \frac{1}{3}$, the ratio is greater than one, and an improvement of FM over ΔM is obtained. The case $m_f = 1/\sqrt{3} \approx 0.6$ is the crossover point from NBFM to WBFM. Narrow band FM has no noise advantage over ΔM for a given carrier power.

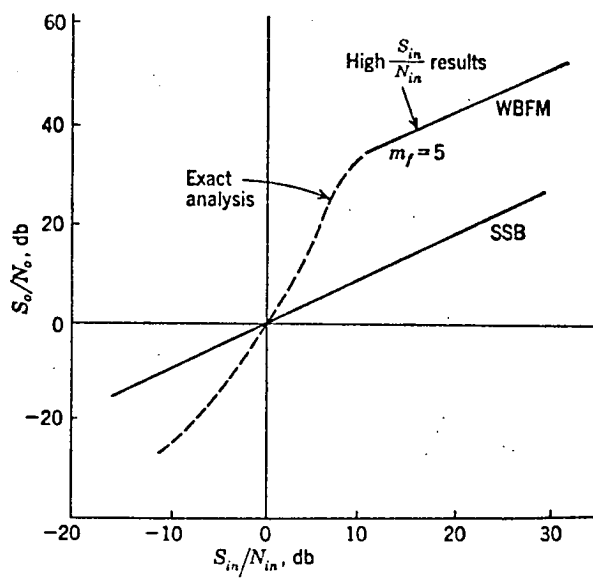


Figure 1.1 Output signal-to-noise ratio versus input signal-to-noise ratio for SSB and WBFM.

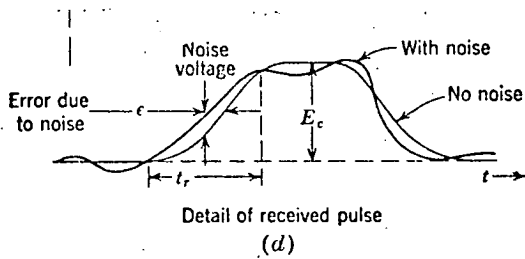


Figure 1.2 Received signals in a PPM system.

If $f_m = 15$ KC and maximum frequency deviation(f_d) is ± 75 KC (this is usual for commercial broadcasting), then for identical carrier powers,

$$\frac{(S_o/N_o)_{\text{WBFM}}}{(S_o/N_o)_{\text{AM-DSB}}} = 3 \frac{75^2}{15^2} = 75$$

This is an improvement of 18.75 db.

These results for FM indicate that, by increasing m_f , unlimited advantage over AM-DSB is achieved for large signal-to-noise ratios. As m_f increases, the bandwidth increases and, therefore, there is a corresponding increase in the noise. It has been shown (1) that the output noise power for FM is given by

$$N_o = \frac{2\eta f_m^3}{3P_c}, \quad (1.11)$$

where P_c = carrier power

η = spectral density of the noise (considered uniform over the bandwidth).

It can be seen from this expression (equation 1.11) that, for a fixed carrier power P_c , the noise power increases with the cube of f_m . As f_m increases, holding the carrier power constant, there is a point reached where the noise suddenly takes over, causing a large reduction in the output signal-to-noise ratio. The region where this reduction occurs is called the threshold.

Figure 1.1 illustrates the performance of FM and AM-SSB. The low value S/N analysis is also shown and clearly illustrates the threshold effect. The carrier-to-noise power ratio should not be below approximately 9db, this minimum being increased to 15 or 16 db if receiver noise is included. Below this 9 to 16 db figure the output signal-to-noise ratio deteriorates rapidly.

1.2 PULSE MODULATIONS

1.2.1 PAM, PWM, PPM

PAM, PWM and PPM have a carrier of an evenly spaced train of pulses, some parameter of which varies according to the modulation signal. The height width or position of the pulses can be varied. The first is known as pulse amplitude modulation (PAM), the second as pulse width modulation (PWM), and the third as pulse position modulation PPM. A fourth is pulse code modulation PCM. The signal is 'quantized' each sampling time, and the quantized value represented by a code of pulses. In all cases, the time function is uniquely determined by sampling every $\frac{1}{2f_m}$ seconds (sampling theorem(2)).

If a PAM system is considered where the pulses are transmitted by AM, then the system (PAM/AM) requires a bandwidth of $2mf_m$, assuming AM-DSB, or mf_m for AM-SSB. (m = the number of message channels). This is the same band width as ordinary AM.

PWM and PPM are closely related, and their signal-to-noise properties are treated simultaneously. Figure (1.2) shows details of a received pulse. For a reasonably sharp band pass characteristic, it can be shown that

$$W = 1/t_r \cdot \quad (1.12)$$

t_r = rise time

t_o = maximum displacement of pulse for a sinusoidal input signal. In terms of the input signal-to-noise ratio, the output signal-to-noise ratio is given by:

$$S_o/N_o = \frac{2t_o^2 W^3}{f_m} \frac{S_{in}}{N_{in}} \quad (1.13)$$

Thus, the output signal-to-noise ratio varies as the cubic of W . This is the same functional relationship as for FM (equation 1.5). Again these results are only for large signal to noise ratios at the input. A comparison between PAM/AM and PPM/AM yields:

$$\frac{(S_o/N_o)_{PPM/AM}}{(S_o/N_o)_{PAM/AM}} = 2 t_o^2 (W)^2 \quad (1.14)$$

where

$$W = 1/t_r$$

Consider a time division multiplex system of 50 channels. Each source of information has a band-width of 5KC, rise time t_r is $0.1 \mu S$, and pulse width $0.2 \mu S$, then the maximum value of t_o is about $0.95 \mu S$. For a PAM/AM system, a band width of $2 \times 50 \times 5000 = 500$ KC is required. For the PPM/AM system, a bandwidth of approximately $\frac{1}{0.1 \mu S} = 10$ MC is required.

$$\begin{aligned} \text{The improvement of PPM/AM over PAM/AM is } & 2(0.95)^2 \cdot (10)^2 \\ & = 180 \text{ or } 22.6 \text{ db.} \end{aligned}$$

As FM was to AM, so is PPM to PAM, in that this useful exchange of bandwidth with signal-to-noise ratio can be made for FM and PPM but not with AM and PAM. PPM has no great advantage over FM and has not been used to the same extent as FM.

In both FM and PPM, the improved signal-to-noise ratio is obtained at considerable expense in bandwidth.

1.2.2 Pulse Code Modulation (PCM)

Pulse code modulation is a very different pulse modulation. In the previous pulse modulations discussed here, modulation was achieved by varying one parameter of a standard pulse. In PCM, the continuous time function is sampled in the

usual manner, then 'quantized'. The signal is transmitted by a code of pulses representing the particular quantized value. The digital code is more favourable because of its simplicity in detection and instrumentation. Usually, the binary digital code is employed, that is, 0 or 1 are the only values the signal can have. This can be achieved by carrier on or off respectively.

Despite the complexity of the mechanism of PCM, there are many advantages in its use. PCM allows for considerable increase in signal-to-noise ratio at the receiver. The only decision that needs to be made by the receiver is whether the pulse is present or not. The receiver need not know its amplitude or width. This is one property which other pulse systems do not possess. Of equal importance, is the fact that the encoded signal can be repeated without introducing significant distortion.

As with other pulse modulations, the signal is sampled at the rate of $2 f_m$ Per second. If there are m signals and n digits per code group, the time interval between pulses is

$$1/2nm f_m$$

(2)

and the minimum bandwidth requirement is ~~(4.5)~~

$$W = nm f_m \quad (1.15)$$

The only source of noise is assumed to be the original 'quantizing noise' inherent in the modulation. The noise over the channel is assumed never to cause a pulse to be misinterpreted. Therefore, any received sample may be in error by as much as half a quantizing level ($V_K/2$). The noise power, for the maximum error $V_K/2$ in each sample is given by

$$N_o = V_K^2/12 \quad (1)$$

and the signal power,

$$S_o = V_K^2/12 (2^n - 1)$$

The output signal to noise ratio is given

$$S_o/N_o = 2^n - 1 \quad (1.16)$$

(This is for large signal-to-noise ratios, 710 db).

For these large signal to noise ratios,

$$S_o/N_o \simeq 2^n \quad (1.17)$$

Equation 1.15 shows bandwidth to be directly proportional to n. Output S/N, however, increases exponentially with n, and hence output S/N increases exponentially with bandwidth. This rate of improvement, with increase in bandwidth, is greater than the other pulse systems and FM. (For FM the signal-to-noise ratio increases with W^3).

Shannon (3) derived a relationship between input and output signal-to-noise ratios from information theory considerations based on channel capacity and Hartley's law. The rate at which the channel supplies information for a PCM system is given by

$$R = 2n W(1 + p \log p + q \log q) \text{ bits/second} \quad (1.18)$$

This rate must be equal to that supplied by the channel (for no information lost), thus giving the output signal to noise ratio as;

$$S_o/N_o = 2^{2n} (1 + p \log p + q \log q) - 1,$$

where

$$p = \frac{1}{2} - \frac{1}{2\pi} \int_0^a \exp(-y^2/2) dy \text{ where } a = \sqrt{\frac{S_{in}/N_{in}}{4}}$$

Figure 1.3 shows output versus input signal-to-noise ratio for n = 1, 5, 10. Below 10 db for S_{in}/N_{in} the output signal-to-noise ratio decreases rapidly. Above 10 db, S_o/N_o levels off to a constant value.

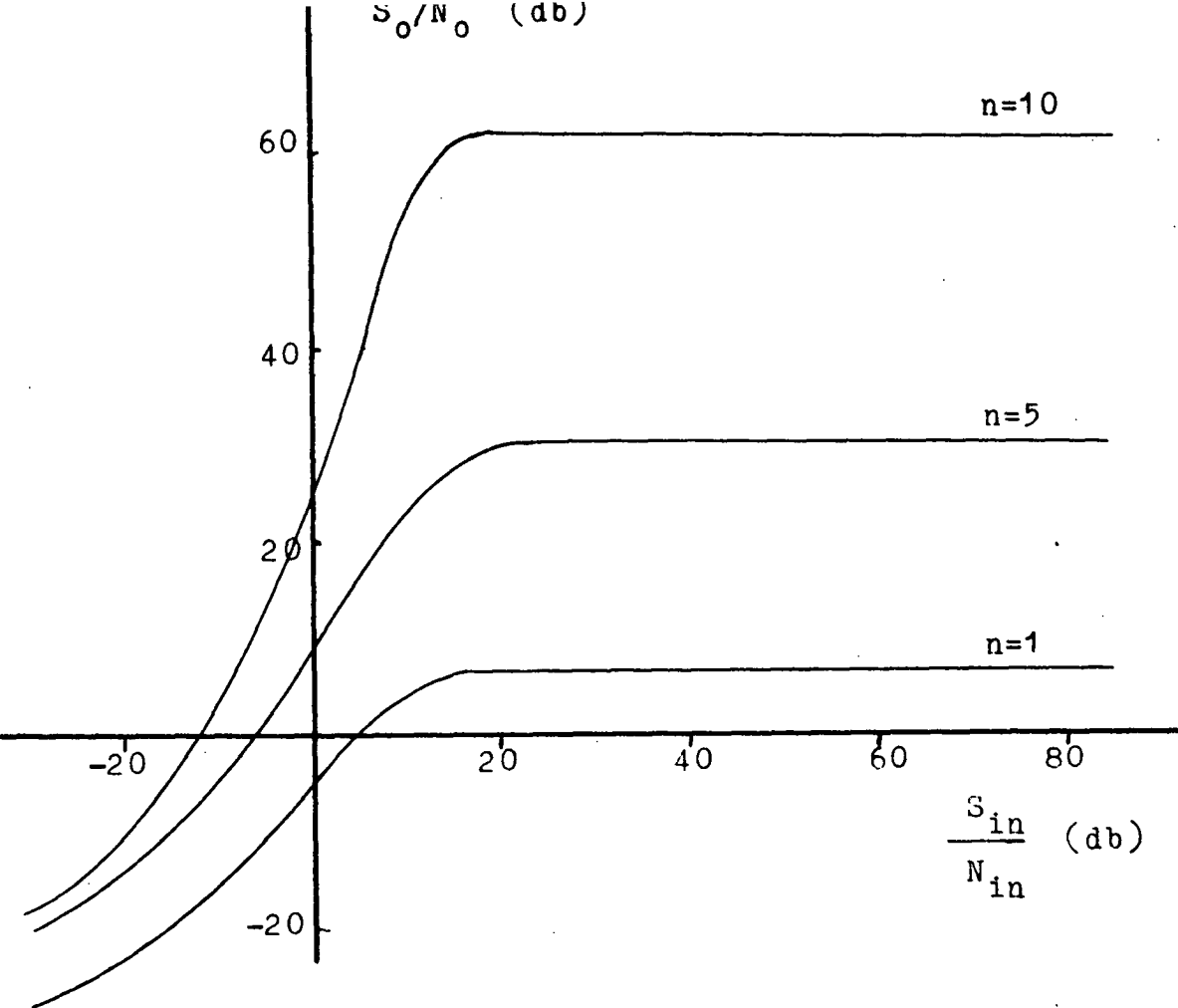


Figure 1.3 OUTPUT VERSUS INPUT S/N FOR PCM

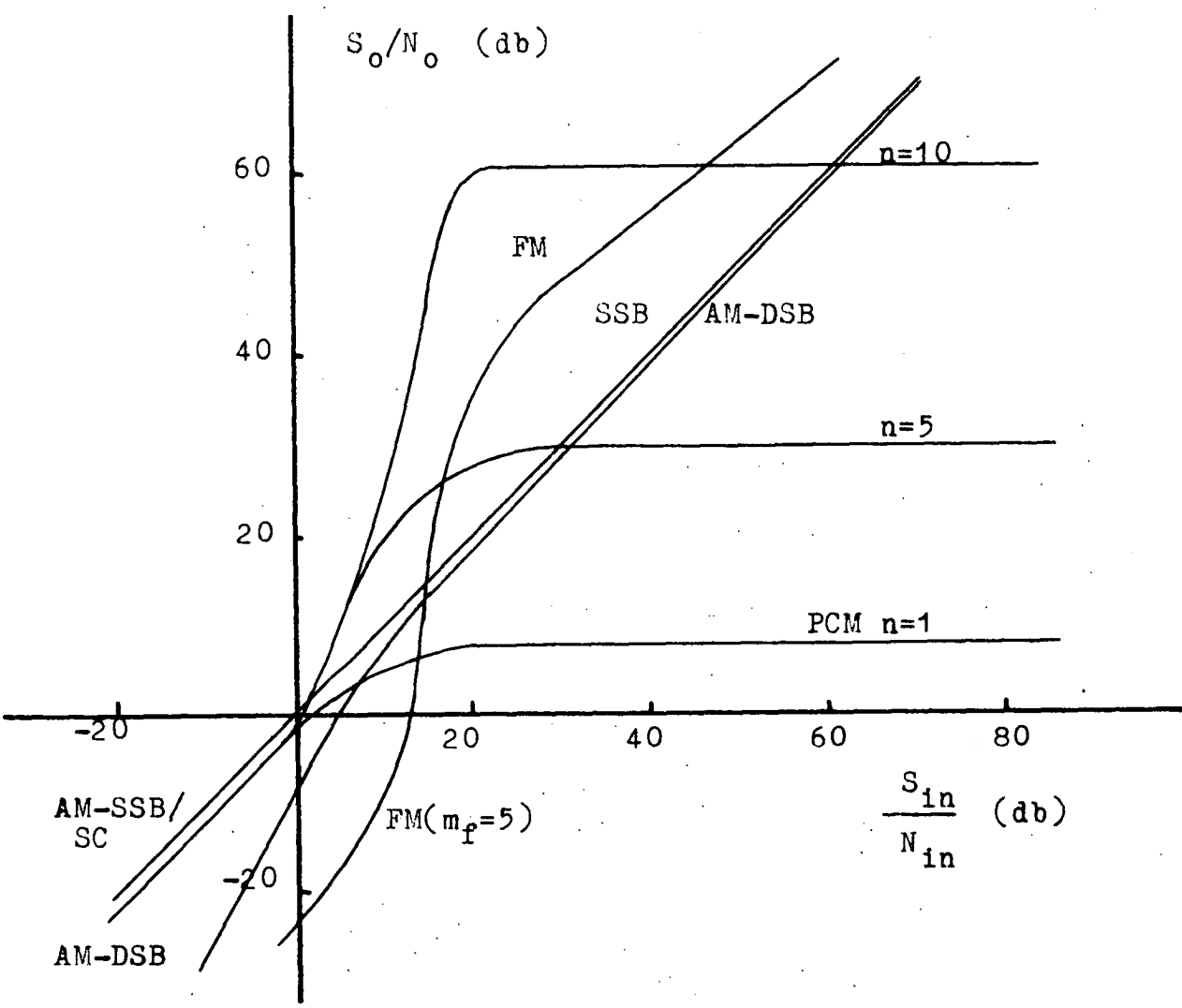


Figure 1.4 COMPARISON OF VARIOUS SYSTEMS

This threshold of 10 db for PCM is an improvement on the 15 to 16 db threshold already described for FM.

1.3 COMPARISON OF MODULATIONS

A comparison of the modulation systems discussed here can be made on a common basis of input signal-to-noise ratio, the noise being contained in the message band width W .

Figure 1.4 shows how various systems compare. Below threshold, (i.e. small signal-to-noise ratio) the ΔM -SSB is superior, in both conservation of band-width and in greater signal to noise ratio.

If the received signal-to-noise ratio is to be large, then a binary PCM system should be used for maximum output signal to noise ratio. A better trade off of S/N with band-width is achieved.

It becomes increasingly difficult to ensure interference free transmission with increasing distances. In modern continuous carrier systems, the signal transmitted by cable over a distance of 100 kilometres is attenuated 240 db, that is a power ratio of 10^{-24} times. The attenuation does not, in itself, constitute any difficulty, for it can be compensated for by a series of repeaters. Besides the attenuation, however, there is interference which is cumulative and is amplified at each repeater, thus decreasing the signal to noise ratio from repeater to repeater. On the other hand, PCM does not accumulate interference. The pulses are regenerated at each repeater.

Although PCM should have been used in preference to WBFM, it was not because of the complexity of instrumentation. The Bell Systems Laboratories (and others) have carried out much research into PCM in order to bring it to a stage of development

such that it be economical to install. PCM is currently in use in the United States of America (fairly extensively) and in small installations in Britain and Holland.

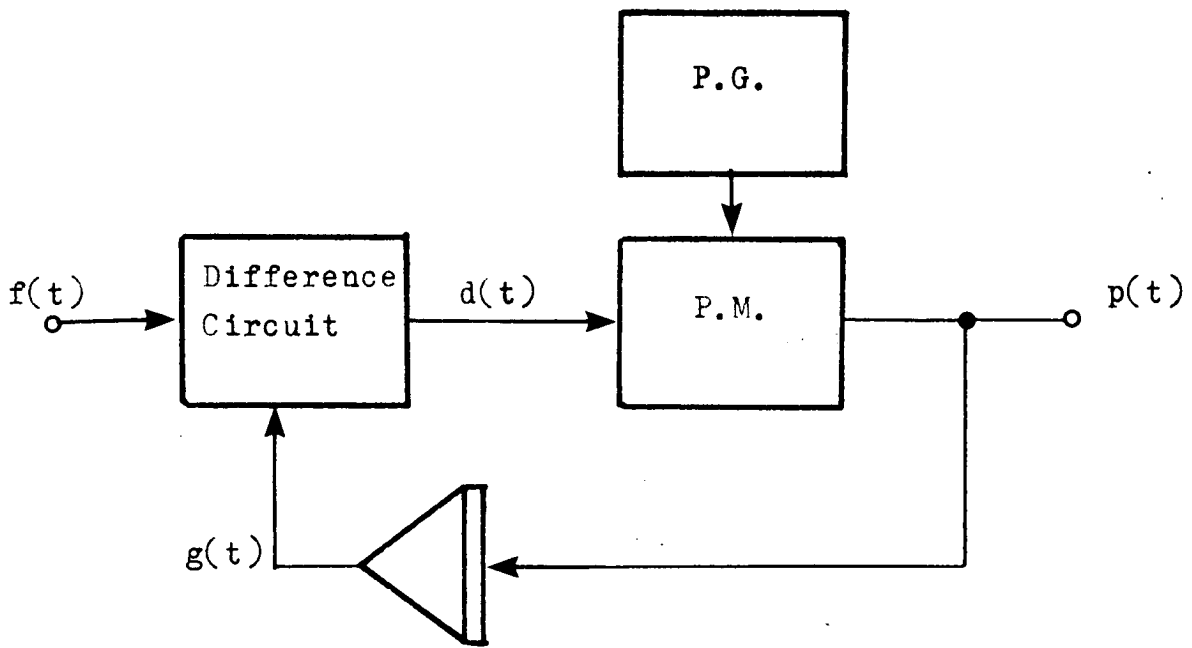
1.4 INTRODUCING DELTA MODULATION

So far there has been no mention of delta modulation (DM). The discussion has gone into the relative merits of the more common methods of continuous carrier modulations, and has briefly compared them. Next the pulse modulations were introduced and compared with the continuous carrier modulations. PCM has emerged the more favourable as regards performance, but is handicapped by the complexity of instrumentation.

Rather than give details of DM here, a few points will be stated. These points form a basis on which further investigation is carried out, and appears in the following chapters.

Delta Modulation is a one-unit binary code. It has the same properties as in PCM, in that pulses need only be recognised as present or absent, without concern for shape. Hence, as in PCM, the only noise which is present in DM is quantizing noise. It could be expected to achieve a similar performance (signal-to-noise ratio) to that of PCM.

The main advantage of delta modulation over PCM is the simplicity of instrumentation. Delta modulation uses a principle of quantized feedback, which results in extremely simple coding and decoding operations. It is in fact so much simpler that it would be used in preference to PCM, were it not for a disadvantage in band width requirements. It is shown later that delta modulation requires about $1\frac{1}{2}$ times the band width of PCM for similar performances.



(a) BASIC BLOCK DIAGRAM FOR DELTA MODULATION

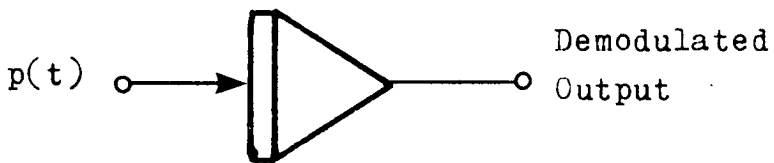
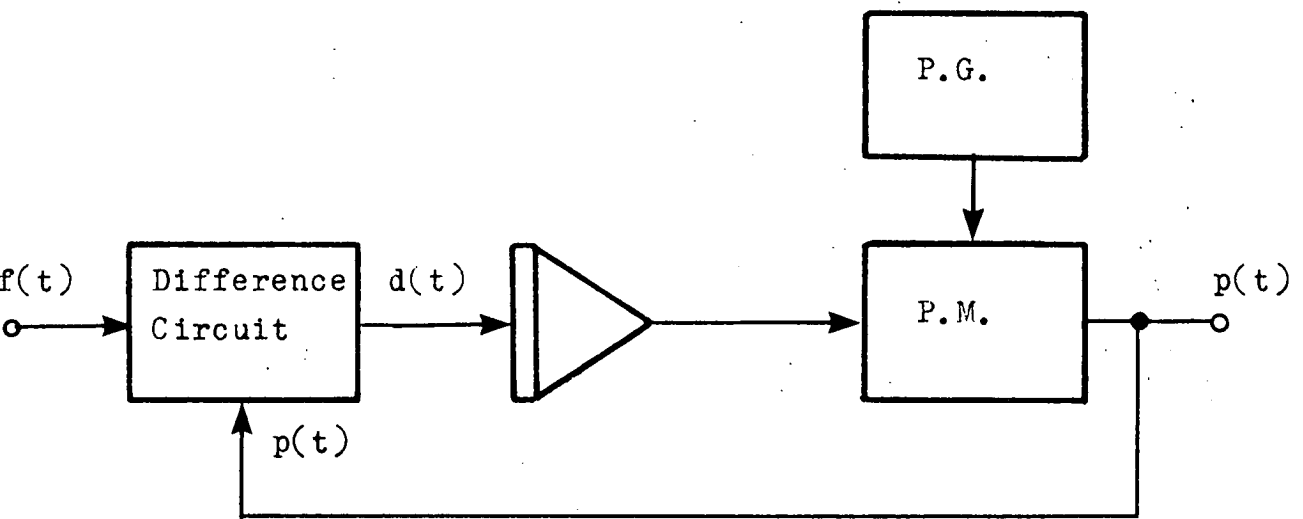
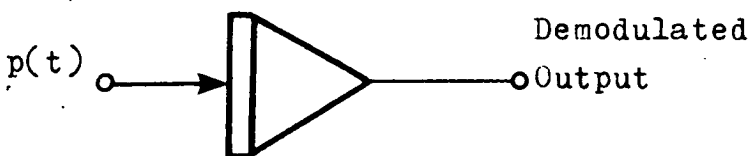


Figure 2.1 BASIC BLOCK DIAGRAM FOR DEMODULATION



(a) BASIC BLOCK DIAGRAM, DELTA-SIGMA MODULATION



(b) BASIC BLOCK DIAGRAM, DELTA-SIGMA DEMODULATION

Figure 2.2

CHAPTER TWO

INVESTIGATION OF DELTA MODULATION

INTRODUCTION

The principles of delta and delta sigma modulation are introduced. Some of the more significant early works on delta modulation are studied and results pertaining to such factors as signal-to-noise ratio, bandwidth, spectral densities and power are discussed.

The discussions are extensive, and conclusions are achieved which indicate delta modulation to be a suitable method of modulation and a competitor with P.C.M.

2.1 THE PRINCIPLES OF DELTA AND DELTA-SIGMA MODULATION

2.1.1 Delta Modulation (4)

The delta modulator is a feedback system (figure 2.1) consisting of a pulse generator (PG), a pulse modulator (PM), a linear network (F) and a difference network.

The output pulses $p(t)$ are fed back through the network F to produce a function $g(t)$ which very closely approximates the input signal $f(t)$. The difference meter produces the difference $f(t) - g(t) = d(t)$ and passes it into the pulse modulator. The pulse modulator passes positive pulses from the pulse generator if $f(t) > g(t)$, and negative pulses if $f(t) < g(t)$. These pulses are the modulator output pulses $p(t)$. Each pulse tries to reverse the polarity of the difference signal $d(t)$. By doing this, the difference between $g(t)$ and the input signal $f(t)$ is kept small. (Essentially, the network F is a low pass filter or an integrator with a large time constant).

At the receiving end (figure 2.1(b)), if the pulses $p(t)$ are applied to a similar network to F, an output signal $e_o(t)$,

which is a close approximation to the input $f(t)$, is obtained. The difference between the original input signal $f(t)$ and the reproduced signal $e_o(t)$ gives rise to the "quantizing noise". This can be reduced by increasing the pulse frequency.

2.1.2 Delta-sigma Modulation (5)

Delta-sigma modulation is similar to delta modulation, the difference being that the input signal $f(t)$ is first integrated. The integrated difference signal $\epsilon(t)$ is fed to the pulse modulator. (see figures 2.2(a) and (b)). The same feedback of the output pulses $p(t)$ applies. In the modulator, the integrated difference signal $\epsilon(t)$ is compared with a predetermined reference voltage V_R . A positive pulse is allowed to pass from the pulse generator if $\epsilon(t) > V_R$, and a negative pulse if $\epsilon(t) < V_R$. In this way, the integrated difference signal is always in the vicinity of the reference voltage V_R , provided the input signal does not have too great a slope, or is too large. The larger the input signal, the more frequently do the output pulses appear.

Demodulation is produced (as with delta modulation) by passing the received pulses through a low pass filter thereby obtaining a reconstruction of the input signal $f(t)$, with of course "quantizing noise". The manner in which the quantizing errors occur determines the signal-to-noise performance that the system will attain. Quantization noise for P.C.M. and delta modulation is discussed in a further section.

As channel interference will distort the pulses $p(t)$, they must be regenerated in the receiving network before filtering. This has been done in the experimental delta-sigma modulator described in chapter III.

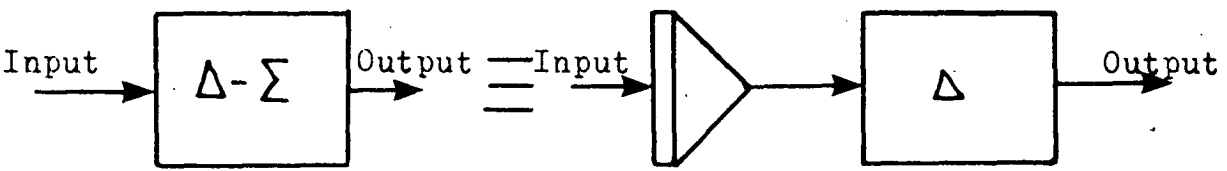


Figure 2.3 BLOCK DIAGRAM SHOWING SIMILARITY BETWEEN DELTA AND DELTA-SIGMA MODULATION

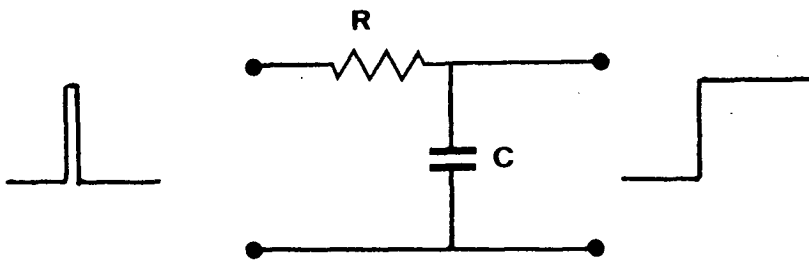


Figure 2.4 SINGLE INTEGRATION (deJager)

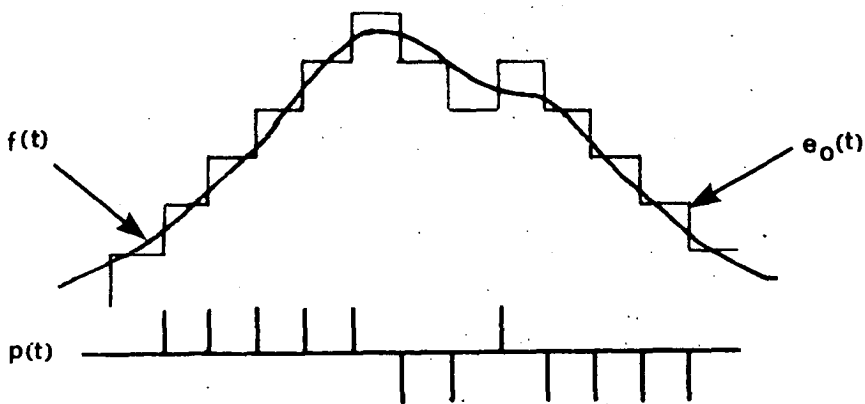


Figure 2.5 STEP WAVEFORM AND INPUT WAVEFORM FOR SINGLE INTEGRATION

2.1.3 Relation Between Delta and Delta-Sigma Modulation.

Essentially, a delta-sigma modulator is the same as a delta modulator, except that the input signal $f(t)$ is first integrated in the delta sigma case. (see figure 2.3). In this way, the delta-sigma modulator carries information according to the amplitude of the input signal, as opposed to delta modulation, where the modulated signal carries information according to the slope of the input signal.

2.2 EARLY WORK BY DEJAGER (4) ON DELTA MODULATION

de Jager, in his paper on delta modulation, as described in section 2.1.1, considered two cases:

- (i) When the demodulator is single integration.
- (ii) When the demodulator is double integration.

2.2.1 Single Integration (figure 2.4)

The network has a large time constant, and the response to an impulse is practically a unit step. Figure 2.5 illustrates the input signal $f(t)$, the step curve and the pulse train. The difference between $e_o(t)$ and $f(t)$ is the quantizing noise.

"This is audible as a type of noise which is more or less correlated to the speech. At a pulse frequency of 40 KC/S the intelligibility of the speech is good, but the quantizing noise has an effect on the speech which may be called 'sandiness' ".

Also, when the slope of the input signal reaches a certain limit, an overloading occurs. For a sine wave of frequency f at the input, the maximum amplitude which can

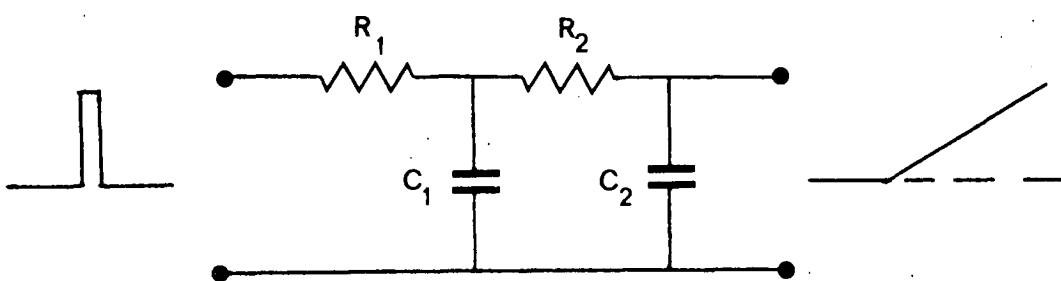


Figure 2.6 DOUBLE INTEGRATION (deJager)

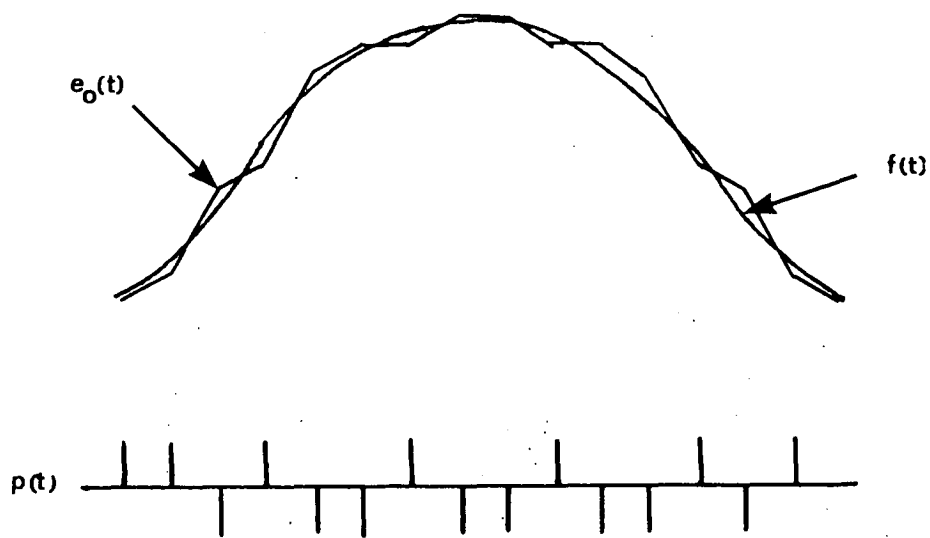


Figure 2.7 SLOPE STEPPING DOUBLE INTEGRATION

be transmitted is

$$a = \frac{f_p}{2\pi f} V_K ,$$

where f_p is the pulse frequency and V_K the height of one step in the approximating function $g(t)$.

de Jager also derived an expression for the signal-to-noise ratio in the case of single integration. The result was:

$$S/N = C_1 \frac{f_p^{3/2}}{f f_0^{1/2}}$$

where f_0 is the cut-off frequency of the low pass filter.

2.2.2 Double Integration (figure 2.6)

By using a double integration linear network, the approximating function now increases or decreases by a unit slope instead of a unit step per input pulse. By making both time constants large, a unit pulse at the input provides a unit pulse at the first condenser and an output signal of constant slope (figure 2.7).

It can be seen by observing figures 2.5 and 2.7, that double integration gives the better approximation to the input signal. deJager goes a little further and introduces prediction methods into the system to give an even better approximation to the input signal (see reference 26).

The expression for the signal-to-noise ratio for double integration is

$$S/N = C_2 \frac{f_p^{5/2}}{f f_0^{3/2}}$$

The improvement in signal-to-noise ratio varies with the $3/2$ or $5/2$ power of f_p , the clock frequency, for single and double integration respectively. Using the digits of a binary code, it varies exponentially. Values of C_1 and C_2 are approximately,

$$C_1 = 0.20 , \quad C_2 = 0.026.$$

2.2.3 Experimental Work

de Jager's experimental measurements of signal-to-noise ratio are shown in figure 19, reference 4. The theoretical calculations agree fairly well with the measured values, and the improvement obtained by using double integration is clearly illustrated.

2.2.4 General Remarks

deJager found that a good reproduction of speech is possible at a pulse frequency of 100 KC/S. Compared with P.C.M. the quality was the same as an eight unit code. In taking 800 C/S as reference frequency, a signal-to-noise ratio of 50 db is observed, while according to a formula by Bennett⁽⁶⁾ the signal-to-noise ratio in db for a full load test tone, in using a code of n digits is

$$D = 6 n + 3$$

which gives $n = 8$ for $d = 50$ db. In this case, the bandwidth needed for transmission with delta modulation is about 50% greater than by using P.C.M.

An experimental system was set up for the high quality reproduction of music. The bandwidth was extended to 12 KC/S, and the signal-to-noise ratio raised to 67 db, by increasing the pulse frequency to 500 KC/S. It was found that the reproduction was very good, but sometimes difficulties arose when the frequency spectrum of the music contained much energy at high frequencies. In this case, the level had to be adjusted to draw a compromise between the quantizing noise and overmodulation. This implied that the method of single integration at the receiver is not well suited to music of this kind.

deJager's concluding comment was:

"it is even possible that in the future the whole system can be constructed in a rather inexpensive way by making use of transistors".

This has been done with the use of not only transistors, but integrated circuits. Chapters III and IV discuss delta and delta-sigma modulations as an efficient and economical means of transmission of signals.

2.3 A REVIEW OF ZETTERBERG'S PAPER "A COMPARISON BETWEEN DELTA AND PULSE CODE MODULATION"⁽⁷⁾

"The systems delta and pulse code modulation are compared from the point of view of information theory and from the study of the quality of transmission with speech -like signals.

It is shown that the systems have almost the same potentiality to transmit information when the number of amplitude levels are the same and reasonably large, more than ten levels. The amplitude distribution of the ideal signal for delta modulation implies a signal power about 60 percent less than for the corresponding signal of pulse code modulation. The spectral distribution of these signals shows for delta modulation only, a marked dependence of frequency which makes the density decrease with increased frequency.

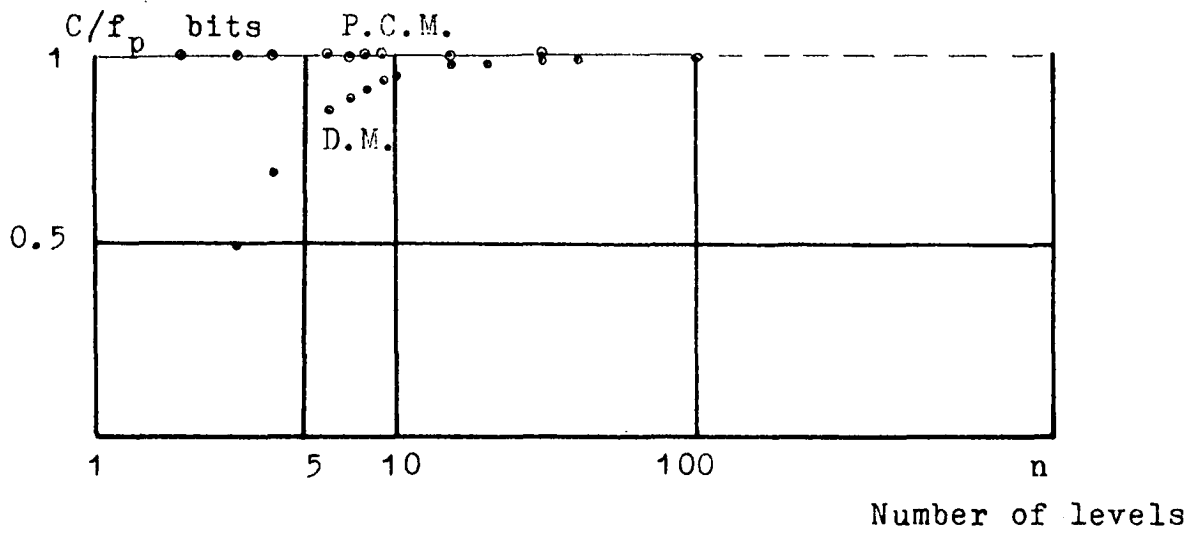
In transmission and reception of speech signals essentially two errors occur, over-loading and granulation. When parameters are chosen to give an optimum of quality expressed as signal-to-noise ratio, delta modulation needs a much larger bandwidth than P.C.M. if the desired quality is moderate or high.

Delta modulation becomes relatively more favourable when the bandwidth of the speech signal is large".⁽¹⁾

It is assumed that the pulses on the transmission channel are of such power that faulty reception of them due to extensive disturbances cannot occur. This assumption is justified by the fact that pulse systems operate almost undisturbed when the noise level on the channel is below a given threshold level, but are completely unusable at a noise level above that value.⁽⁸⁾

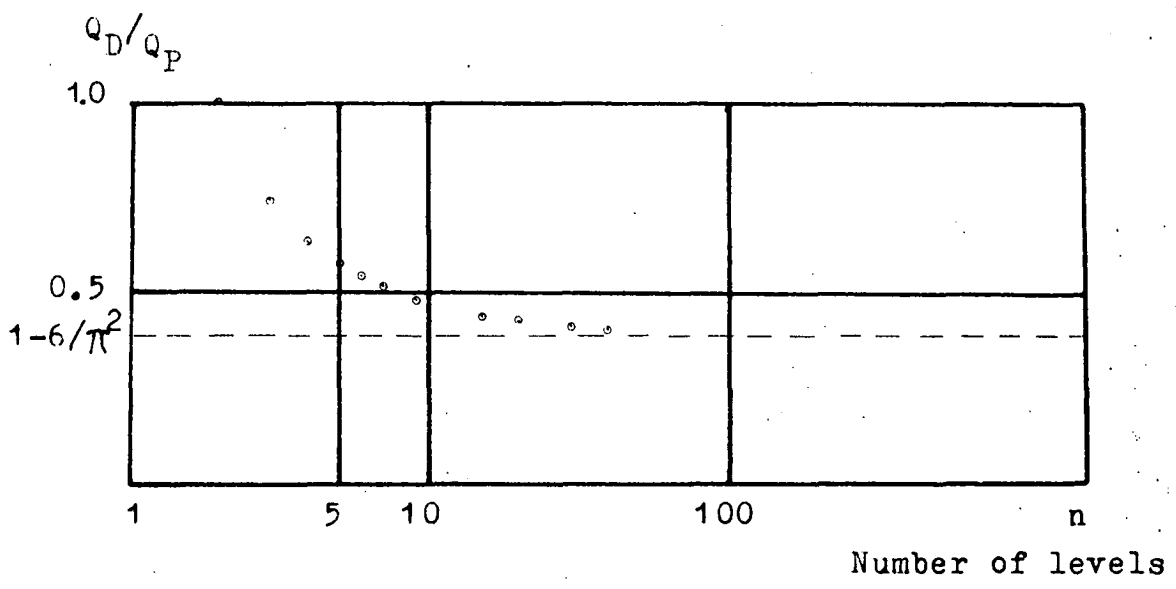
Zetterberg's methods of analysis are as follows:

- (i) The discrete case: With certain restrictions on the source, a rate of information can be defined which constitutes a statistical measure of the ensemble of messages transmitted. The greatest value of the information rate is named "channel capacity", and the corresponding ensemble is called optimal. He determines the statistical characteristics for the optimum message ensemble from which the amplitude, power and spectral characteristics have been calculated for P.C.M. and delta modulation.
- (ii) Continuous Signal: A common measure of the quality of transmission is used. This is called signal-to-noise ratio. In the examination of transmission quality, it has been assumed that the ensemble of messages has been generated by a stochastic normal process, with the energy lying within a determined frequency range f_1 to f_2 , and with a comparatively arbitrary distribution in this range.



CHANNEL CAPACITY FOR P.C.M. AND D.M. AT SAME PULSE FREQUENCY

figure 2.8



POWER RATIO Q_D/Q_P IN OPTIMAL ENSEMBLE FOR DIFFERENT N^0 LEVELS n .

figure 2.9

2.3.1 Channel Capacity for P.C.M. and D.M.

The channel capacity which corresponds to the maximum information rate, and, therefore, to the optimal ensemble, is for P.C.M.,

$$C = \frac{1}{\tau} \log 2$$

where τ = pulse interval in seconds. For Delta modulation,

$$C = \frac{1}{\tau} \log \left(2 \cos \frac{\pi}{n+1} \right)$$

where n = the number of quantizing levels.

Figure 2.8 shows channel capacity versus n for the same pulse frequency. For n greater than 10, the difference is less than 5 percent.

2.3.2 Power of the Modulation Signal

For the optimal ensemble (as before), the power of the modulation signals are:

For P.C.M.,

$$Q_P = V_K^2 \frac{n^2-1}{12}$$

For DM,

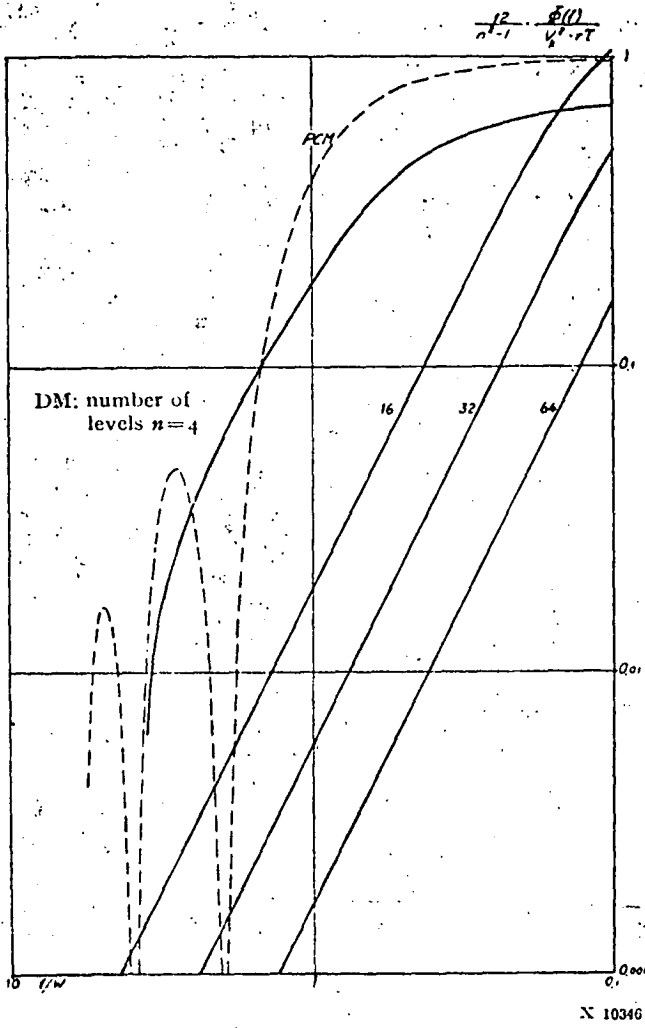
$$Q_D = V_K^2 \left\{ \frac{(n+3)(n-1)}{12} - \frac{1}{2} \cot^2 \frac{\pi}{n+1} \right\}$$

V_K = quantizing step .

Figure 2.9 shows Q_D/Q_P versus n . Q_D/Q_P approaches a number $1-6/\pi^2$ which corresponds to about 60 percent smaller power for delta modulation than PCM. (Note; this is for the optimal ensemble of functions at the input to each modulator).

2.3.3 Spectral Density Functions

The spectral analysis was done to throw light on the question of overloading in delta modulation. This occurs when the change in signal between two sample times is greater than the system can reproduce. (see also deJager on overloading).



Standardized spectral density for optimal ensemble
 with PCM and DM. $f/W = 0$ gives for

| | |
|------------|-------|
| PCM: | 1.0 |
| DM, n = 4: | 0.72 |
| n = 16: | 4.18 |
| n = 32: | 12.09 |
| n = 64: | 37.6 |

Figure 2.10

In a composite signal with a continuous spectrum, the energy should be less at greater frequencies in order to avoid trouble with overloading. This last remark ties in with experimental observations made by deJager on music transmission (see section 2.2.4) where, in a satisfactory music transmission system, overloading did occur at large amplitudes and high frequencies.

The analysis was done for the optimal ensemble of functions and was based on the original information theory analysis done by Shannon (9). Figure 2.10 shows the standardized (w.r.t. power) spectral density function for delta and pulse code modulation. For P.C.M., the same curve is obtained for different n because of standardization. It shows that a small part of the energy exists above W (where f_1 to $f_2 = 0$ to W), because the reconstruction was not done by ideal low pass filtering.

The curves for delta-modulation show a growing concentration of energy to low frequencies with increase in n .

Chapter III describes an experimental delta-sigma modulation system. It would be desirable to be able to apply Zetterberg's theory on delta modulation to the delta-sigma system. Section 2.1.3 shows how a delta-sigma system can be considered as a delta system preceded by an integrator. Zetterberg's work would apply to this delta system. The problem is, therefore, reduced to the relatively simple task of interpreting the effect of integration before delta modulation.

The optimal ensemble of functions is defined as the ensemble for which the information rate is at a maximum. Zetterberg does not find the actual optimal ensemble but works from the condition of maximum information rate. In this way, he finds the autocorrelation function and, therefore, the spectral density function. The same theory applies for the delta section of the delta-sigma system. Thus, the figure of

2.10 would apply to delta sigma modulation for its optimal ensemble.

The optimal ensembles for delta and delta-sigma modulation are, of course, different. They are related by the transfer characteristics of the integrator, but, as the analysis is carried out from the maximum information rate (thus giving the optimal condition), the theory applies in either case.

The theories by Zetterberg and deJager consider the pulses as impulses and the integrators as "pure integrators". In a practical system, the integrators are low pass filters (either with large time constants or with appropriately adjusted time constants) and the impulses square finite pulses. The analyses given by Zetterberg and deJager are, therefore, a first order description only. They do give an indication of the spectral properties of the delta and delta-sigma systems, and enable them to be compared on a spectral basis with P.C.M.

In section 2.6 an attempt is made to show how a more general (and more accurate) method of analysis could be developed. Auto-correlation techniques are suggested and used, and a problem posed.

2.3.4 Transmission of Continuous Signals

Zetterberg makes certain assumptions upon which he bases his calculations. They are:

- (i) The transmitted signal is continuous and is generated by a stochastic process.
- (ii) The spectrum is absolutely continuous.

The difference between the transmitted and received signals is the error signal. Zetterberg then shows how the

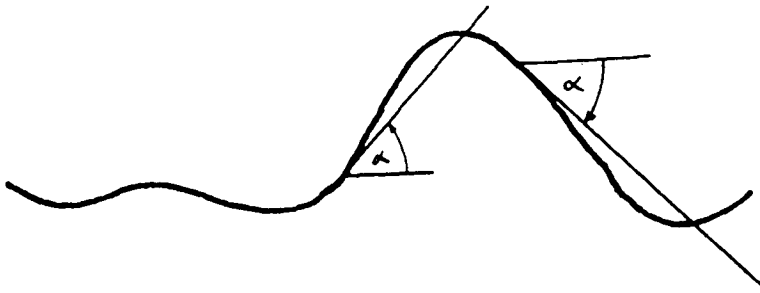


Figure 2.11 OVERLOADING IN DELTA MODULATION

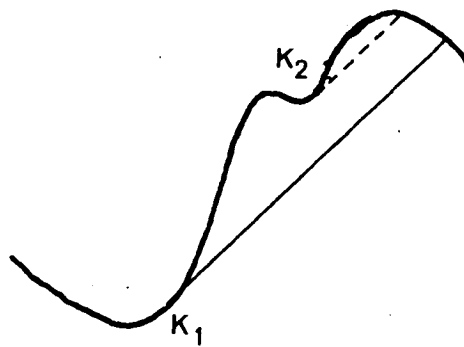


Figure 2.12 SECOND CONTACT POINT INSIDE THE FIRST
(OVERLOADING)

error signal can be broken down into three statistically independent parts. The total noise power, N , is the sum of the part powers N_e , N_g , N_o for extrapolation⁽⁷⁾, granulation and overloading, respectively. He shows N_e can be made arbitrary small, so the expression for noise power becomes,

$$N = N_g + N_o$$

A result for overloading is derived based on deJagers experiments on over loading. If

$$f_p/f_3 \geq 2\pi \frac{2V_E}{V_K} \quad (2.1)$$

where f_3 is given by

$$f_3^2 \int_{f_1}^{f_2} \Phi(f) df = \int_{f_1}^{f_2} f^2 \Phi(f) df.$$

$\Phi(f)$ is the power spectral density function of the signal. Zetterberg's investigations lead to a generalisation of this result.

2.3.5 Overloading in Delta Modulation

To find the total effect of overloading in delta modulation, Zetterberg fixes the value of $V_K f_p$ at γ and lets V_K diminish to zero. In this way, the granulation error is effectively reduced to zero and the expression for N_o holds good. Figure 2.11 shows how overloading occurs. The reconstructed signal follows the transmitted signal some of the time, and the secant corresponding to the slope γ or $-\gamma$ for the rest of the time. The point of transition from one case to the other is known as a "contact point". Figure 2.12 shows how a second contact point can fall within the effect of the first. Zetterberg takes this into account in his analysis.

He then calculates the number of contact points for a given ensemble of functions, and the noise energy per contact point. The product is the total noise energy due

$$\sqrt{\psi_0} = \sqrt{V_H}$$

It is also shown that

loading.

result of deager's condition of transmission without over-
This latter expression (F/F_3) is the more general

$$\text{or } \frac{F}{F_3} = 2\sqrt{2} \frac{V_H}{V_K} y$$

$$y = \frac{F}{F_3} \cdot \frac{2\sqrt{2} V_H}{V_K}$$

$$r(s) = \frac{\psi(s)}{\psi(0)}$$

$$\Phi(x) = \int_{-\infty}^x e^{-u^2/2} du$$

$$Q(x) = \frac{7}{2} x^5 + \frac{7}{5} x^7$$

$$P(x) = \frac{1}{2} x^6 - \frac{4}{3} x^4 - \frac{2}{5} x^2 - 1$$

$$h(x) = 1 + \exp(-x^2/2) P(x) - Q(x) \Phi(x)$$

$$s_1 = \frac{2 F_3}{\sqrt{8} C}$$

$$-r''_0 = (2\pi F_3)^2$$

$$y = \frac{3}{\sqrt{2}} \frac{y_0 \cdot 2\pi F_3}{y} \cdot \left[2 \psi_0(-r''_0) \right]^{1/2}$$

$$a = \frac{3}{\sqrt{2}} y_0 \cdot 2\pi F_3$$

$$c = \frac{-r''_0}{(r''_0)^{1/2}}$$

$\psi(s)$ is the autocorrelation function.

$$as_1 = \frac{2\sqrt{3}}{3} y \int_0^y$$

$$N_0 = \psi_0 = \frac{243}{35 \pi^{3/2}} \frac{1}{(as_1)^2} e^{-y^2} \quad (2.2)$$

to overloading and is given by:

the effective value of the input signal. Therefore, the signal-to-noise ratio (for overloading) is easily obtained.

$$\frac{\Psi_0}{N_0} = \frac{35 \pi^{3/2}}{243} \frac{v^5 C^2 \exp(v^2)}{L(aS_1)} \quad (2.3)$$

2.3.6 Granulation Noise in Delta Modulation

The granulation noise is isolated from the total error by holding V_K fixed and increasing the value of the pulse frequency to a theoretically infinitely great value. All overloading disappears without any essential change in the granulation error.

The result derived for granulation noise is;

$$N_g = 2 \Psi_0 \frac{K}{(2\pi)^3} \sqrt{\frac{2}{\pi}} \frac{f_2 - f_1}{f_3} \left(\frac{V_K}{V_E} \right)^3 \quad (2.4)$$

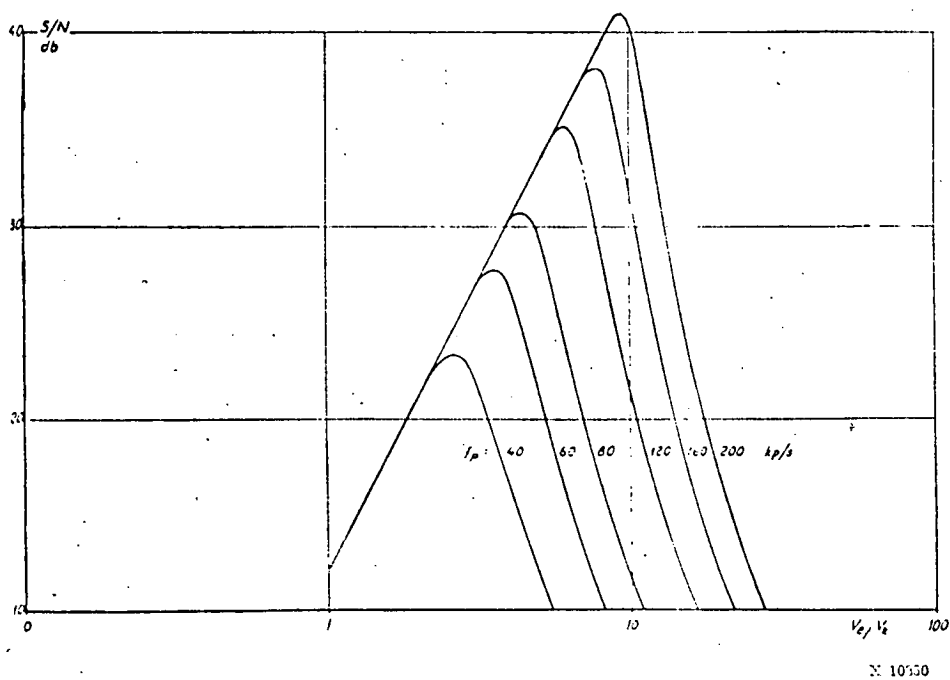
$$K = \sum_{n=1}^{\infty} 1/n^3$$

The signal-to-noise ratio due to granulation is given by,

$$\frac{\Psi_0}{N_g} .$$

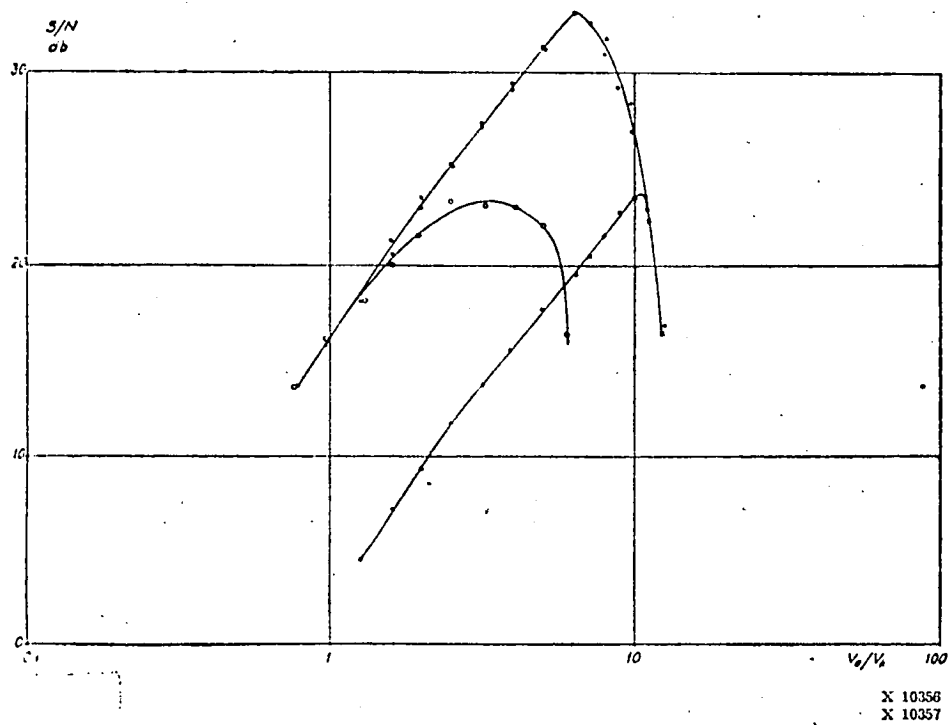
2.3.7 Comparison with Measurements for Delta Modulation

Zetterberg illustrates measurements made and how they compare with theory. At sufficiently low values of V_E/V_K , measured curves for different pulse frequencies coincide. This implies that signal-to-noise ratio is independent of pulse frequency when overloading is negligible. It also verifies the assumption that the pulse frequency in technical applications is so large that it can be considered infinite, when the granulation error is to be calculated.



Signal-noise ratio with DM dependent on V_e/V_k and f_p . Frequency range II

Figure 2.13



Measurement results. Signal-noise ratio with DM for sine wave signal, $f = 800$ c/s.

- $f_p = 60$ kc/s, with filter
- $f_p = 30$ kc/s, with filter
- $f_p = 60$ kc/s, without filter

Figure 2.14

The curve of signal-to-noise ratio versus V_E/V_K consists of two branches: in one (small V_E/V_K) the granulation is dominant, and in the other, overloading dominates. The granulation branch in reference 7 has different slopes in theory than in measurement. (See figures 2.13, 2.14). The difference is suspected to be due to different input signals and dissimilarities in the spectral distribution of the noise. A test is described in reference 7 to verify this assumption.

2.3.8 Noise Power for Overloading and Granulation in P.C.M.

The noise power through overloading in P.C.M. is given by

$$N_o = \frac{V_o^2}{V_o} \sqrt{\frac{2}{\pi}} \left[(1+b^2) \int_0^{\infty} \exp(-y^2/2) dy - b \exp(-b^2/2) \right]$$

where $b = \frac{V_K}{2V_E} (N - 1)$

$N =$ number of roots of maximal modulus of equation $\lambda^N - 1 = 0$. (reference 7 page 103).

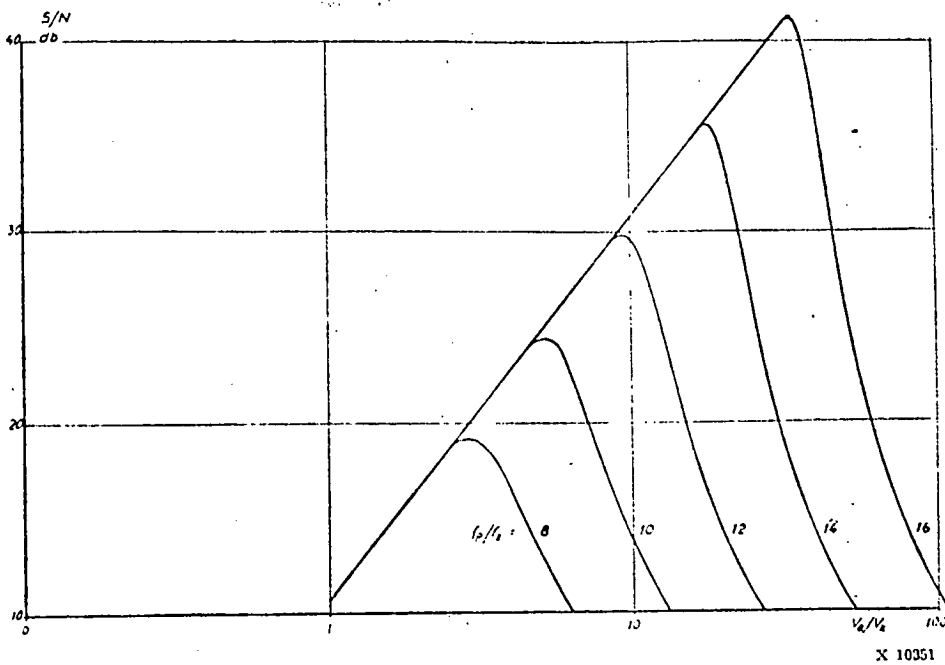
Noise power through granulation in PCM

$$N_g \approx \frac{1}{12} V_K^2$$

Figure 2.15 illustrates signal-to-noise ratio versus V_E/V_K and its dependence on f_p . There is a great similarity between the curves of figures 2.13 and 2.15.

2.3.9 Discussion

Zetterberg has set up a mathematical model for the analysis of quantizing noise in delta modulation. Using this model he has obtained analytical values for the signal to noise ratio versus V_E/V_K , which he then compares with experimental results to test out the model. The difference between the theoretical and measured values is shown to be small, and in most cases is explained.



Signal-noise ratio with PCM dependent on V_c/V_k and f_p .

Figure 2.15

Results for quantizing noise for P.C.M. are also derived. Based on the theoretically derived results for delta modulation and P.C.M., a comparison between the two is made.

The noise power through granulation errors for a certain V_E/V_K is less for delta modulation. Overloading is less trouble, the greater the pulse frequency. It occurs more quickly in P.C.M. than in delta modulation.

A comparison was made on the basis "equivalent" systems, from the point of view of quality. By equivalent, one means the same maximum signal to noise ratio for the same pulse frequency and input signal. The determination of when PCM and delta modulation are equivalent must depend upon the character of the input signals and their bandwidths.

A table from Zetterberg for the equivalence of PCM and delta modulation, is shown below:

| cut off frequency of signal (KC/S) | Pulse frequ. ΔM. & P.C.M. KC/S | (S/N) _{MAX} db | No. pulses per code sp. (PCM) |
|------------------------------------|--------------------------------|-------------------------|-------------------------------|
| 5.4 | 65 | 30 | 6 |
| 3.3 | 33 | 24 | 5 |

Zetterberg's concluding comment is made regarding commercial telephone systems, in which the signal frequency range is about 3.5KC/S and a transmission quality of 35 db is desired. Delta modulation requires a channel bandwidth approximately twice that required for P.C.M. It is only at low qualities of transmission that the two systems will be comparable at the required pulse frequency.

This result compares favourably with deJager's result where, for a pulse frequency of 100 KC/S, delta modulation is equivalent to an eight digit PCM system. Another author Libois⁽¹⁰⁾, showed that, for a system with $f_p = 100\text{KC/S}$, it gave the same quality as a P.C.M. system with six pulses per code group with compression, and 7 pulses per group without compression.

2.4 DELTA-SIGMA MODULATION

H. Inose, Y. Yasuda and J. Murakami⁽⁵⁾ described the principle of delta-sigma modulation (section 2.1) and discuss advantages of delta-sigma over delta modulation. In their introduction, it is implied that delta modulation is only suited to signals which do not require the d.c. level transmitted, and delta-sigma is an extension of delta to overcome this disadvantage.

These assumptions are based on the use of pure integrators in the feedback and demodulator, where in fact, no author has suggested the use of pure integrators in a practical system. The suggested sources of error are noise and hit, but in any such system the pulses are regenerated (to remove sources of error which would accumulate on integration) before demodulation.

J. C. Balder and C. Kramer⁽¹¹⁾ in their paper "Analogue-to-Digital Conversion by means of Delta Modulation", show that a d.c. level can be transmitted. The cut-off frequency of the integrator should be at least as large as the highest signal frequency in order to avoid overloading of the delta modulator. On the other hand, the cut-off frequency of the integrator should be small with regard to the pulse frequency.

Delta-sigma modulation is a high quality method of producing the transmission of d.c. signals with virtually the same simple circuitry, the same bandwidth and the same signal-noise characteristics as delta modulation.

Inose showed analytically that

$$S/N = M \cdot \frac{3}{4\pi} \left(\frac{f_p}{f_2} \right)^{3/2}$$

M = ratio of signal amplitude to the maximum amplitude that does not overload the modulator.

For Delta modulation,

$$S/N \sim \frac{f_p^{3/2}}{f_2^{1/2} f}$$

where f = signal frequency.

The above values for S/N have the same functional relationship. Each was derived for the different systems by different methods. Inose's method is only approximate.

2.4.1 Stability

The stability of the delta-sigma system is dependent on the variation in reference level of the comparator. For a variation ϵ' in the comparator reference, the corresponding variation d' in the integrator input is

$$d' \sim \frac{\epsilon'}{A}$$

where A is the gain of the integrator amplifier. By increasing the gain to a high enough value, the variation in level after integration barely effects the system performance.

2.5 THE PROBLEM OF OBTAINING THE OUTPUT SPECTRUM OF A DELTA MODULATOR IN TERMS OF THE INPUT SPECTRUM.

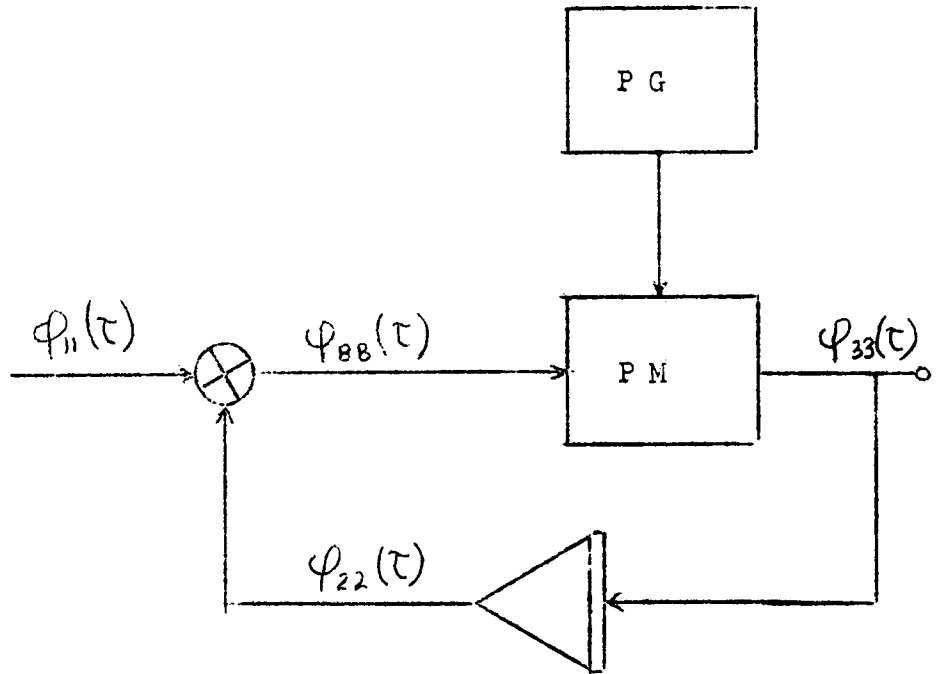


Figure 2.16 Delta Modulator

2.5.1 The Problem

Given $\varphi_{11}(\tau)$, the input auto-correlation function, ($\Phi(\omega)$ is the corresponding spectrum) what is output auto-correlation function $\varphi_{33}(\tau)$ (and what is the corresponding $\Phi_{33}(\omega)$)?

The three operations of interest are, the subtraction of the feedback loop from the input, the integration in the feedback loop, and the pulse modulation which contains both quantizing and sampling.

$$\varphi_{BB}(\tau) = \varphi_{11}(\tau) + \varphi_{22}(\tau) - \varphi_{21}(\tau) - \varphi_{22}(\tau)$$

$\varphi_{22}(\tau)$ is easily obtained in terms of $\varphi_{33}(\tau)$ (the required quantity) and $\varphi_{11}(\tau)$ is given. The difficulty which so far has prevented the full solution of this spectral

problem is finding the cross correlation functions $\varphi_{12}(\tau)$ and $\varphi_{21}(\tau)$ ($\varphi_{12}(\tau) = \varphi_{21}(-\tau)$) for a non-linear forward loop. (The pulse modulator).

If the forward loop were linear, a complete description of the system in terms of the auto-correlation function at the input would be possible.

2.5.2 $\varphi_{22}(\tau)$ in terms of $\varphi_{33}(\tau)$

If $\varphi_{22}(\tau) \leftrightarrow f_2(t)$, then

$$\varphi_{22}(\tau) = \lim_{T \rightarrow \infty} \frac{1}{2T} \int_{-T}^T f_2^1(t) f_2^1(t + \tau) dt .$$

Therefore, $\varphi_{22}''(\tau) = -\varphi_{33}(\tau)$.

2.5.3 Pulse Modulator

The pulse modulator can be suitably described in terms of the autocorrelation functions. Use is made of Price's theorem⁽²²⁾ (for two variables only) in order to obtain the output autocorrelation function of the "two level quantizer". The input must be assumed gaussian as well as ergodic and stationary.

Summary of Price's Theorem

Let $x_1(t)$, $x_2(t)$ be random variables with zero mean value taken from a gaussian process having the joint frequency function

$$p(x_1, x_2) = \frac{1}{2\pi\sigma^2 \sqrt{1 - \left(\frac{R_{12}}{R_{11}}\right)^2}} \exp \left\{ - \frac{\left(x_1^2 + x_2^2 - 2 \frac{R_{12}}{R_{11}} x_1 x_2 \right)}{2\sigma^2 \left(1 - \left(\frac{R_{12}}{R_{11}}\right)^2 \right)} \right\}$$

where $R_{12} = \overline{x_1 x_2}$.

Let $x_1(t)$, $x_2(t)$ be passed through zero memory devices and denote outputs by $h_1(x_1)$ $h_2(x_2)$.

The output cross co-variance can then be written as;

$$\Psi = \overline{h_1(x_1) h_2(x_2)}$$

Define the normalized input correlation coefficient to be

$$\rho_{12} = R_{12}/R_{11} \quad .$$

Theorem:

Under the above hypothesis, if the input process is gaussian and if $h_j(x)$ satisfies certain integrability conditions, then

$$\frac{\partial^K \bar{\Psi}}{\partial \rho_{12}^K} = \frac{h_1^{(K)}(x_1) h_2^{(K)}(x_2)}{h_1(x_1) h_2(x_2)} ,$$

where

$$h_j^{(K)}(x_j) = \left. \frac{\partial^K h_j(x)}{\partial x^K} \right|_{x=x_j}$$

2.5.4 Application to a Two Level Quantizer

The quantizer of the delta-modulator is two levelled with transfer characteristics as shown in figure 2.17.

$$h_1(x_1) = h_2(x_2) = h(x) = \begin{cases} -1, & x < 0 \\ +1, & x > 0 \end{cases}$$

or $h(x) = -1 + 2u(x)$, $u =$ step function

with $K = 1, \frac{\partial h}{\partial x} = 2 \delta(x)$.

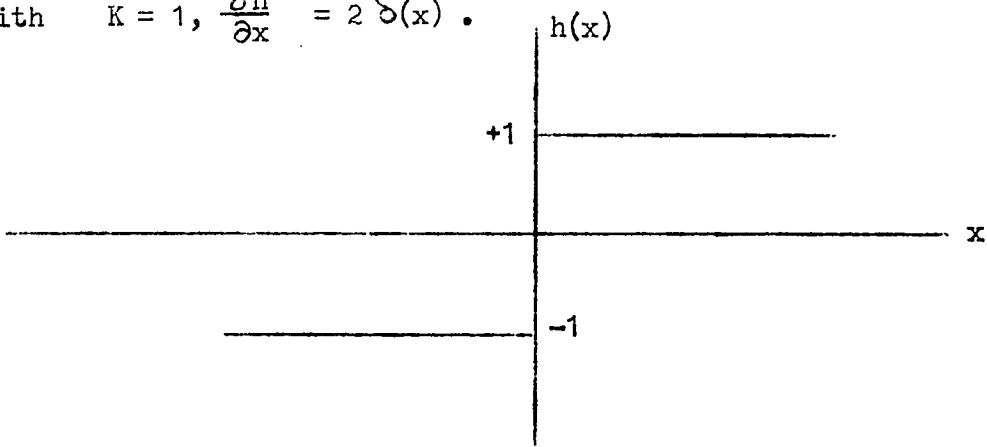


Figure 2.17 Quantizer Characteristic

The output autocorrelation function is required, so putting

$$x_1(t) = x(t) , x_2(t) = x(t + \tau) ,$$

and using the joint frequency function as described above,

$$\frac{\partial^k \Psi}{\partial \rho^k} = \frac{h_1^{(k)}(x(t)) h_2^{(k)}(x(t + \tau))}{2\pi\sigma^2 \sqrt{1-\rho^2}} \exp\left[-\frac{x_1^2 + x_2^2 - 2\rho x_1 x_2}{2\sigma^2(1-\rho^2)}\right] dx_1 dx_2$$

for $k = 1$,

$$\begin{aligned} \frac{\partial \Psi}{\partial \rho} &= \frac{1}{2\pi\sigma^2 \sqrt{1-\rho^2}} \int_{-\infty}^{\infty} \int_{-\infty}^{\infty} 2\delta(x_1) 2\delta(x_2) \exp\left[-\frac{x_1^2 + x_2^2 - 2\rho x_1 x_2}{2\sigma^2(1-\rho^2)}\right] dx_1 dx_2 \\ &= \frac{4}{2\pi\sigma^2 \sqrt{1-\rho^2}} \int_{-\infty}^{\infty} \delta(x_1) \exp\left[\frac{-x_1^2}{2\sigma^2(1-\rho^2)}\right] dx_1 \\ &= \frac{2}{\pi\sigma^2 \sqrt{1-\rho^2}} \left[-\exp\left[\frac{-x_1^2}{2\sigma^2(1-\rho^2)}\right] \right]_0^{\infty} \\ &= \frac{2}{\pi\sigma^2 \sqrt{1-\rho^2}} \end{aligned}$$

$$= 0 \text{ when } \rho = 0 .$$

$$\Psi(\tau) = \int_0^{\rho} \frac{2}{\pi\sigma^2} \frac{1}{\sqrt{1-\rho^2}} d\rho$$

Substituting $\cos \theta = \rho$

$$\begin{aligned} \Psi(\tau) &= \frac{2}{\pi\sigma^2} \int_{\arccos \rho}^{\pi/2} 1 d\theta \\ \text{i.e. } \Psi(\tau) &= \frac{2}{\pi\sigma^2} \left(\frac{\pi}{2} - \arccos \rho \right) \end{aligned}$$

Knowing the input correlation coefficient, the autocorrelation function of the output may thus be determined.

Its inverse fourier transform gives the spectrum.

The above analysis has been based upon quantizing only.

No consideration has been given to sampling.

2.5.5 The Effect of Sampling

The delta modulator is controlled by a clock pulse.
 regular
 The effect of/sampling must therefore be considered.

A gaussian process is sampled and held, at periodic intervals. The sampled and held waveform has a gaussian distribution in amplitude, provided the input signal has no periodic component at a frequency commensurate with the sampling frequency. The input $q(t)$ to the quantizer thus still satisfies the conditions required by Price's theorem although its spectrum is not that of $f(t)$.

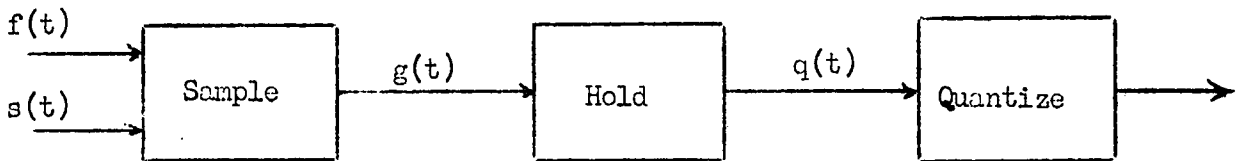


Figure 2.18

Suppose the sampling procedure consists of multiplying the signal $f(t)$ by a sampling waveform $g(t)$ with pulse height 'a' and width 2ϵ as shown in figure 2.18.

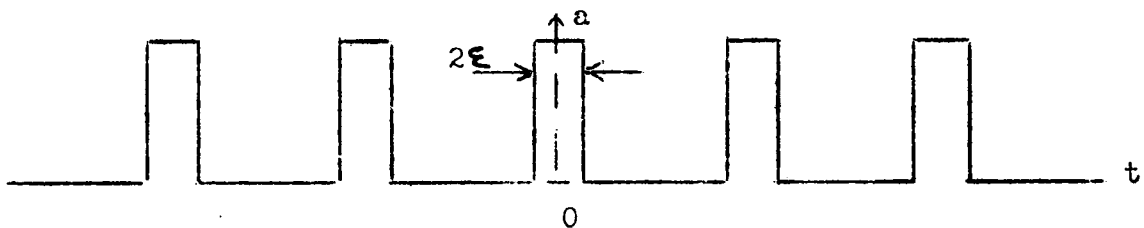


Figure 2.19 Sampling Waveform

The fourier transform of the sampling waveform is,

$$\begin{aligned}
 S(\omega) &= \int_{-\infty}^{\infty} s(t) \exp(-j\omega t) dt \\
 &= \sum_{n=-\infty}^{\infty} \int_{nT-\xi}^{nT+\xi} a \exp(-j\omega t) dt \\
 &= \sum_{n=-\infty}^{\infty} \Delta \frac{\sin \xi \omega}{\xi \omega} \exp(-jn\omega T)
 \end{aligned}$$

$\Delta = 2a\xi$, pulse area.

The fourier transform of $g(t) = f(t) s(t)$ is obtained as the convolution of the two fourier transforms $S(\lambda)$, $F(\omega - \lambda)$ of f and s respectively.

$$\begin{aligned}
 G(\omega) &= \int_{-\infty}^{\infty} S(\lambda) F(\omega - \lambda) d\lambda \\
 &= \int_{-\infty}^{\infty} \frac{\Delta \sin \xi \omega}{\xi \omega} \left[\sum_{n=-\infty}^{\infty} \exp(-jn\lambda T) F(\omega - \lambda) \right] d\lambda
 \end{aligned}$$

It can be shown (Reference 23, problem 4.2) that

$$\begin{aligned}
 \sum_{n=-\infty}^{\infty} \exp(-jn\lambda T) &= \frac{1}{T} \sum_{n=-\infty}^{\infty} \delta\left(\frac{n}{T} - \frac{\lambda}{2\pi}\right) \\
 G(\omega) &= \frac{\Delta}{T} \sum_{n=-\infty}^{\infty} \int_{-\infty}^{\infty} \frac{\sin \xi \lambda}{\xi \lambda} F(\omega - \lambda) \delta\left(\lambda - \frac{2\pi n}{T}\right) d\lambda \\
 &= \frac{\Delta}{T} \sum_{n=-\infty}^{\infty} \frac{\sin \frac{2\pi n \xi}{T}}{\frac{2\pi n \xi}{T}} f\left(\omega - \frac{2\pi n}{T}\right)
 \end{aligned}$$

Put $\frac{2\pi}{T} = \omega_0$, the angular sampling frequency ,

$$G(\omega) = \frac{\Delta}{T} \sum_{n=-\infty}^{\infty} F(\omega - n\omega_0) \frac{\sin(n\omega_0 \xi)}{n\omega_0 \xi}$$

If $\xi \rightarrow 0$ whilst Δ remains finite, then we have, in fact, delta function sampling and,

$$G(\omega) = \frac{\Delta}{T} \sum_{n=-\infty}^{\infty} F(\omega - n\omega_0) , \quad (24) \quad \text{a familiar result.}$$

If $\xi \neq 0$, then the factor $\frac{\sin n\omega_0 \xi}{n\omega_0 \xi}$ indicates how the repeated but shifted parts of the spectrum fall off in amplitude with increase in n .

If $f(t)$ is band limited to W cycles/sec., and sampling is carried out at a rate of $2W$ times per second, then

$F(\omega - K\omega_0)$ does not overlap with $F(\omega - (K \pm 1)\omega_0)$ and the spectrum is

$$\Phi_{GG}(\omega) = \frac{A^2}{T^2} \sum_{-\infty}^{\infty} |F(\omega - n\omega_0)|^2 \frac{\sin^2 n\omega_0 \tau}{n^2 \omega_0^2 \tau^2}$$

2.5.6 Spectrum of Held Signal

The holding process is assumed ideal with no return to zero between samples.

Time response of the holding circuit.

For an input $f(nT) \delta(t)$, the output is required to be

$$\theta(t) = \begin{cases} 1, & 0 < t < T \text{ linear network} \\ 0, & t \geq T \end{cases}$$

The frequency transfer function $H(\omega)$ is then given by the fourier transform of the impulse response.

The Wiener-Khinchine theorem leads to spectrum of $q(t)$ ⁽²³⁾

$$\begin{aligned} \Phi_q(\omega) &= \Phi_{GG}(\omega) |H(\omega)|^2 \\ |H(\omega)|^2 &= \frac{4 \sin^2 \omega T/2}{\omega^2} \\ \Phi_q(\omega) &= \left(\frac{4 \sin \frac{\omega T}{2}}{\frac{\omega T}{2}} \right)^2 \sum_{n=-\infty}^{\infty} \Phi_{ff}(\omega - n\omega_0) \end{aligned}$$

This gives the energy spectrum to the quantizer for suitably sampled band-limited signals with delta function sampling.

The fourier transform of $\Phi_q(\omega)$ gives the auto correlation function $\psi(\tau)$ at the input to the quantizer. Since $q(t)$ is still gaussian, the previous results based on Price's theorem still apply, and give the quantizer output auto-correlation function, and, in taking the fourier transform, gives its spectrum.

It has been shown how the output auto-correlation function can be obtained for the pulse modulator, given the input auto-correlation function. However, it does not appear possible to obtain an explicit expression for $\varphi_{BB}(\tau)$ in terms of known quantities.

$$\varphi_{BB}(\tau) = \varphi_{11}(\tau) + \varphi_{22}(\tau) - \varphi_{12}(\tau) - \varphi_{21}(\tau)$$

The reason being that, to date, it is not possible to calculate the input-output cross-correlation ($\varphi_{12}(\tau)$) for a non-linear system.

The solution to the problem is very simple if the forward loop is linear. Application of the theorem in section 13.8 of reference 25 gives the input-output cross-correlation function.

To the author's knowledge, no ready solution is available to the input-output cross-correlation function for a non-linear system such as that of the delta-modulator. A solution to this problem would enable a complete description of the output power spectral density function in terms of that at the input, and of the sampling frequency.

2.6 THERMAL NOISE

In the analyses contained in this thesis, the system has been considered to be operating at a signal-to-noise ratio above the threshold value. That is, the effect of the channel noise in causing incorrect reception of a pulse does not occur.

In the same way thermal noise is considered to be below threshold and is, therefore, neglected throughout the analyses. This would not be possible if the system were operating near threshold where the effect of the

thermal noise would be significant.

Overloading and granulation are the only noise types considered.

2.7 CONCLUSIONS

The bulk of the work reviewed in this chapter is on analytical discussions, with some experimental work to verify the results. DeJager's work was more a qualitative description of the principle, and did not go too far into the practicability of the delta system. Zetterberg's work was a highly analytical investigation. Results were achieved which could be closely followed in experiment. Inose's work introduced the principle of delta-sigma modulation as a means of d.c. transmission which is not so easily achieved by straight delta modulation.

Only Zetterberg went to the extent of subdividing the quantizing noise into "granulation" and "over-loading". The author feels this is an important consideration. Usually, when a system is designed, it is done so to fulfil a given specification, and overloading is virtually avoided in the design. Granulation cannot be avoided. In the system considered in chapter III, the effects of overloading are negligible throughout the range of operation of the system, where as granulation (for a given pulse frequency) noise for low level signal is very significant. For the transmission of d.c., it is granulation noise that must be considered thoroughly.

Another important aspect of Zetterberg's work, upon which a majority of his paper was based, was the comparison with P.C.M. He showed under what conditions delta modulation is the more favourable.

Economic considerations are also a very important factor and must be given due consideration. This has been done in chapter IV.

From information gathered from the bibliography, and especially the work reviewed here, it appears that delta and delta-sigma modulations are a cheap and simple means of transmitting continuous signals to a high degree of accuracy.

Many factors come into consideration as to which modulation to choose for a particular application. An attempt is made in chapter IV to place delta and delta-sigma modulations in perspective with other forms of pulse modulation, (especially P.C.M.)

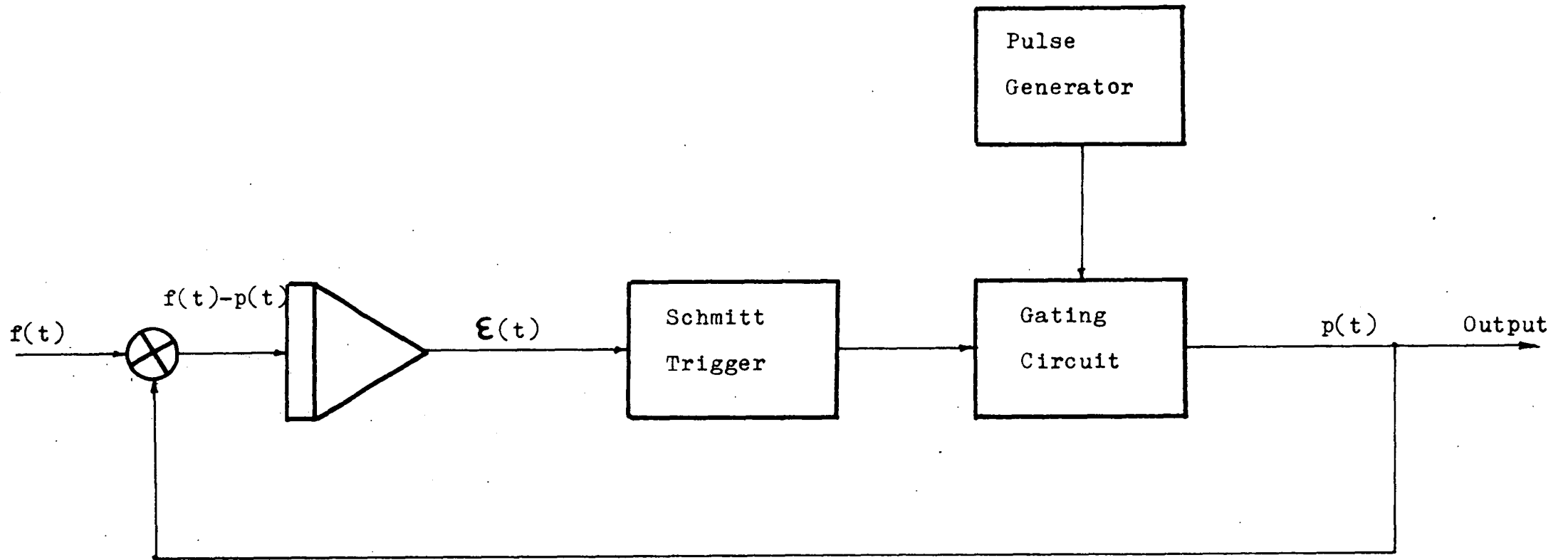


Figure 3.1 DELTA-SIGMA MODULATION BLOCK DIAGRAM

CHAPTER THREE

AN EXPERIMENTAL DELTA-SIGMA MODULATION SYSTEM

INTRODUCTION

In order to investigate delta modulation in a practical case, an experimental delta-sigma modulator was designed, built and tested.

A member of the Electrical Engineering Department, at the University of Tasmania was interested in a data transmission system for dc signals. It was decided to use his specification in the prototype modulator.

The system was required to transmit dc signals from an angle/voltage transducer. The transducer measured between $\pm 90^\circ$ and converted to voltages between $\pm 7\frac{1}{2}$ V.d.c. The rate at which the dc varies is low. The limitations on the frequency that can be transmitted (to a suitable accuracy) will be discussed in a further section. The channel bandwidth specified is 2 kilocycles.

Delta-sigma is chosen instead of straight delta modulation because of the dc advantages (5). Figure 3.1 is the basic block diagram for the experimental modulator.

3.1 THE DELTA-SIGMA MODULATION SYSTEM

3.1.1 Logic Simplification

A simplification to the delta sigma modulator (as described in section 2.1.2) can be made by deleting the generation of both positive and negative clock pulses. Positive pulses only are generated, and where a negative pulse would occur, "no pulse" occurs instead. On demodulation, a negative current is produced when "no pulse" occurs and a positive current when "pulse" is present.

When there is an equal number of 'pulses' and 'no pulses' the negative current will flow for a longer period of time than the positive current. For a period of time T , for which the number of pulses equals the number of no pulses ($T \gg$ clock period), the integrator amplifier will saturate unless the currents are weighted in such a way that

$$I T = 0 \quad (I = \text{total current})$$

over the period of time T . (see appendix A).

The weighted current values are,

$$I^+ = -3I^-$$

With this modification, the block diagrams of figures 2.1 and 2.2 still apply.

3.1.2 Sequential Circuit

The gating circuit must be such that whole pulses are passed. That is, if the output of the schmitt trigger changes from low to high during a pulse from the pulse generator, that pulse and any part thereof must be inhibited. On the other hand, if the schmitt trigger output changes from high to low whilst a pulse is present, all of that pulse must be passed. This procedure is necessary in order to maintain the average $I T = 0$ for equal number of 'pulses' and 'no pulses'.

This can be accomplished by using sequential logic networks (12).

3.1.3 Clock Pulse Generation

Now that only positive pulses are required, the clock becomes a simple device. A free running astable multivibrator triggering a bistable multivibrator is most suitable. The bistable is used to assure an even mark-space ratio. Small variations of clock frequency with temperature or component

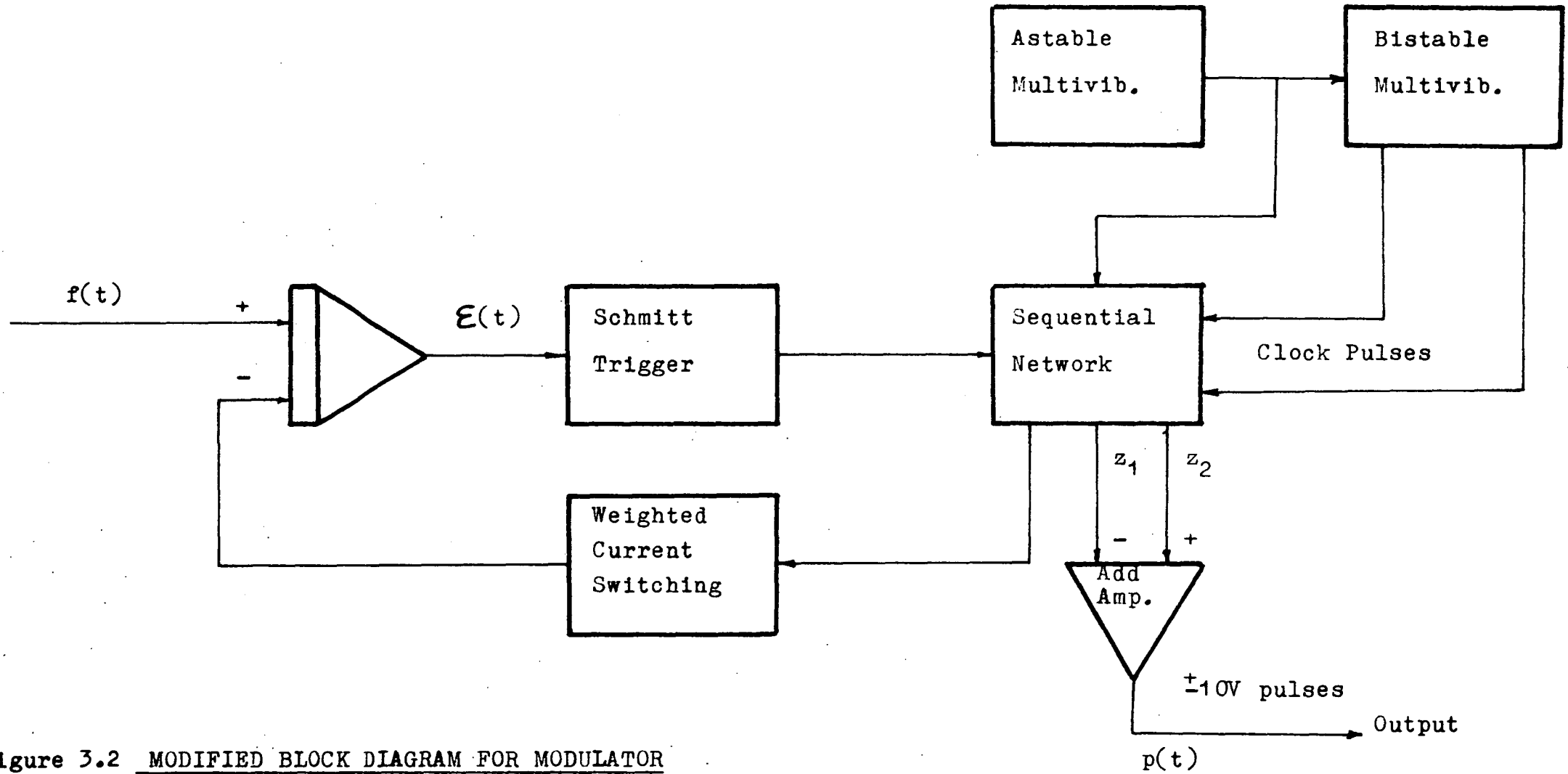


Figure 3.2 MODIFIED BLOCK DIAGRAM FOR MODULATOR

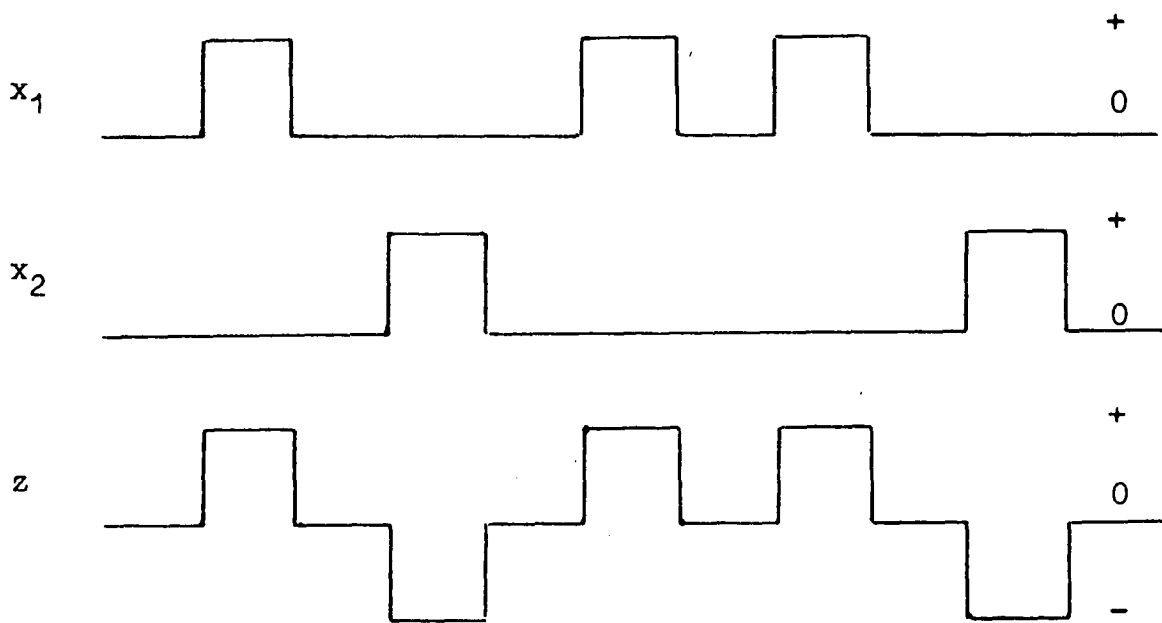


Figure 3.3 SEQUENTIAL NETWORK OUTPUTS AND SUM ON ADDING AMPLIFIER

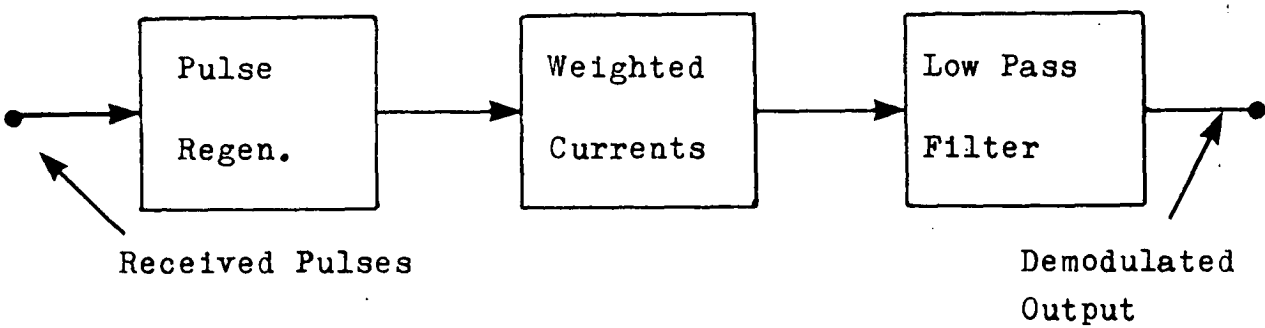


Figure 3.4 PRINCIPLE OF DEMODULATION

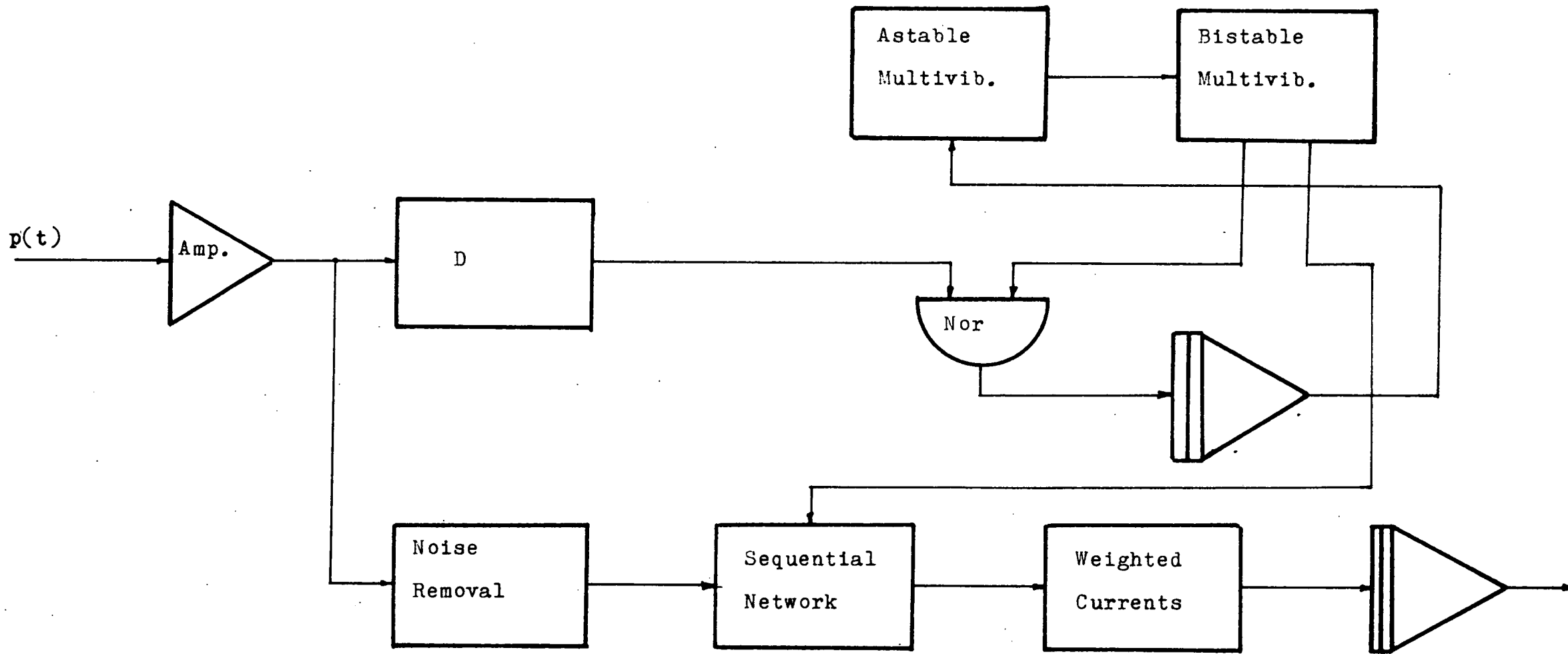


Figure 3.5 DETAILED BLOCK DIAGRAM FOR DEMODULATION

aging will not matter, as it is not the frequency that is critical, (as regards accuracy) but the necessity for an even markspace ratio.

3.1.4 Modified Modulator Block Diagram

Figure 3.2 shows the modified block diagram depicting the modulation system. The sequential network has two outputs, one the negation of the other. These outputs can be added on opposite inputs to an adding amplifier, thereby producing a second output with positive and negative pulses. By having the output wave in this form, regeneration of the clock pulse at the receiving end is simplified. Figure 3.3 shows typical sequential network output waveforms and their sum on the adding amplifier.

3.1.5 The Demodulator

As mentioned previously, demodulation consists of a very simple process, that of passing the pulse train (consisting of positive and negative pulses) through a low pass filter. With the modification of generating positive pulses only, the currents have to be weighted in the receiver in the same way as in the transmitter.

Noise, distortion, and other forms of interference will necessitate the regeneration of the pulses in order to maintain the even mark-space ratio and switch the weighted currents. Figure 3.4 illustrates basically how the demodulator is to operate. Figure 3.5 shows in more detail the demodulation block diagram.

The astable and bistable multivibrators have nominally the same characteristics as those in the transmitter. The incoming pulse train is amplified and passed into block D where it is rectified. This rectified signal is gated with the

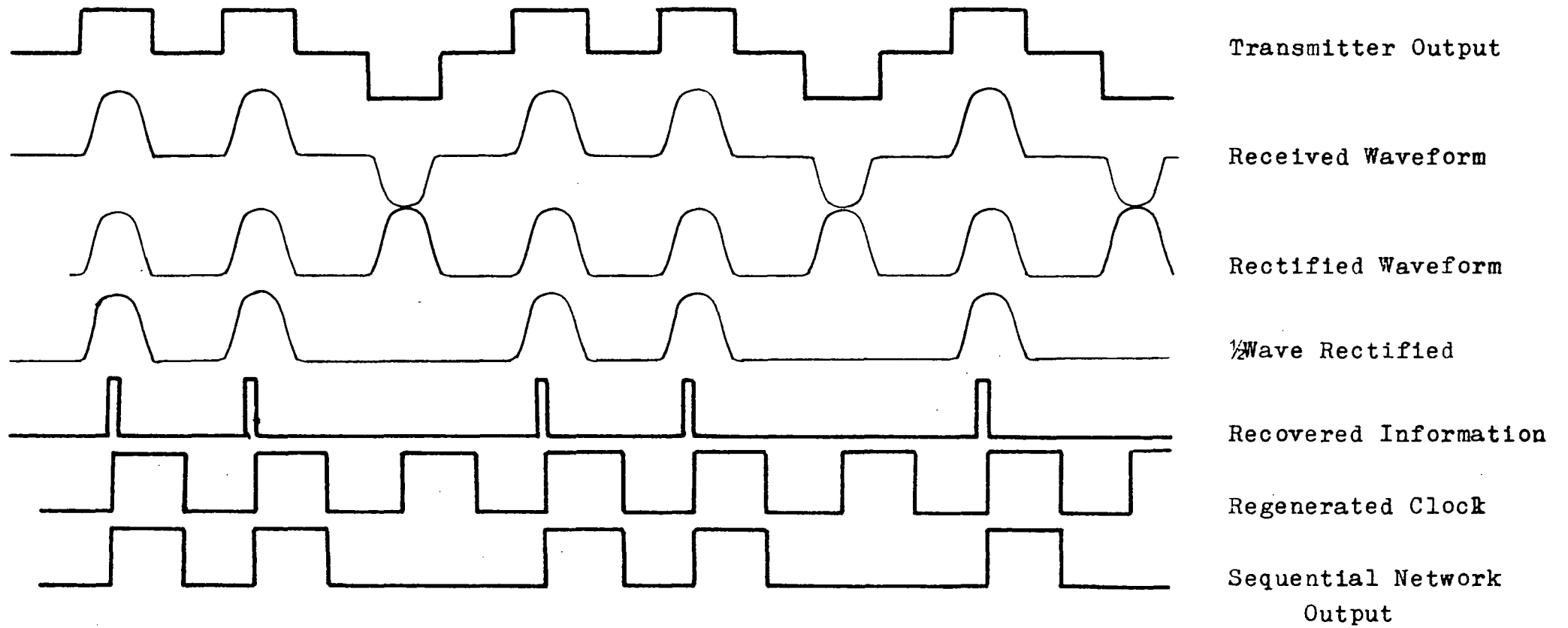


Figure 3.6 WAVEFORMS DURING REGENERATION

output from the bistable multivibrator. The output from the NOR gate, $(A + B)'$, is filtered through the first low pass filter. This gives the d.c. value of $(A + B)'$. This dc output from the filter controls the output frequency of the astable multivibrator to within ± 10 percent of the nominal frequency determined by RC.

The information signal is half wave rectified, that is, the negative pulses are removed. The positive pulses are passed through a "noise removal" circuit which identifies the presence or absence of a pulse and gives a narrow square pulse output.

This train of narrow pulses containing the required information is gated with the regenerated clock pulse to give a waveform the same as that at the output of the transmission sequential circuit. This even mark-space ratio waveform is used to switch weighted current generators (weighted in the same proportion as in the transmitter, see appendix A) into the second low pass filter. The output of the second low pass filter is the demodulated output signal. This signal is the required reproduction of the input signal plus the noise due to quantization.

Figure 3.6 shows the transmitted and received waveforms. Also shown are the various waveforms during regeneration, the final output being the current switching waveform.

3.2 MODULATION CIRCUITRY

Figure 3.7 shows a complete circuit diagram of the delta-sigma modulator. Integrated circuits have been used wherever possible. This has been done because of their low cost, low power consumption, high operating speeds, small

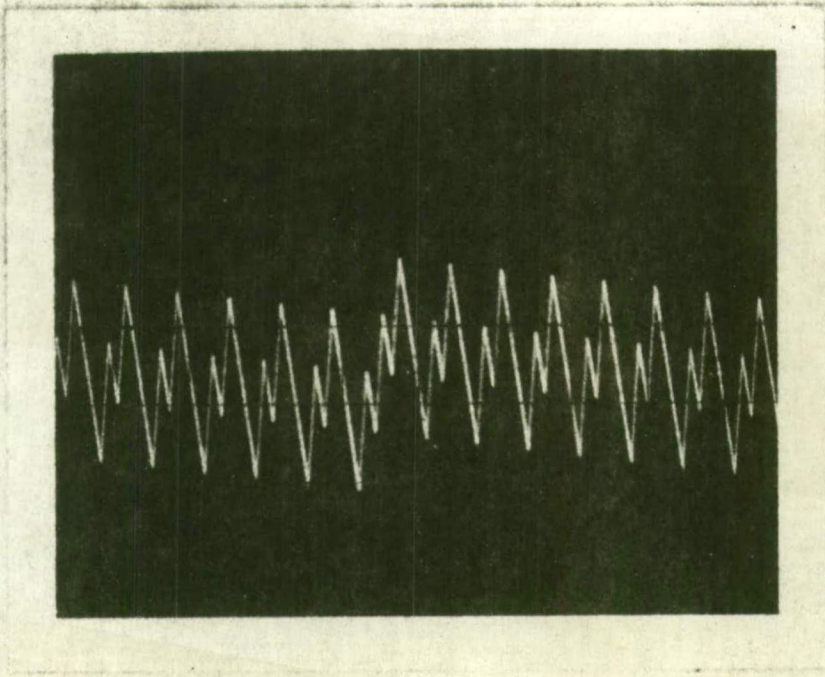


Figure 3.8 INTEGRATOR OUTPUT WAVEFORM

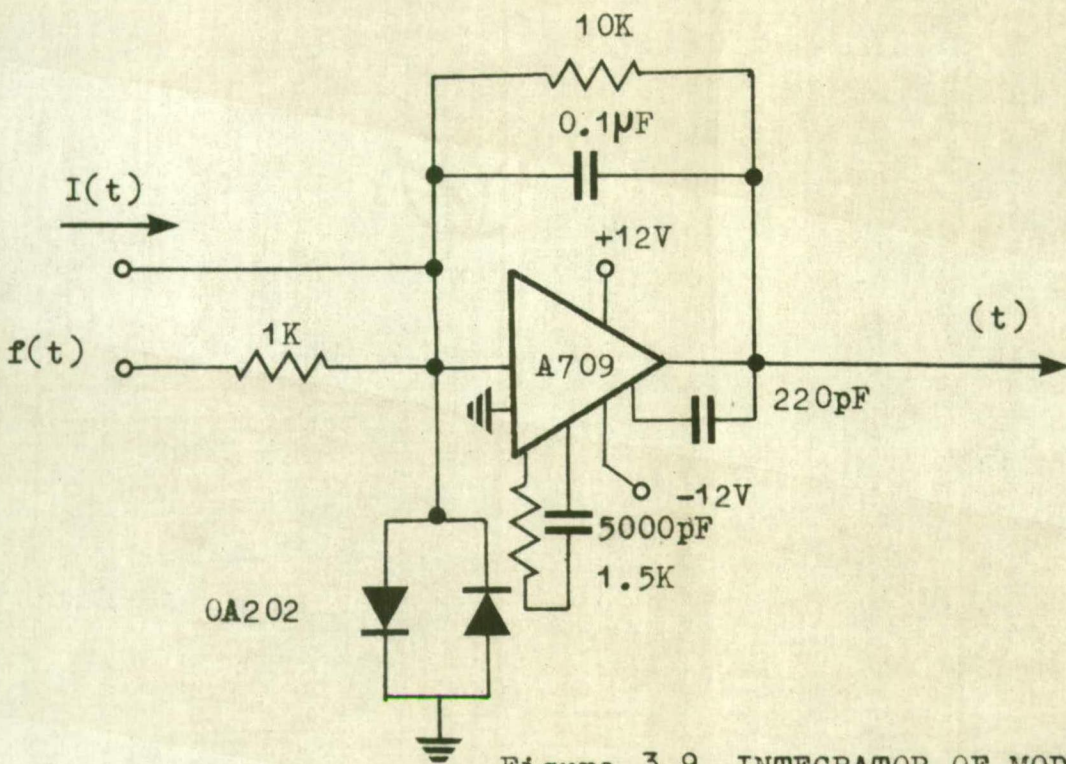


Figure 3.9 INTEGRATOR OF MODULATOR

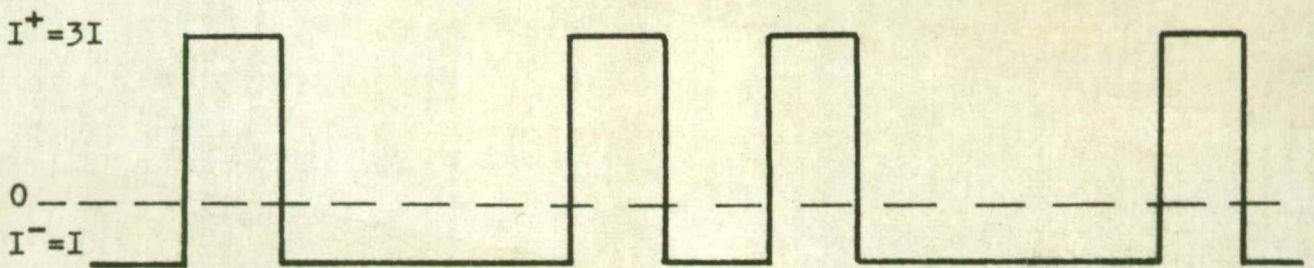


Figure 3.10 CURRENT WAVEFORM

physical size and intercompatibility.

3.2.1 The Integrator

The weighted currents (section 3.1) are added to the input signal at the integrator, and the sum (i.e. the difference signal $d(t)$) is integrated.

The integrator is a Fairchild $\mu A709$ operational amplifier⁽¹³⁾ with capacitive feedback and the necessary frequency compensation (according to chapter 14, reference 13).

Referring to figure 3.9, the output signal $\mathcal{E}(t)$ is given by:

s = Laplace operator

$I(t)$ = Input current from feedback loop.

$$sC \mathcal{E}(s) = -\left(\frac{f(s)}{R} + I(s)\right)$$

$$\mathcal{E}(s) = -\frac{1}{s} \cdot \frac{1}{RC} \cdot f(s) - \frac{1}{s} \cdot \frac{I(s)}{C}$$

$$\text{That is, } \mathcal{E}(t) = -\frac{1}{RC} \int f(t) dt - \frac{1}{C} \int I(t) dt.$$

$I(t)$ is a square wave of the form in figure 3.10 (pulse width 0.5mS) and $f(t)$ is a slowly varying dc voltage. It is clear then, that these two waveforms when added and restricted to remain in the vicinity of the reference voltage V_R , will have a resulting waveform like that in figure 3.8.

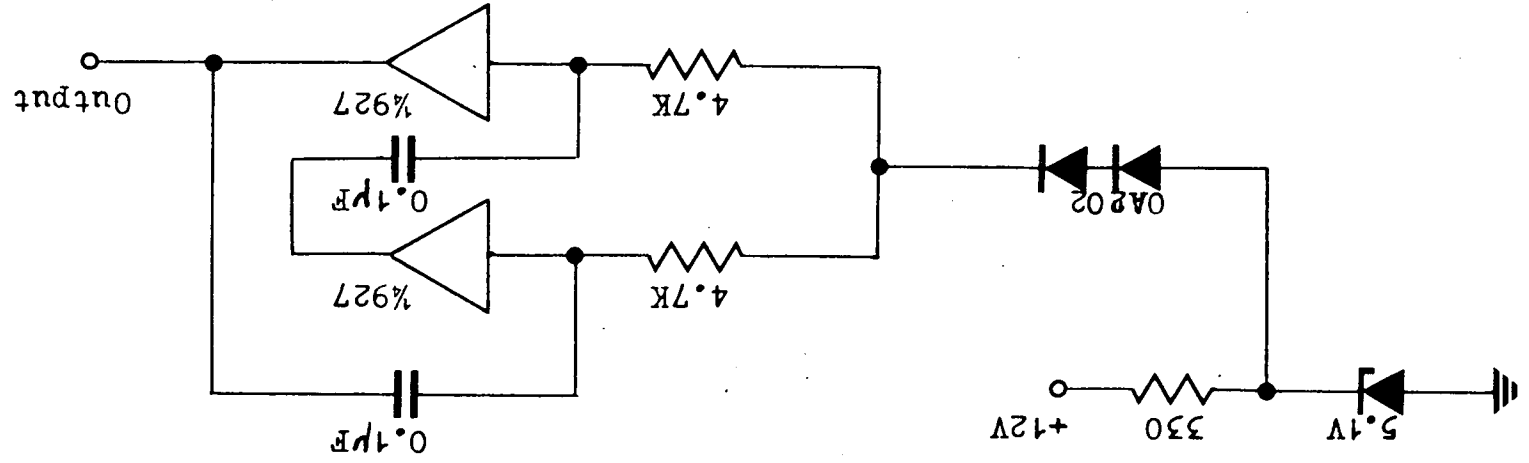
3.2.2 Schmitt Trigger

The Schmitt trigger consists of half a Fairchild RT $\mu L9927$ ⁽¹⁴⁾ quad inverter connected as in figure 3.7.

The integrator output is fed into the schmitt trigger which gives an output "one" (3.5V) or "zero" (0V) depending on whether the input is above or below the reference of the schmitt trigger. The reference level at which the schmitt

ASTABLE WITH TEMPERATURE COMPENSATION

Figure 3.11



trigger fires is dependent on the ratio of the feedback resistance to the input resistance. This ratio is adjusted to give the best performance of the system. This occurs when zero volts are applied at the input and the modulator produces alternately "pulse" and "no pulse" at the output (further discussion in a later section, 3.7). The 4.7V zener diode limits the input to the schmitt trigger.

The output from the schmitt trigger is fed to the sequential network where it regulates the pulses from the clock to the output.

3.2.3 Clock Generator

The clock is an astable multivibrator made from two inverting amplifiers (Fairchild RT μ L9927)⁽¹⁴⁾ coupled with R_s and C_s , and a bistable multivibrator (RT μ L9923)⁽¹⁴⁾. The astable produces a square wave of frequency nominally 2000 c/s (see figure 3.7).

Temperature tests were carried out on the clock, and frequency was found to vary directly with temperature. It varied inversely with supply voltage. Compensation for these variations was achieved by using the circuit shown in figure 3.11. A zener diode of 5.1 volts, supplying the astable multivibrator through two OA202 silicon diodes in series, gave (approximately) the required 3.5V supply. As temperature increases, the drop across the two diodes from the 5.1V zener decreases, and hence increases the supply voltage. This causes a decrease in frequency, and offsets the increase caused by the direct action of the temperature on the integrated circuit.

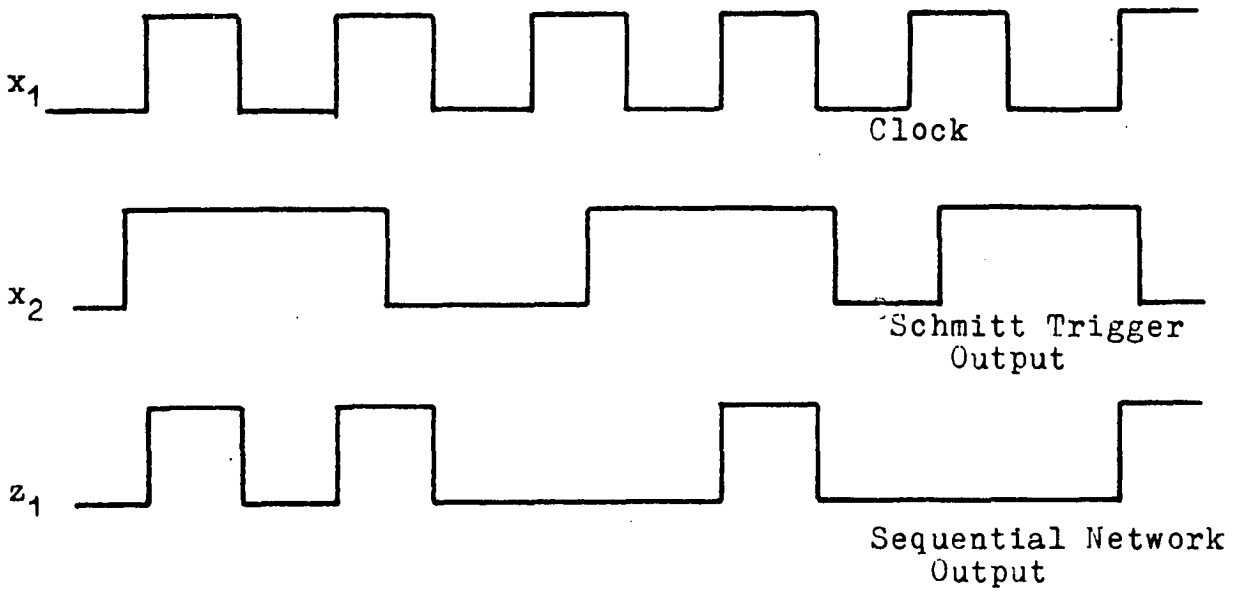


Figure 3.12 SEQUENTIAL NETWORK INPUTS AND OUTPUT

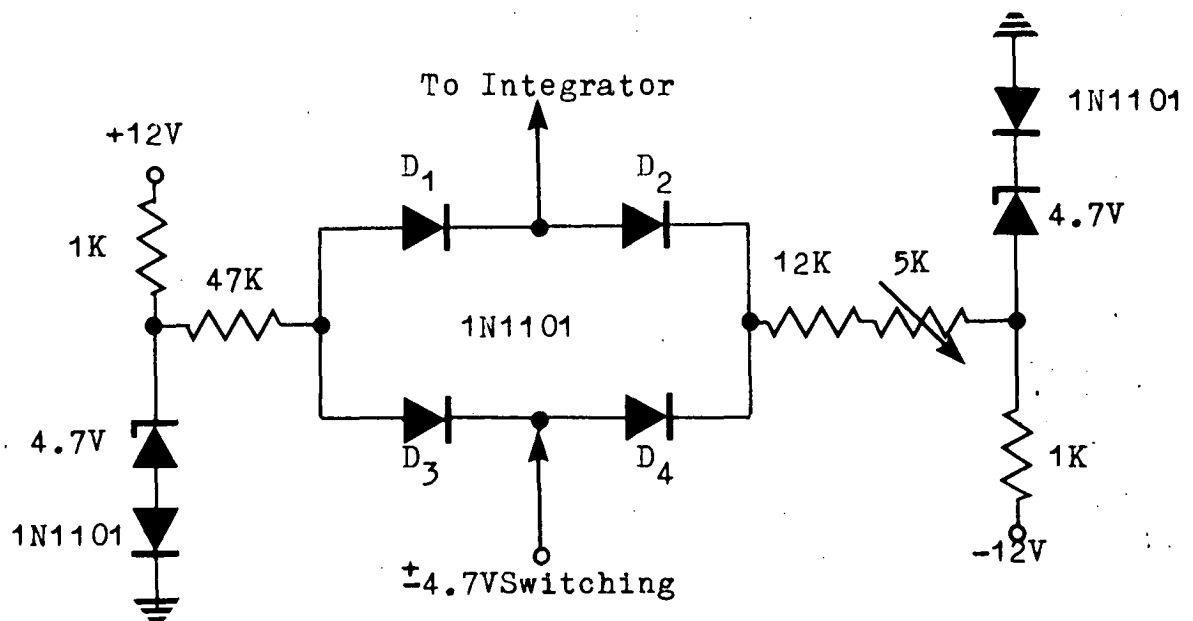


Figure 3.13 DIODE TRANSMISSION GATE AND CURRENT GENERATORS

This compensation technique kept the clock frequency accurate to 2 per cent over 40°C temperature range from room temperature. It should be mentioned again that the stability of the clock frequency is not critical. All that is critical is the necessity for an even mark-space ratio.

With the two percent variation over the 40°C range of the transmitter clock, the receiver clock remained synchronised.

3.2.4 Sequential Network

As described in section 3.1, in order to simplify the regeneration of the clock pulses, both positive and negative pulses are transmitted. This is done by adding two signals (one the negation of the other) from the sequential network on the inverting and non-inverting inputs of an operational amplifier.

The sequential network used has the information signal and its negation as outputs. This network is derived in appendix B, using sequential network logic calculations (12). The circuit is shown in figure 3.7.

Figure 3.3 shows the two outputs z_1 , z_2 from the sequential network. Also shown is the transmitted signal z_1 plus z_2 inverted (negative voltage).

One of the outputs z_1 is fed back to the transistor T (figure 3.7) and is converted to switching signals operating between $\pm 4.7\text{V}$ (instead of 0 to 3.5V). These switching voltages are used to operate the diode transmission gate.

Figure 3.12 shows the schmitt trigger output, the clock pulse and sequential network output.

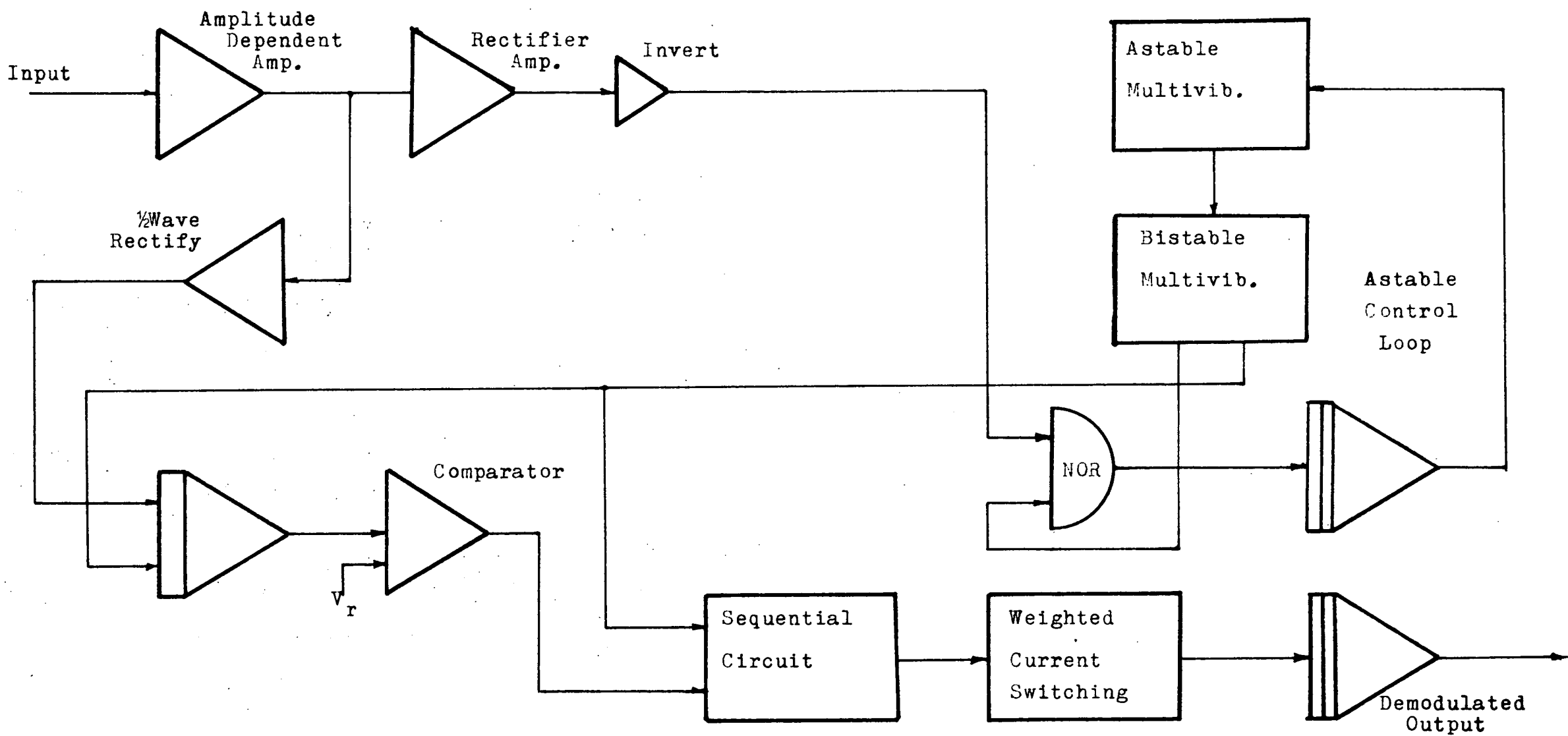


Figure 3.14 RECEIVER DETAILED BLOCK DIAGRAM

3.2.5 Weighted Current Generators

The transmission gate switches the weighted currents into the integrator from the zener diode current generators. To temperature compensate the zener diodes, a diode identical to those in the transmission gate is inserted in series with the zener diode. The accuracy of modulation depends on these currents being weighted in a ratio exactly three to one. (section 3.1). Over the 40°C temperature rise, the two currents varied 15 per cent in value but remained substantially at the 3 to 1 ratio.

The value of the current affects the distribution or pattern of the output pulses. That is, for a given input signal, the pulse pattern representing that signal can be varied depending on the value of the weighted currents $-I$ and $+3I$. Any one of many different patterns represent the signal and each will produce different quantizing noise. This has been observed and discussed in section 3.7.

Referring now to figure 3.13, with +4.7V on the input to the transmission gate, D_2 and D_3 are biased off, D_1 and D_4 biased on. The current flows from the +4.7 volt supply, through the 4.7K resistor to the virtual earth at the input to the integrator. With -4.7V on the input, D_1 and D_4 are reverse biased and current (negative) flows from the virtual earth through D_2 to the -4.7V supply. The currents are weighted 3 to 1 negative to positive (as the integrator inverts).

3.3 DEMODULATOR CIRCUITRY

A complete block diagram of the receiver is shown in figure 3.14.

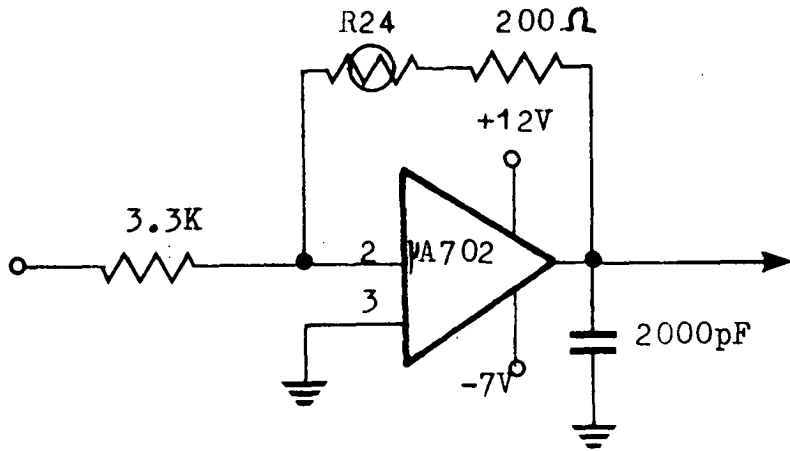


Figure 3.15 AMPLITUDE DEPENDENT AMPLIFIER

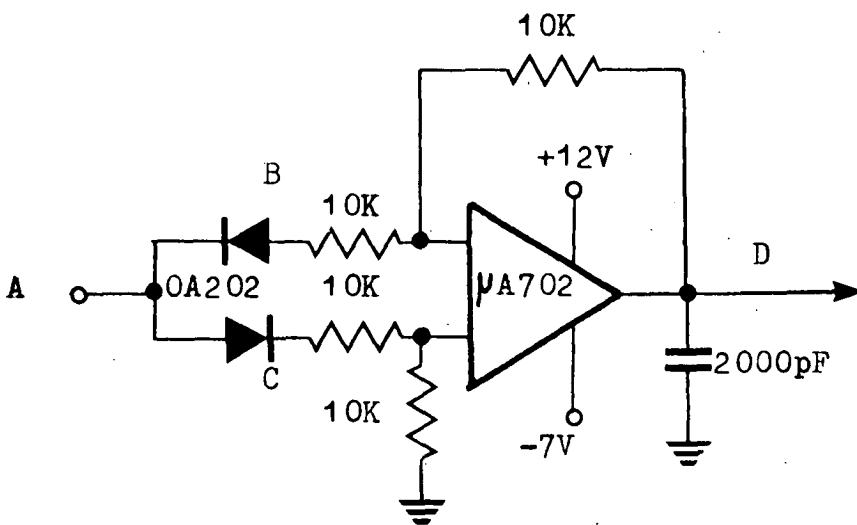


Figure 3.16 RECTIFIER AMPLIFIER

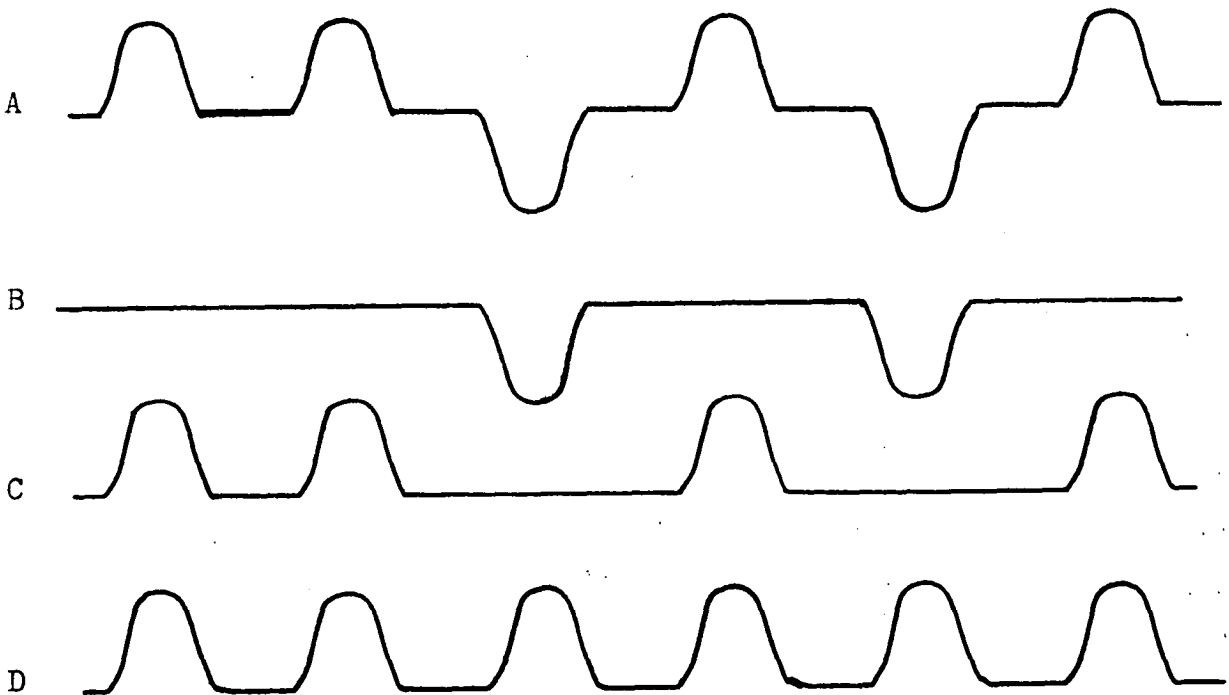


Figure 3.17 WAVEFORMS AT RECTIFIER AMPLIFIER

3.3.1 Amplitude-Dependent Amplifier

The incoming signal is amplified by an amplitude-dependent amplifier. This is done in order to give approximately a constant amplitude to the incoming pulses before demodulation. The amplifier is a Fairchild $\mu A702$ wide-band amplifier, with appropriate feedback and frequency compensation⁽¹³⁾ (see figure 3.15).

Part of the resistive feedback is a thermistor. If the input amplitude is increased, the power dissipated in the thermistor is increased, and its resistance decreases, reducing the gain, and keeping the output amplitude substantially constant. In the system built, the output amplitude was 4 volts (approximately) for a range of input amplitudes from 1.5 volts to 7 volts. This 4 volt value is suitable for the rest of the demodulator to process.

The amplifier inverts the signal but this inversion is compensated for by reversing the inputs to the output amplifier at the transmission end.

The output signal from this amplifier is processed through two separate circuits, one, the clock regeneration circuit, the other, the reshaping circuit for the information signal.

3.3.2 Rectifier Amplifier (figure 3.16)

The amplifier has a gain of one. The input is clipped at zero in both directions, and fed in at the inverting and non-inverting inputs. The waveforms at A, B, C and D are shown. The output waveform is at the same frequency as the original clock in the transmitter, but distorted, and possibly some pulses are displaced.

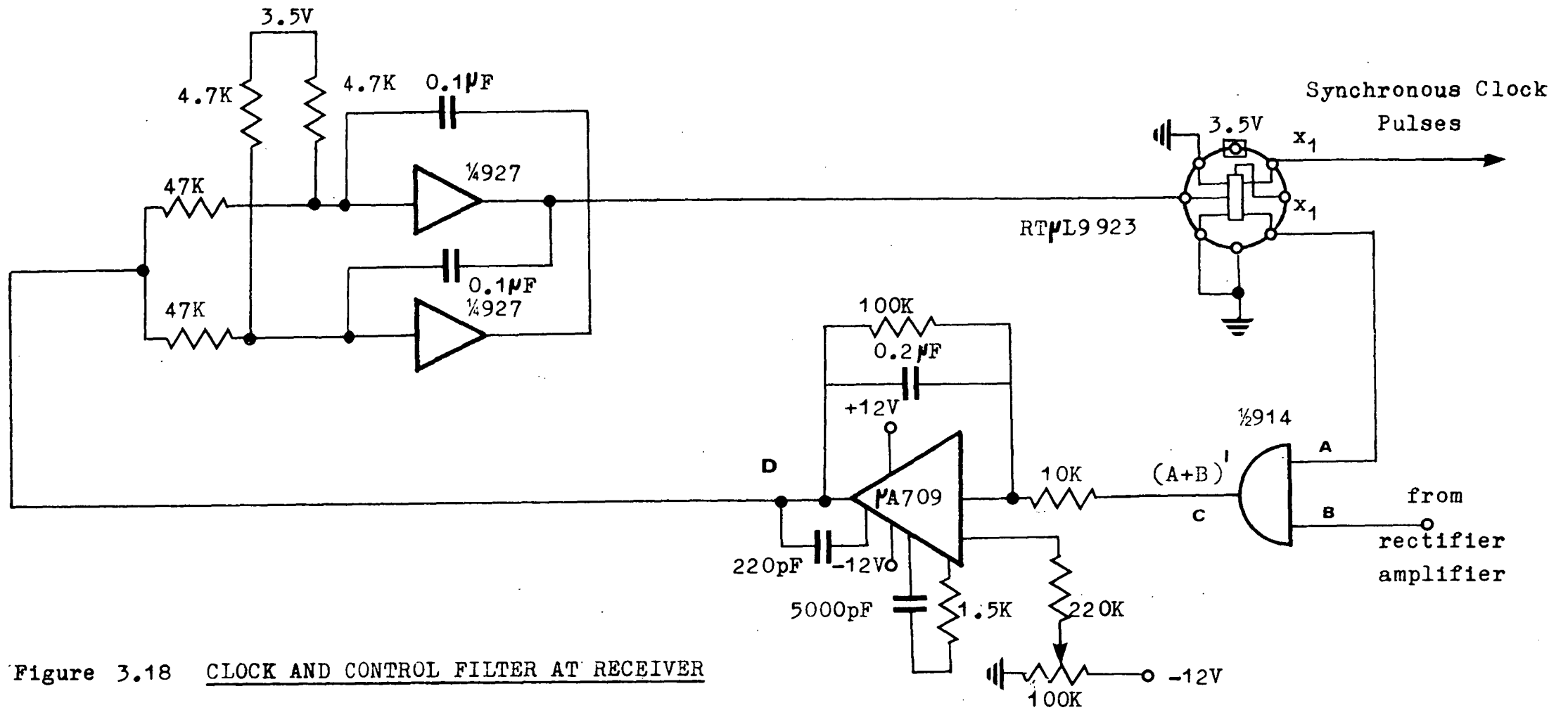


Figure 3.18 CLOCK AND CONTROL FILTER AT RECEIVER

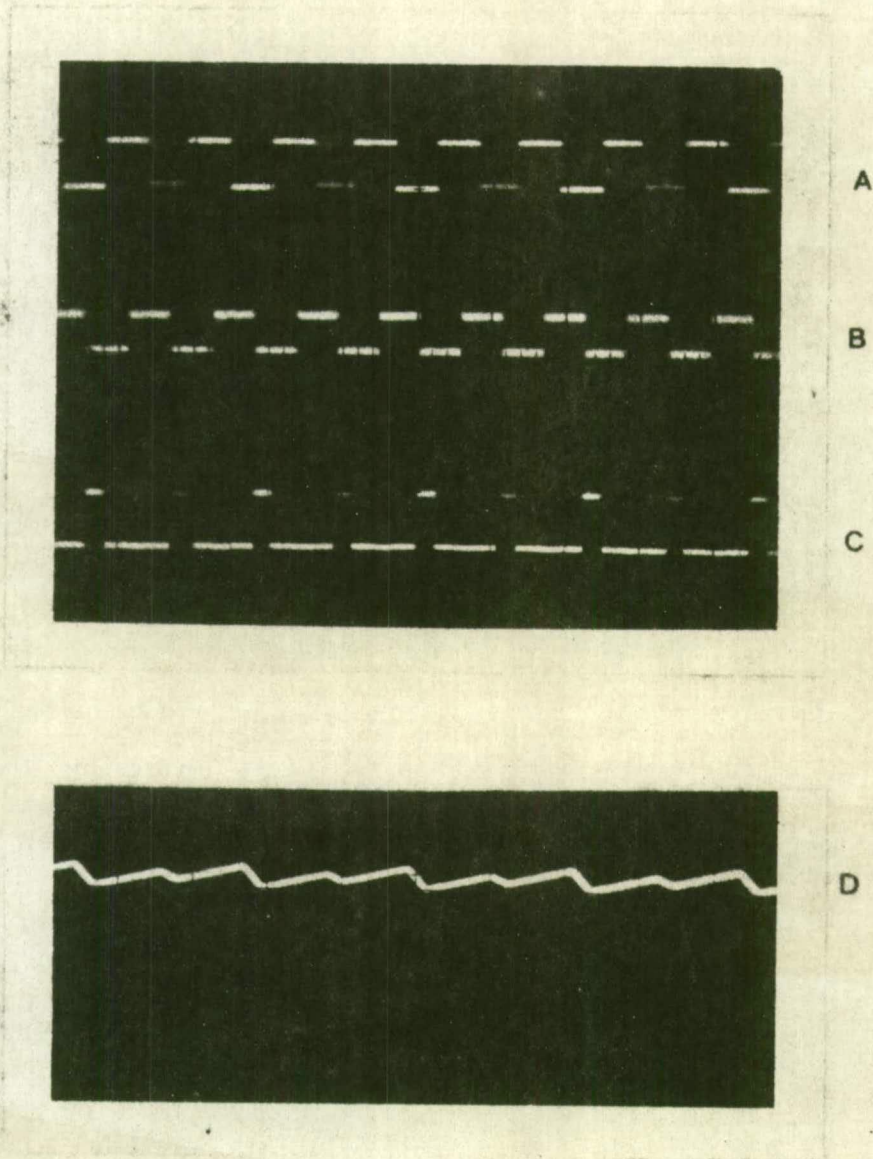


Figure 3.19 WAVEFORMS AT THE POINTS A,B,C,D IN
FIGURE 3.18

It is this waveform D that is used to regulate the receiver clock (see figure 3.17).

3.3.3 Clock and Filter

The clock is the same as in the transmitter, that is, an astable coupled to a bistable multivibrator. However, the astable has feedback control (as described in 3.1.5, also see figure 3.18).

The rectified signal is gated with the bistable output. The gate output $(A + B)'$ is filtered by the low pass filter (shown), and fed back to the astable multivibrator through the two 47K resistors. The dc level at the output of the low pass filter can be adjusted by feeding a d.c. value in at the non-inverting input. It is made to have a value in the vicinity of 3.5 V.D.C. so that the effect of the 47K resistor inputs to the astable multivibrator have approximately ± 10 percent effect on the output frequency.

By altering this d.c. input to the filter, the phase relationship between the two clocks can be altered.

Figure 3.19 shows the wave forms at the various points A, B, C, around the circuit, as well as the transmitter and receiver clock pulses.

3.3.4 Information Recovery

The output from the amplitude dependent amplifier is passed through a diode in the forward direction in order to remove the negative pulses. The resulting information signal is then fed into an integrator (non-inverting input), along with the new clock pulse (inverting input) which is adjusted to be 180° out of phase with the information signal. The output is clamped such that it cannot exceed values 0V in the negative direction and +3 volts in the positive direction.

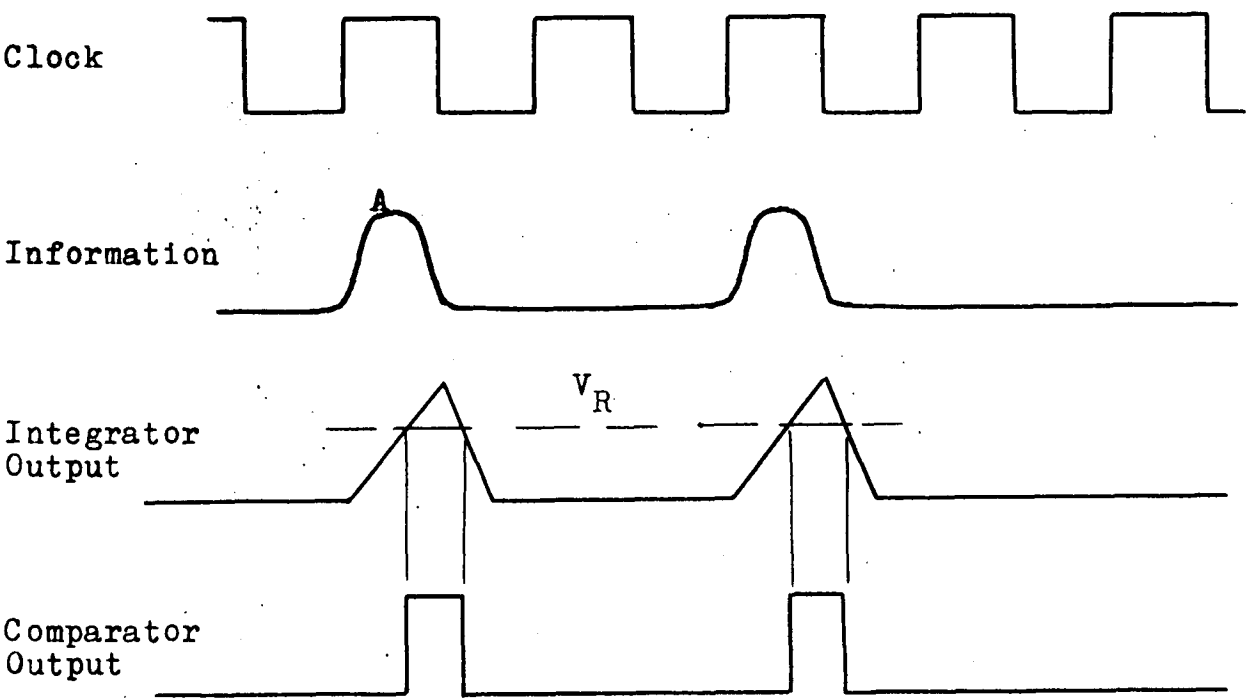


Figure 3.20 INFORMATION RECOVERY WAVE FORMS

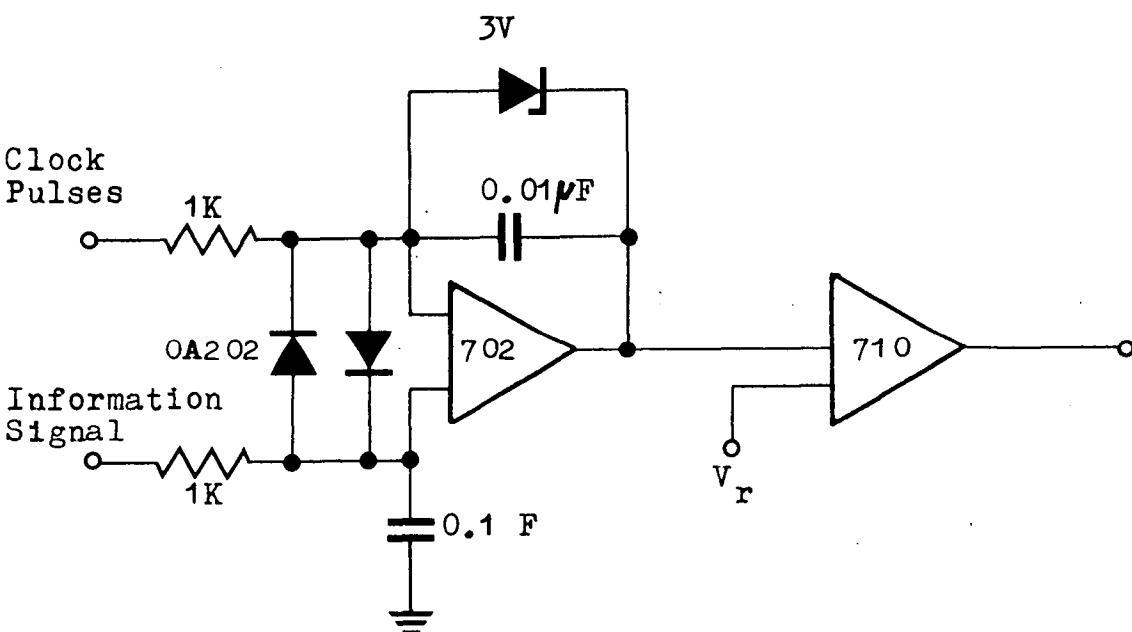


Figure 3.21 INTEGRATOR AND COMPARATOR

When an information pulse is present (as at Δ in figure 3.20), the output integrates up (perhaps to its maximum obtainable value + 3 volts), then a clock pulse integrates downwards to 0 volts. The gain on the clock pulse integration is made sufficiently large so that the output voltage is always returned to zero.

When an information "no pulse" is present, the output remains zero during the period of the clock pulse, as it cannot take values below zero.

Figure 3.21 shows the integrator circuit connected to the comparator. The comparator gives an output of "one" for the time that the integrator output is greater than the reference voltage. This output is a square, narrow, well-defined signal, representing the original information signal. (see figure 3.20).

Ideally the output waveform of the integrator would be triangular, but because of the pulse distortion it is not. In figure 3.20 it has been shown to be triangular.

The comparator used is a Fairchild $\mu A710$ high speed comparator⁽¹³⁾.

3.3.5 Reforming Comparator Output

Before the sequence of information pulses from the comparator can be filtered in order to give the original signal they must be converted back into pulses derived from a square wave-form with even mark-space ratio. This is necessary to satisfy the criterion

$$I T = 0 ,$$

for a period of time $T(T \gg 1/f_p)$, see section 3.1.1).

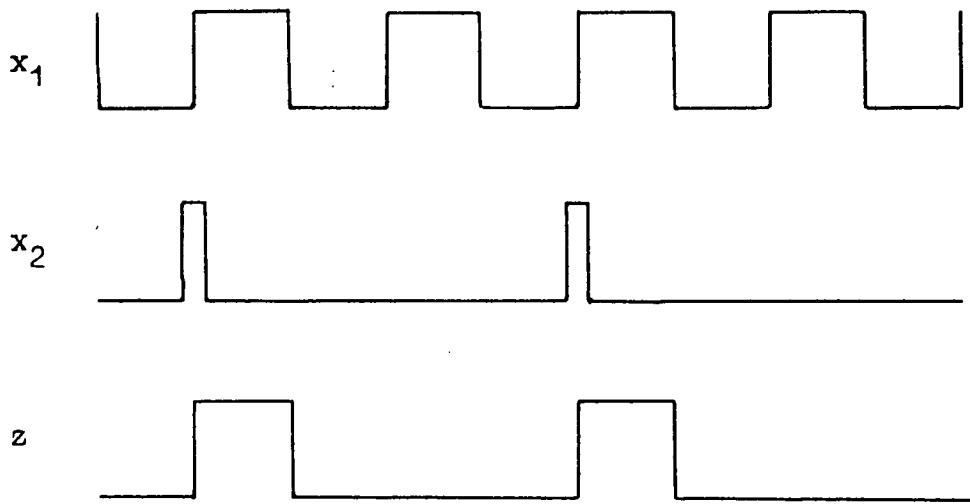


Figure 3.22 INPUT-OUTPUT WAVEFORMS

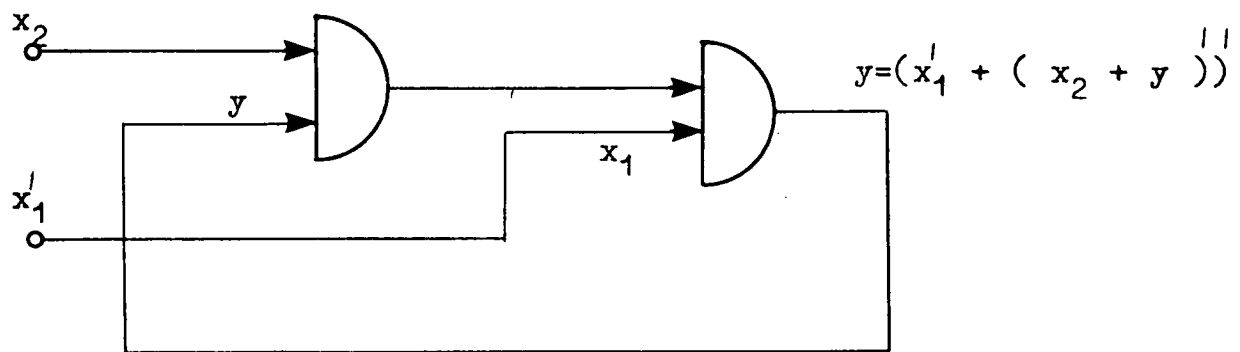
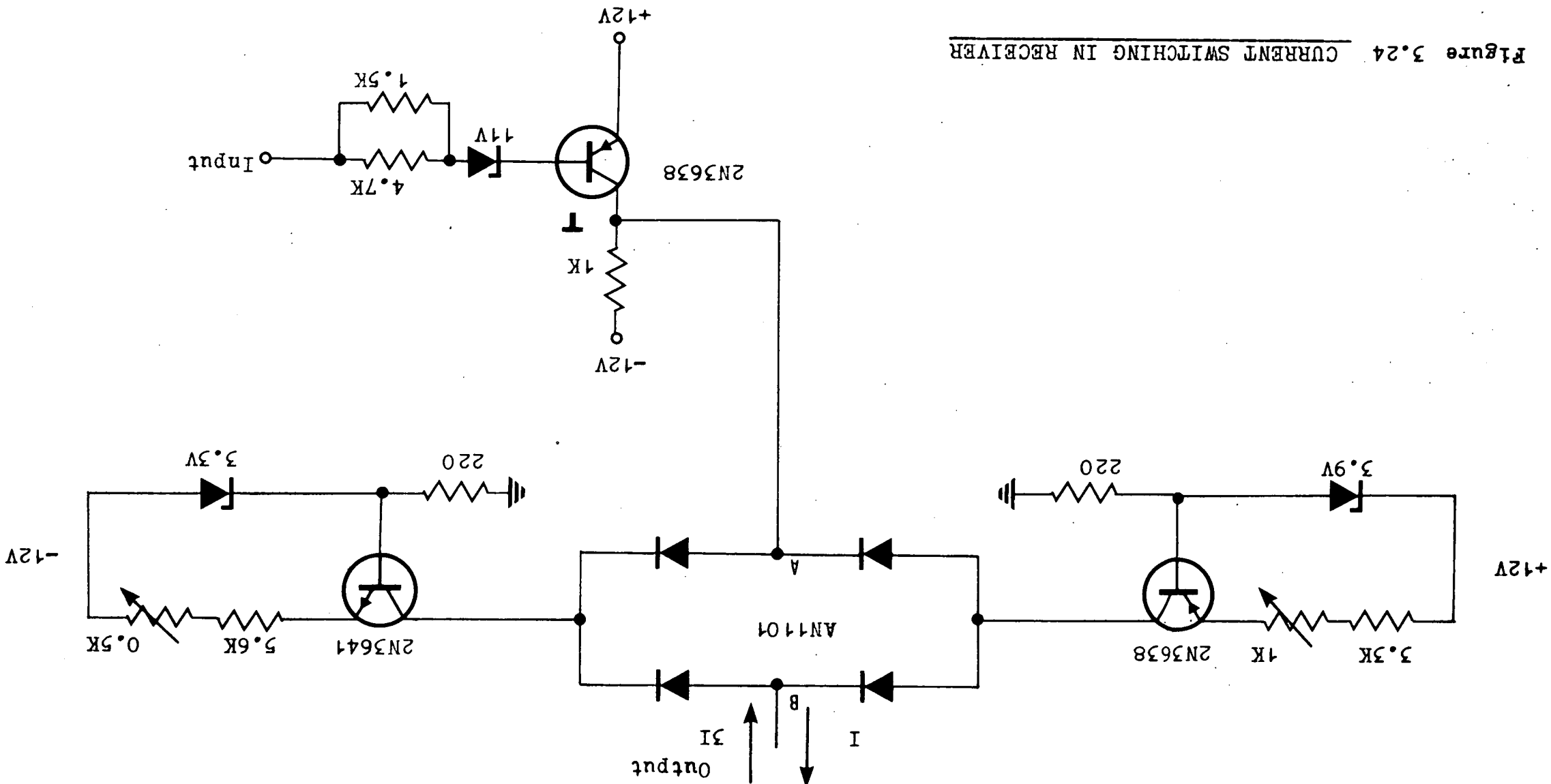


Figure 3.23 REALIZATION OF SEQUENTIAL CIRCUIT

Figure 3.24 CURRENT SWITCHING IN RECEIVER



The phase of the information signal is adjusted so that they overlap the leading edge of the clock pulse at all times. In this way, a simple sequential network can be designed to pass a clock pulse whenever an information pulse is present. The inputs x_1 and x_2 , and the output z are shown in figure 3.22. Appendix C contains the derivation of the circuit, and figure 3.23 shows the circuit.

The output z is the same as the pulse output at the modulator. In this form it can be used to switch weighted currents into an active low pass filter using simple RC networks.

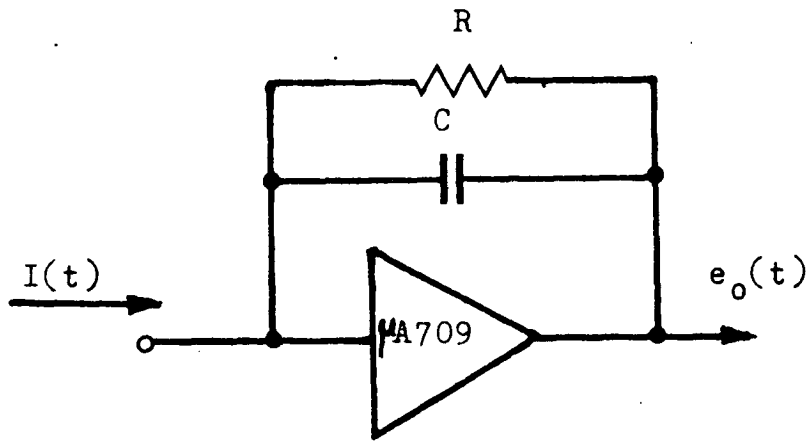
3.3.6 Current Switching

The incoming information pulses operating between 0 and +3.5V are inverted by transistor T (figure 3.24) to approximately +11 V and -11V. These voltages ($\pm 11V$) are required to operate the diode transmission gate, which switches the weighted currents into and out of the low pass filter.

The fixed current values are generated by transistors in the grounded base configuration (figure 3.24) from $\pm 12V$ supplies. Zener diodes are used to supply the bases with $\pm 8V$ respectively.

The value of the voltage at A (the switching voltage) must always exceed the voltage at B for the transmission gate to operate. The voltages at B are generated by the injected currents, and have a maximum value of approximately 5 volts.

The emitter resistances are made variable, so that the current values can be adjusted exactly in the ratio 1 to 3. The currents are nominally 1mA and $\frac{1}{3}$ mA.



(a) Single RC Filter

Transfer Impedance $\frac{e_o(S)}{I(S)} = \frac{R}{(RCS + 1)} \dots \dots (b)$

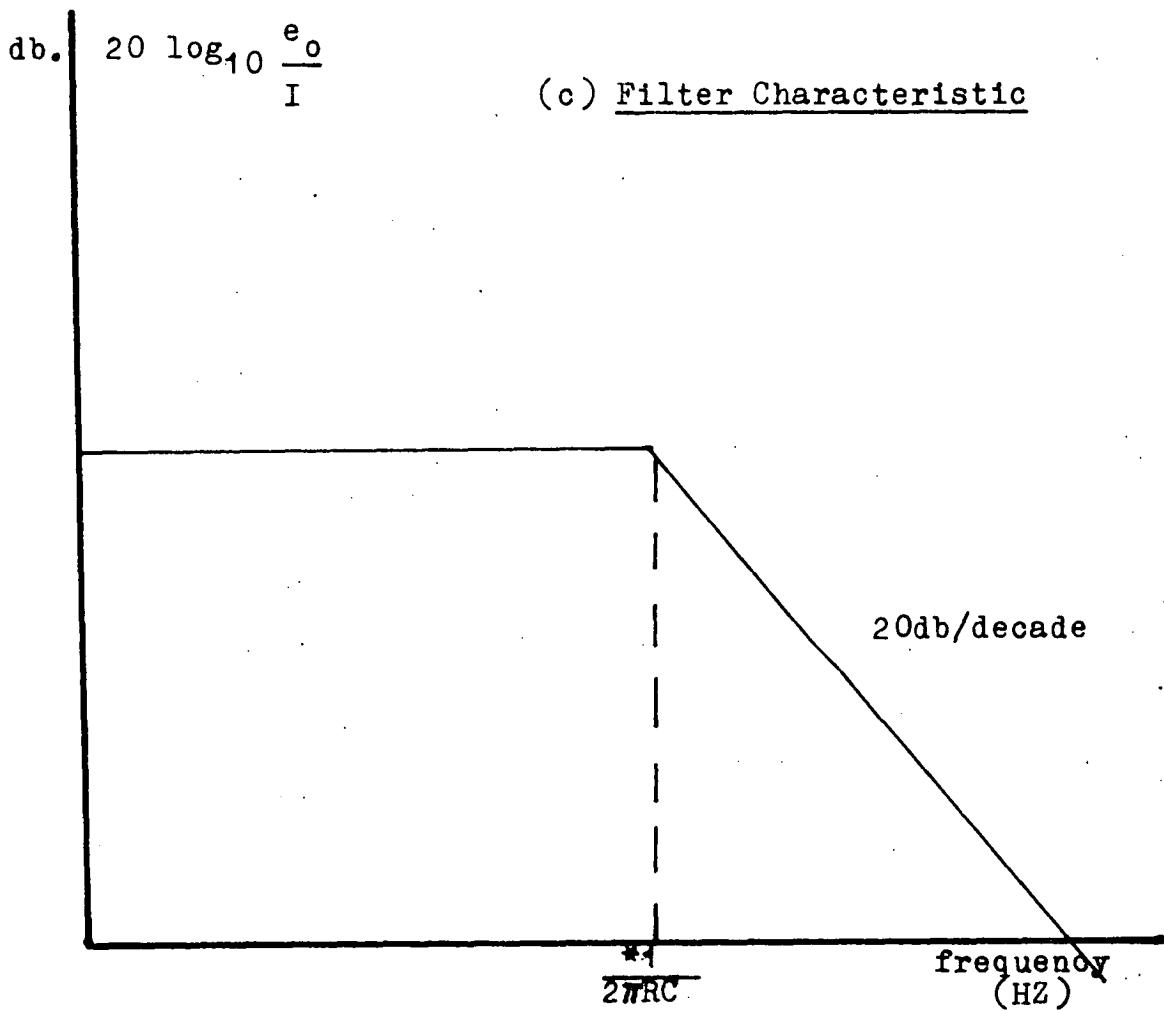
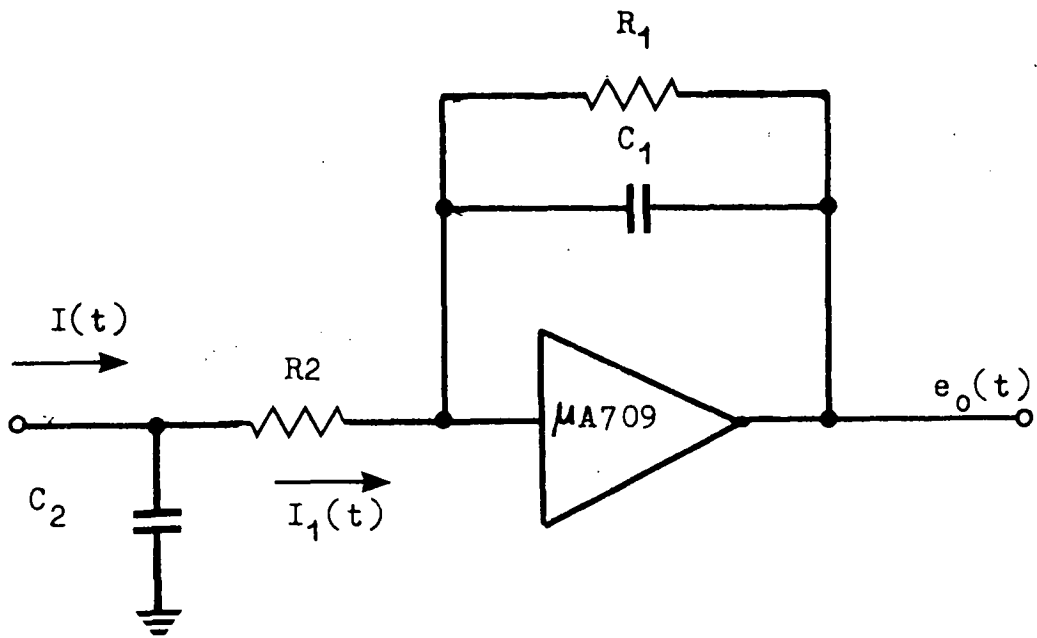


Figure 3.25 SINGLE NETWORK FILTER



(a) Double RC Filter.

Transfer Impedance $\frac{e_o(t)}{I(t)} = \frac{R_1}{(R_1 C_1 S + 1)(R_2 C_2 S + 1)}$ (b)

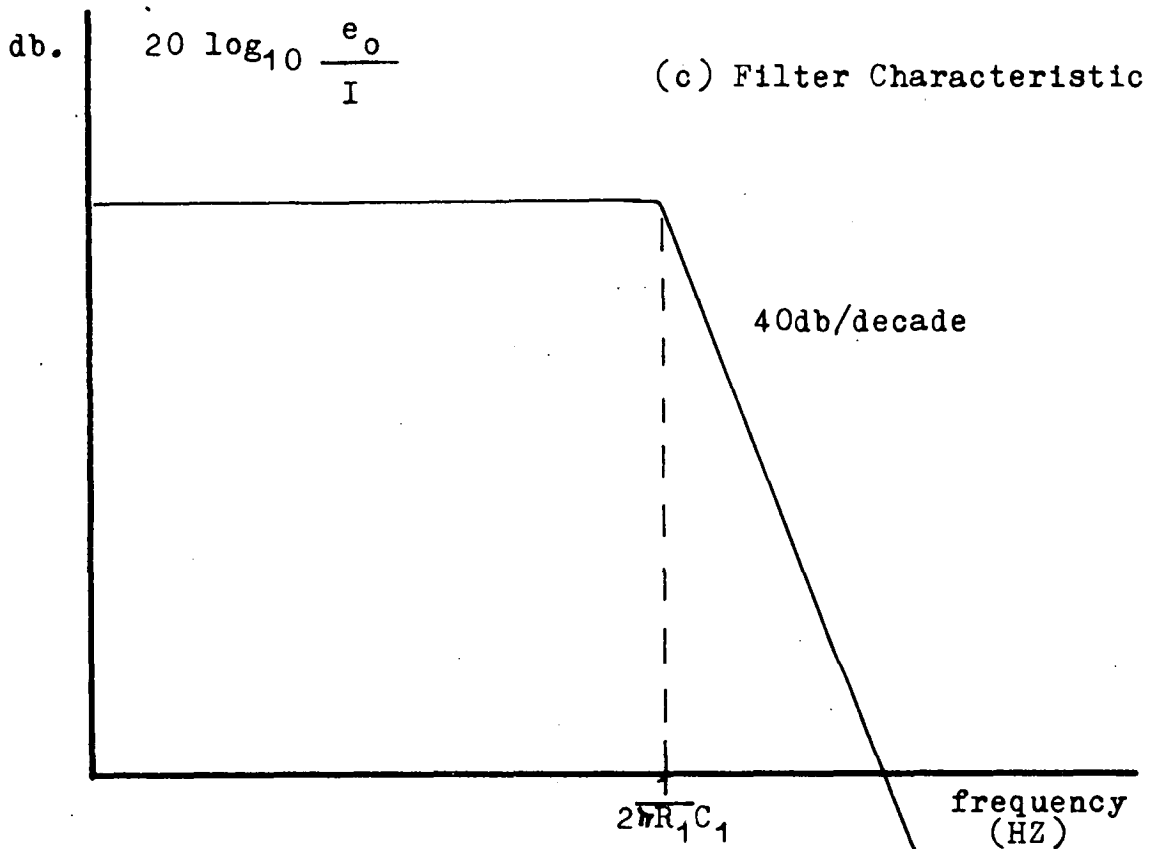


Figure 3.26 DOUBLE NETWORK FILTER

3.3.7 Low Pass Filter

A filter is required with a cutoff frequency, such that it will pass signals at the required transmitted frequencies, and cutoff the quantizing noise to a sufficiently low level. The fundamental frequency of the quantizing noise is 1000 c/s.

The simplest filter to use was a single RC network made active by including it as the feedback loop on an operational amplifier (figure 3.25). With this filter, a demodulated signal with a satisfactory signal-to-noise ratio was obtained for a bandwidth of only 2.5 cycles (0 to 2.5 c/s).

This can be improved upon by using a double RC network*. It produces twice the attenuation of the quantizing noise for a given pole ($1/RC$) than does the single filter. This corresponds in principle to deJager's double integration in his delta modulation system (figure 3.26).

$$I_1(s) = \frac{I(s)}{(R_2 C_2 s + 1)}$$
$$e_o(s) = \frac{R_1 I_1(s)}{(R_1 C_1 s + 1)}$$
$$e_o(s) = \frac{R_1}{(R_1 C_1 s + 1)(R_2 C_2 s + 1)} I(s)$$

$R_2 C_2 = R_1 C_1$ is the optimum condition for a given band-width and maximum attenuation of the quantizing noise produced.

$$\frac{e_o(s)}{I(s)} = \frac{R_1}{(R_1 C_1 s + 1)^2}$$

* The performance can be improved considerably by means of a more elaborate network. However, the design is aimed at simplicity and the network used was confined to the double RC type.

V_{in}/V_{out}

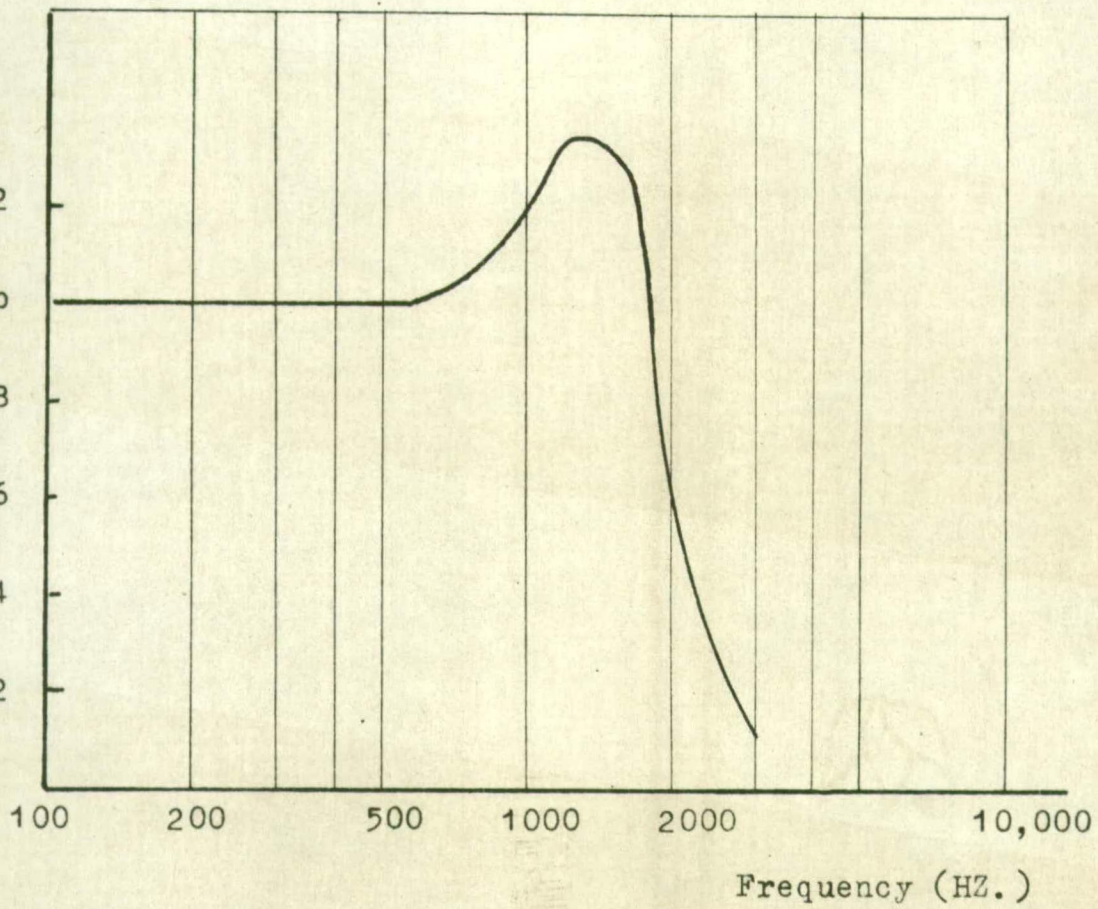


Figure 3.27 CHANNEL SIMULATION FILTER CHARACTERISTIC

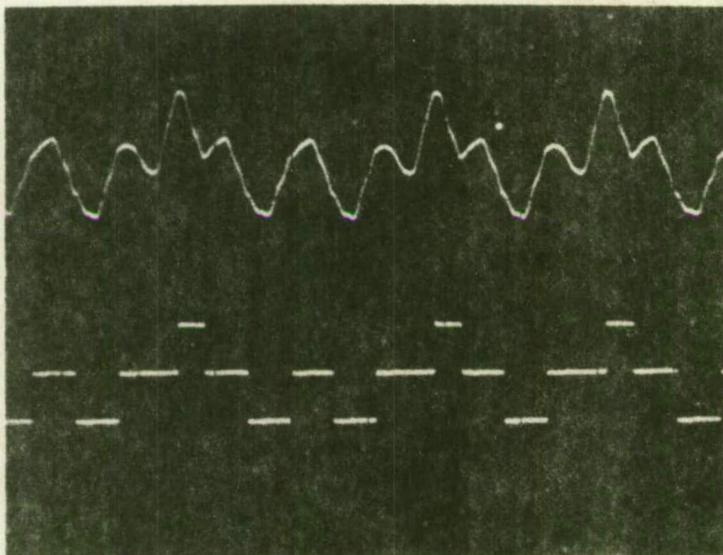


Figure 3.28 CHANNEL OUTPUT AND INPUT PULSES

For a cutoff frequency of 20C/S

$$R_1 = 10K \quad C_1 = 0.79 \mu F$$

$$R_2 = 1K \quad C_2 = 7.9 \mu F .$$

R_1 must be small in order to keep the voltage at B on the transmission gate (figure 3.24) low enough for the gate to operate. R_1 controls the gain and is given a value such that the overall system gain is about unity.

For the same quantizing noise level obtained in the single network case, the double network gives a decade extra bandwidth. An investigation of the signal-noise characteristics appears in a further section.

3.4 CHANNEL SIMULATION

The transmission channel over which this modulation system is to operate is assumed to be band-limited to approximately 2000 C/S. To simulate these operating conditions a low pass filter with characteristics as shown in figure 3.27 was introduced in the line between the modulator and demodulator.

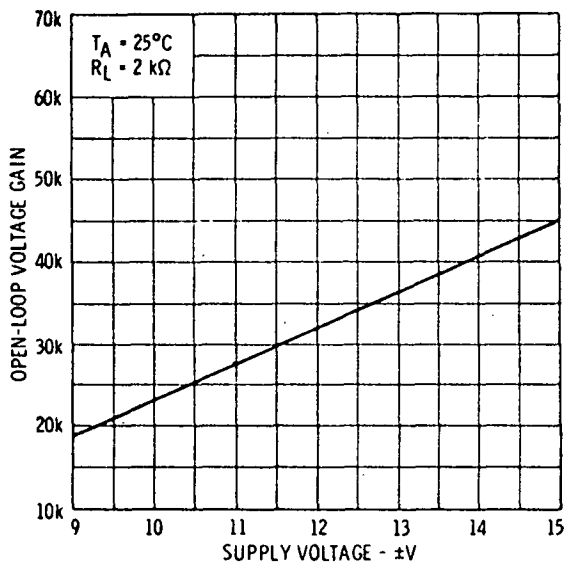
Figure 3.28 shows the pulse input and output of the filter. Pulses received over a transmission line would be distorted in this manner hence the need for regeneration before demodulation.

All tests carried out on the prototype delta-sigma modulator were done with this filter in the circuit.

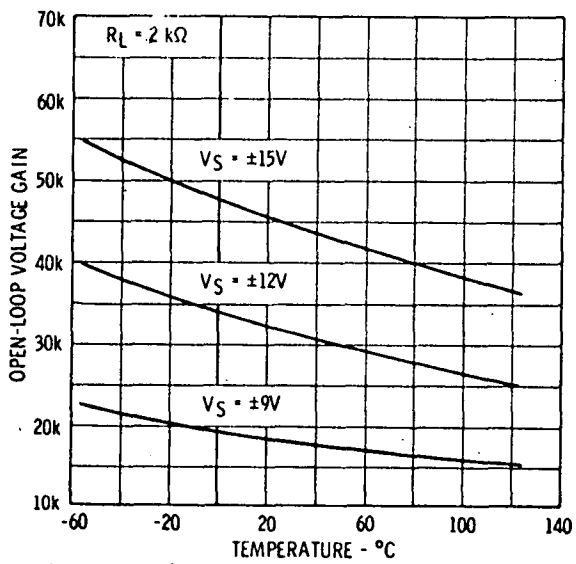
3.5 PERFORMANCE OF SYSTEM

3.5.1 Zeroing and Calibration of Demodulator

Zeroing of the demodulator is easily achieved. The input to the modulator is earthed, that is, the signal to be transmitted is made 0 volts dc. With the receiver and transmitter clocks synchronized (as it always remains,



Voltage Gain as a Function of Supply Voltages.



Voltage Gain as a Function of Ambient Temperature.

Figure 3.29

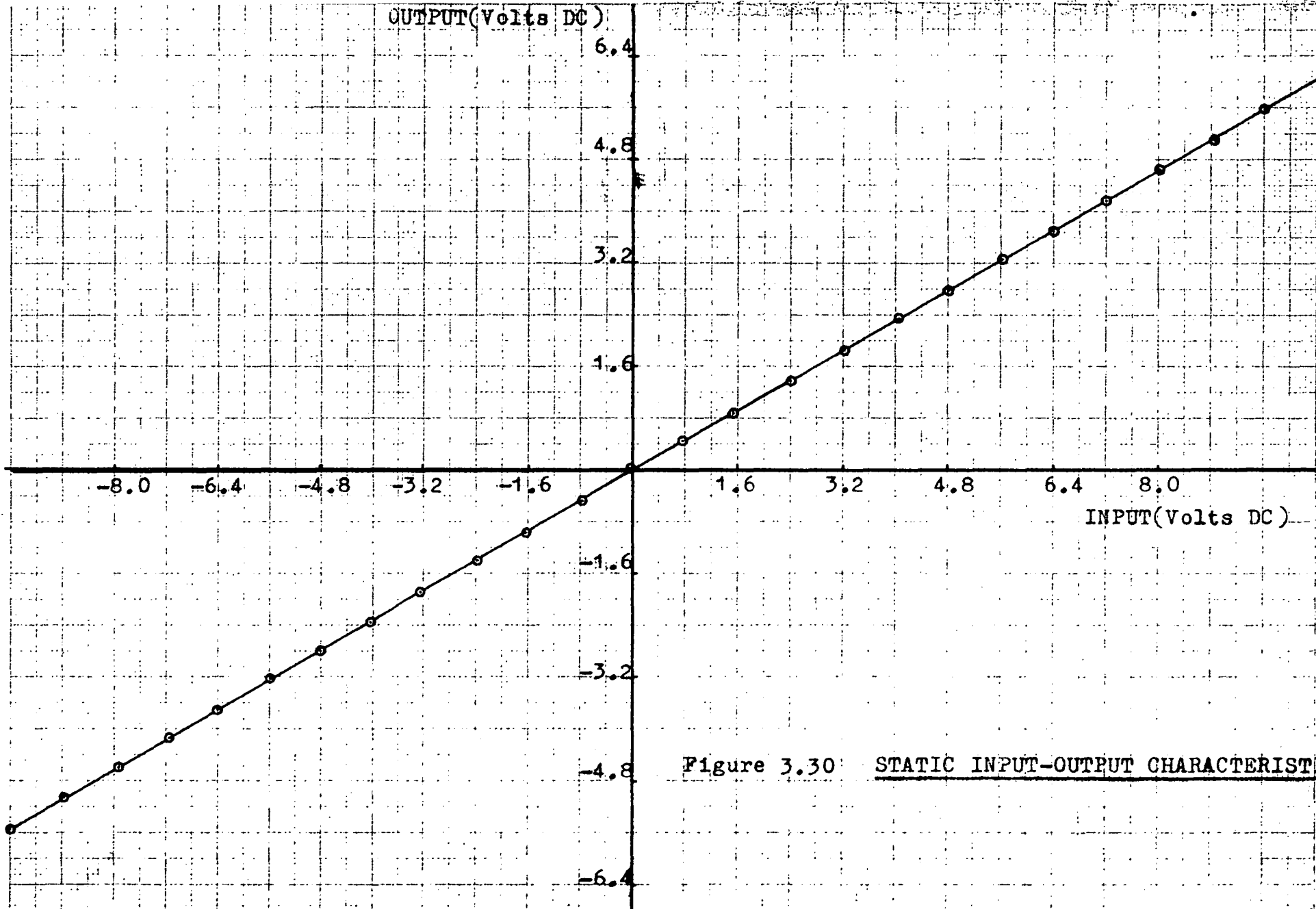


Figure 3.30 STATIC INPUT-OUTPUT CHARACTERISTIC

once adjusted), the weighted currents in the demodulator are adjusted until the output reads zero. This was done, reading the output on a digital voltmeter to an accuracy of 0.01 percent.

This adjustment was necessary often during the experimental development of the circuitry. This was due to variations in the regenerated power supplies which were necessary at times, and to the use of different operational amplifiers in the demodulator low pass filter.

The $\mu 4709$ operational amplifiers have an open loop voltage gain which varies with ambient temperature (figure 3.29). Because of these temperature effects, a calibration run had to be made each time the system was used to counteract the variations obtained in the output. Although this method is functional, it is not practicable, and a chopper stabilized operational amplifier would be preferred in a circuit put to practical use.

3.5.2 Static Accuracy

Figure 3.30 is the input-output characteristic for the delta-sigma modulator system. The slope of the line can be adjusted by varying R_1 in the low pass filter network of the demodulator. The line was plotted by an EAI model 1100-E X-Y plotter. The static accuracy of the pen and arm is 0.075 percent. As the plotter acts as a second filter, the quantizing noise, seen on the CRO trace of the output, is further reduced. The output is also read on a digital voltmeter to 3 digits, in this case, 0.01 volts in $\pm 7\frac{1}{2}$ volts.

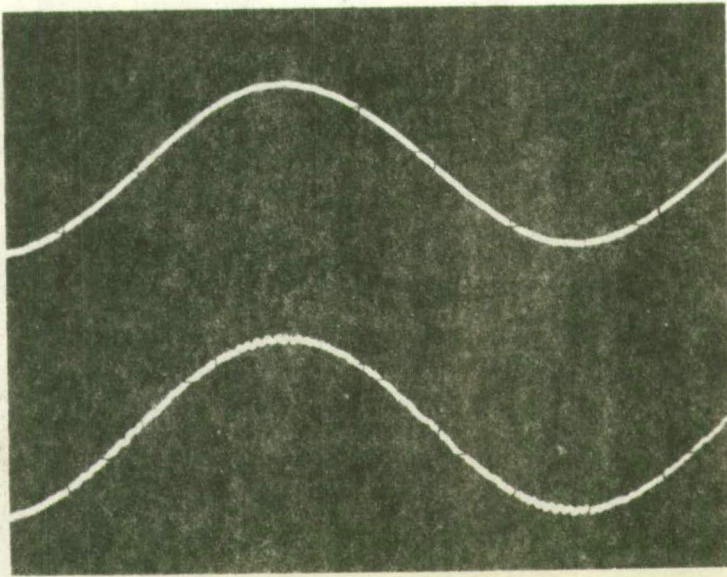


Figure 3.31 INPUT TO MODULATOR(top)
OUTPUT OF DEMODULATOR(bottom)

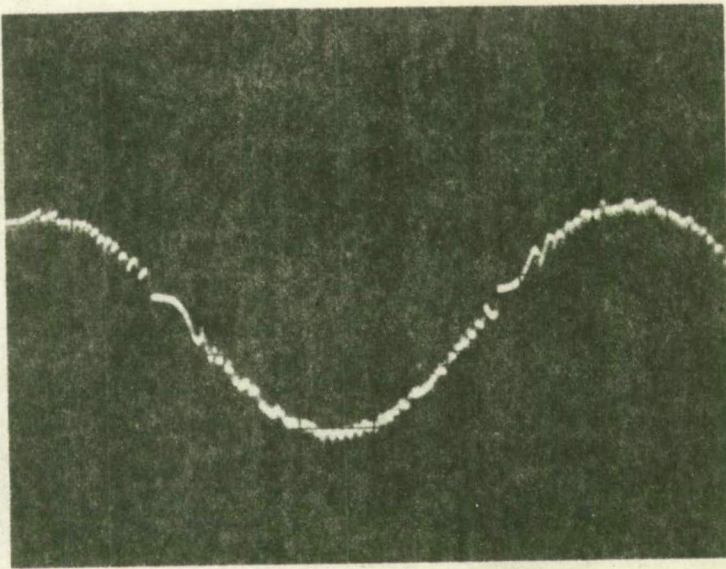


Figure 3.32 OUTPUT 12½ c/s, 3VOLTS PEAK TO PEAK

3.5.3 A.C. Performance

The accuracy at frequencies up to 20 C/S is less than the d.c. accuracies for the same effective value (V_E) of the input signal. Figure 3.31 shows the input to the modulator and the output from the demodulator at a frequency of $12\frac{1}{2}$ c/s and a peak to peak value of 12 volts at the output. It was observed that the accuracy of transmission is affected by the level of the input signal. This is discussed in section 2.3.6 relating to signal-noise properties.

Because of the smaller signal-to-noise ratio at low level signals, the overall accuracy is considerably reduced, compared to the accuracy at high levels. (Improvements of this deficiency in the form of companding are discussed in chapter IV).

The A.C. accuracies were measured on a cathode ray oscilloscope. For low level signals (less than 0.8V r.m.s.) at frequencies between 10HZ and 20HZ, the accuracy was 0.5 percent. At frequencies less than 10HZ it is 0.2 percent, and as mentioned previously, 0.085 percent static accuracy.

This system was designed primarily for d.c. and V.L.F. signals. The accuracy of the system/^{as}it stands could be improved upon considerably with a sacrifice in bandwidth.

The system operates over a band-limited channel (2000 HZ) to the above mentioned accuracies. It employs relatively simple means to modulation and demodulation. From the discussion so far, some advantages of delta-sigma modulation are beginning to emerge.

3.5.4 Observations made on Character of Quantizing Noise

On observing a low level signal, the effect of the quantizing appears as granulation noise (see figure 3.32 and description in section 2.3.6), which, at these low levels,

Figure 3.34 OUTPUT 12% c/s, 12VOLTS PEAK TO PEAK

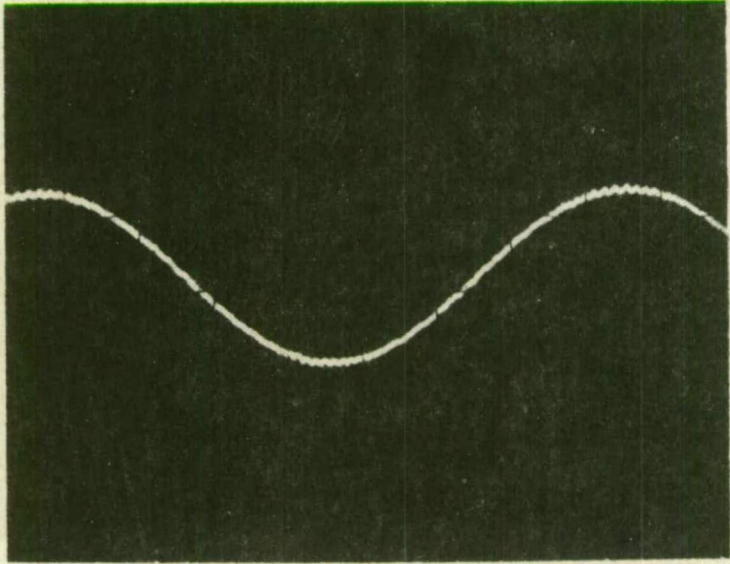
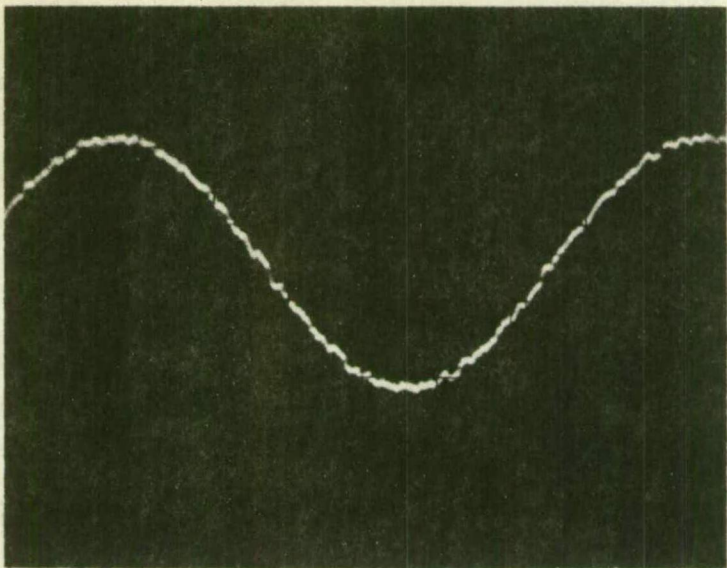


Figure 3.33 OUTPUT 12% c/s, 7 VOLTS PEAK TO PEAK



reduces the a.c. accuracy. Figure 3.33 shows the same frequency with a greater peak to peak value (7V), and figure 3.34 an even higher level still (12V). The reduction in the effect of the granulation noise with the increase in signal level can be seen. This variation of granulation noise with signal level observed here, verifies that result derived by Zetterberg⁽⁷⁾ and shown in section 2.3.6.

Overloading noise, which for any given system would occur more at high level A.C. signals, was almost non-existent in this system. As the r.m.s. value of the signal was increased, the effect of the granulation was reduced, and a stage was reached at which granulation was small and overloading became apparent. With a further increase in the r.m.s. value of the signal the modulator soon saturated. At this stage the input signal is beyond the design value of the system.

To overload the system without reaching saturation was not possible. In order to attempt this the frequency must be increased at an r.m.s. value below saturation. However, the cut-off frequency of the output filter would not allow an overloading frequency to be transmitted.

It can be said that, for the specified ranges of amplitude and frequency, the system cannot be overloaded. All limitations of accuracy due to quantizing noise come from granulation.

3.6 MEASUREMENT OF SIGNAL-TO-NOISE RATIO

To investigate the signal-to-noise ratio only the double RC network filter will be considered.

V_E = effective value of the modulation signal,

V_K = quantizing step.

3.6.1 deJager's Approximate Method

Use is made of deJager's⁽⁴⁾ result which states:

The system can transmit a random signal with power spectral density function $\Phi(f)$ with no overloading if the amplitude of the signal does not exceed the maximum amplitude that can be transmitted at a frequency f_3 , where f_3 is given by

$$f_3 = \frac{\int_0^{f_2} \Phi(f) f^2 df}{\int_0^{f_2} \Phi(f) df},$$

and f_2 is the maximum frequency to be transmitted.

Consider the system described in this chapter under the above conditions for a random signal of a given power spectral density function $\Phi(f)$. If this single frequency f_3 is transmitted for varying values of V_E until overloading begins to occur, an evaluation of granulation noise in the form of signal-to-noise ratio for various V_E/V_K can be obtained.

DeJager compared the signal to noise ratio in a delta system with those in amplitude limited systems. His comparison suggests that it is justifiable to consider the signal-to-noise ratio for a sine wave of f_3 cycles per second as a representative of the signal-to-noise ratio of the given power spectral density function $\Phi(f)$.

To apply this result to delta-sigma modulation, use is made of the relationship existing between the two as shown in section 2.1.3.

If the power spectral density function is that of band-limited white noise (figure 3.35), then the power spectral density function at the input to the delta section is given by

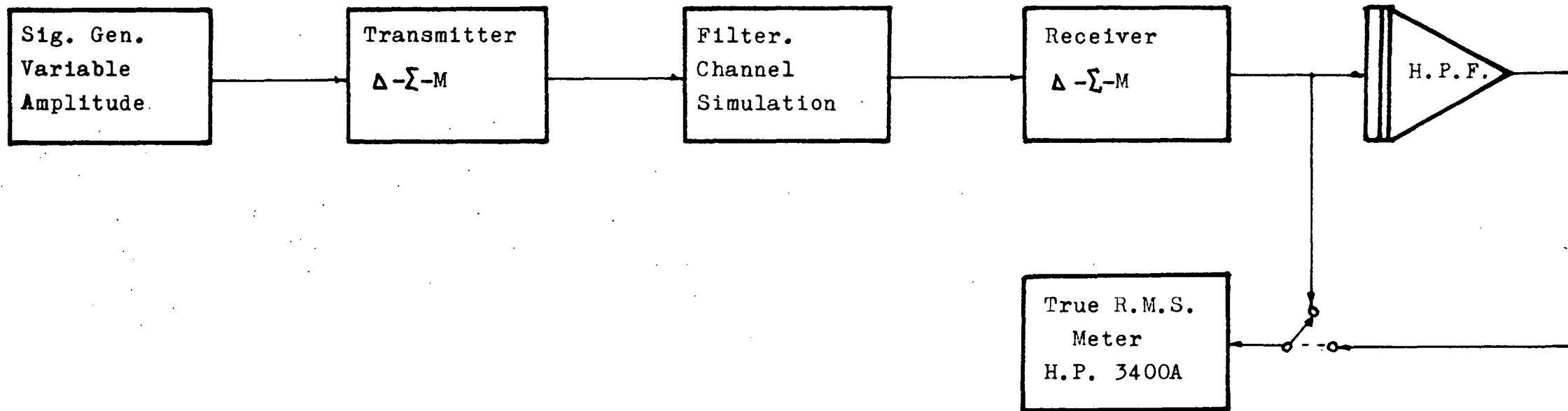


Figure 3.36 ARRANGEMENT FOR MEASURING SIGNAL-TO-NOISE RATIO VERSUS V_E/V_K

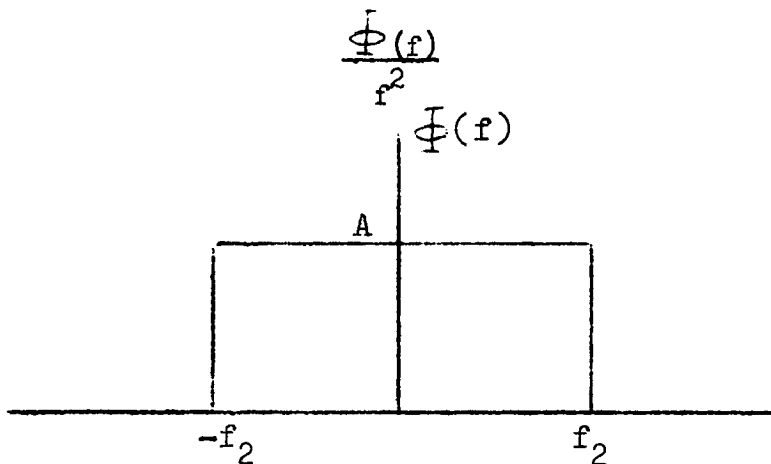


Figure 3.35 POWER SPECTRAL DENSITY FUNCTION

The equivalent f_3 corresponding to $\frac{\Phi(f)}{f^2}$ is

$$f_3^2 = \frac{\int_0^{f_2} \frac{\Phi(f)}{f^2} f^2 df}{\int_0^{f_2} \frac{\Phi(f)}{f^2} df}$$

$$= f_2^2$$

This result can be extracted directly from the result derived in deJager's⁽⁴⁾ appendix.

By transmitting a single sine wave of frequency f_2 over the delta-sigma system, an evaluation of the signal-noise properties until overloading can be obtained.

A signal of frequency 15HZ was transmitted, and the output signal to noise ratio measured for varying V_E . For the purposes of measurement,

$$\frac{S + N}{N} \approx \frac{S}{N}$$

as the noise power is small compared with the signal power.

Figure 3.36 shows the arrangement used for measuring signal to noise ratios. To measure the noise power, most of which occurs at the fundamental 1000 HZ and at 500 HZ, the low frequency must be filtered out, leaving the noise signal (granulation) which is measured on a true r.m.s.

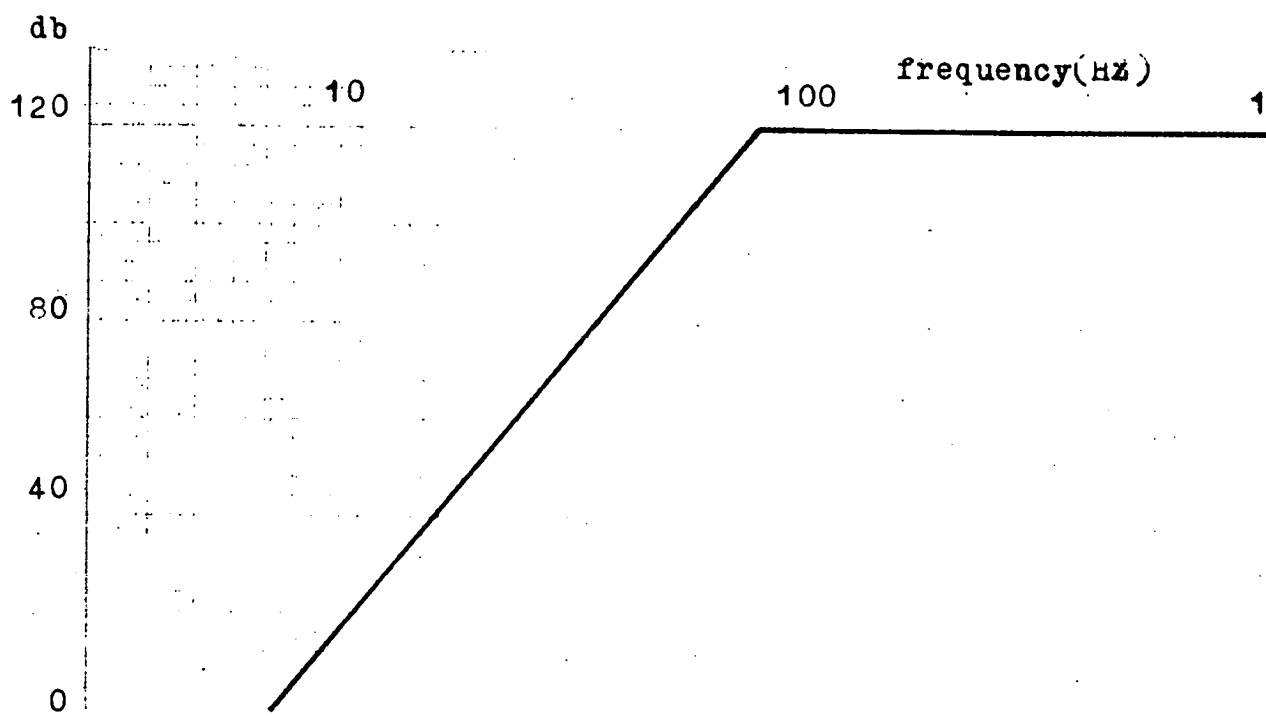


Figure 3.37(i) HIGH PASS FILTER CHARACTERISTIC

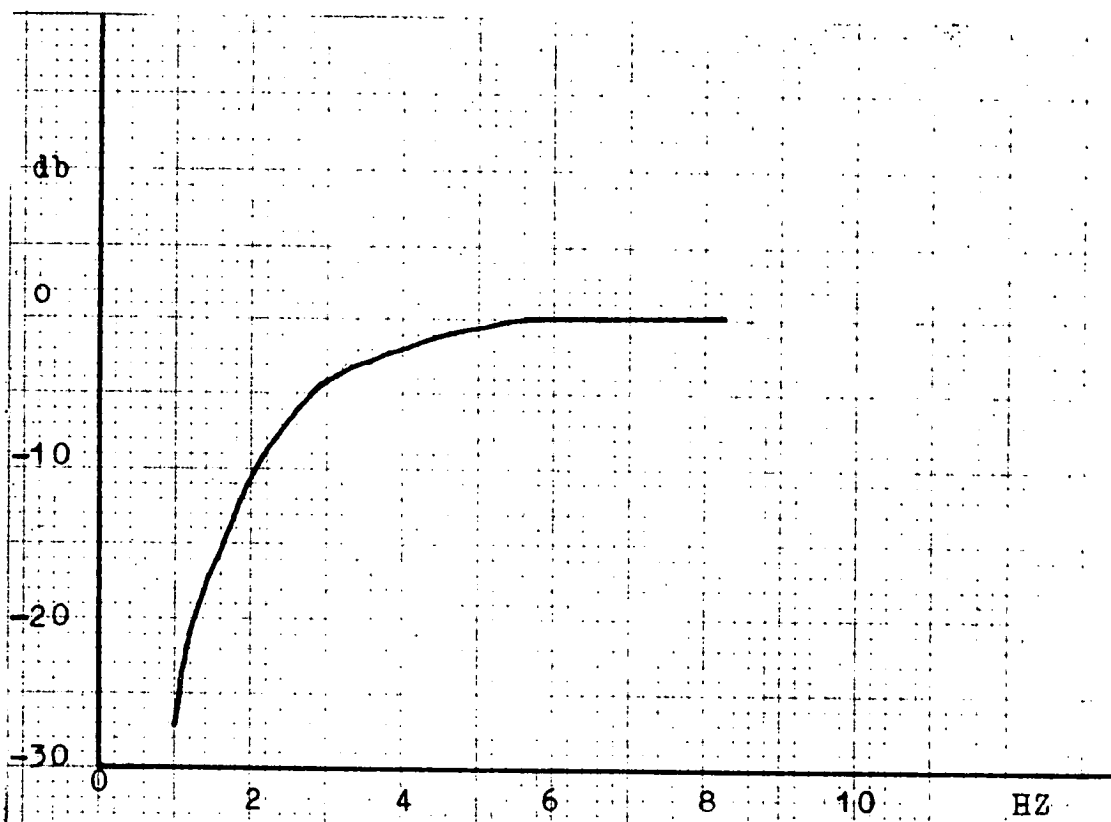


Figure 3.37(ii) TRUE R.M.S. METER RESPONSE

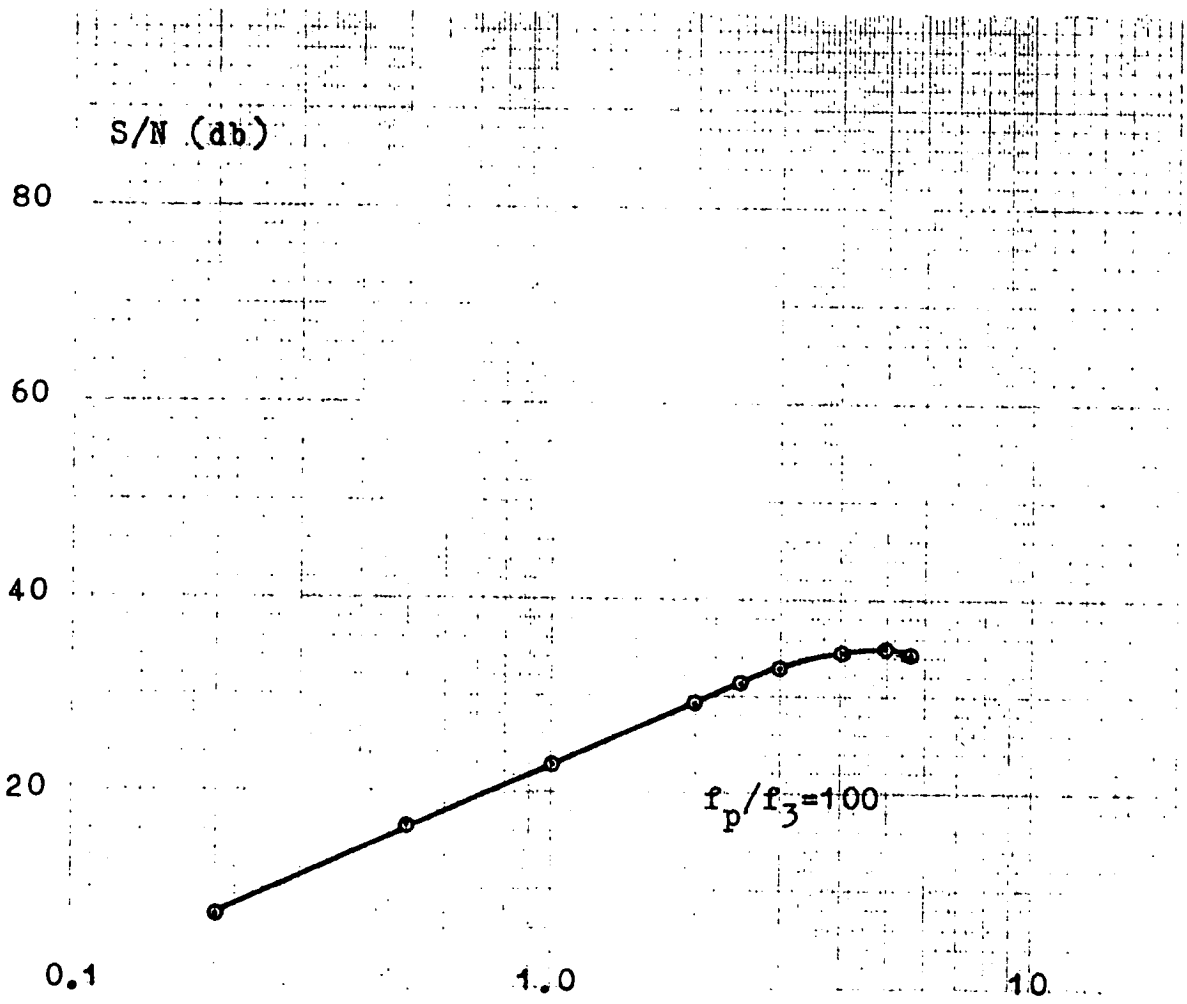


Figure 3.38 S/N VERSUS V_E/V_K FOR TEST SIGNAL (FIRST METHOD)

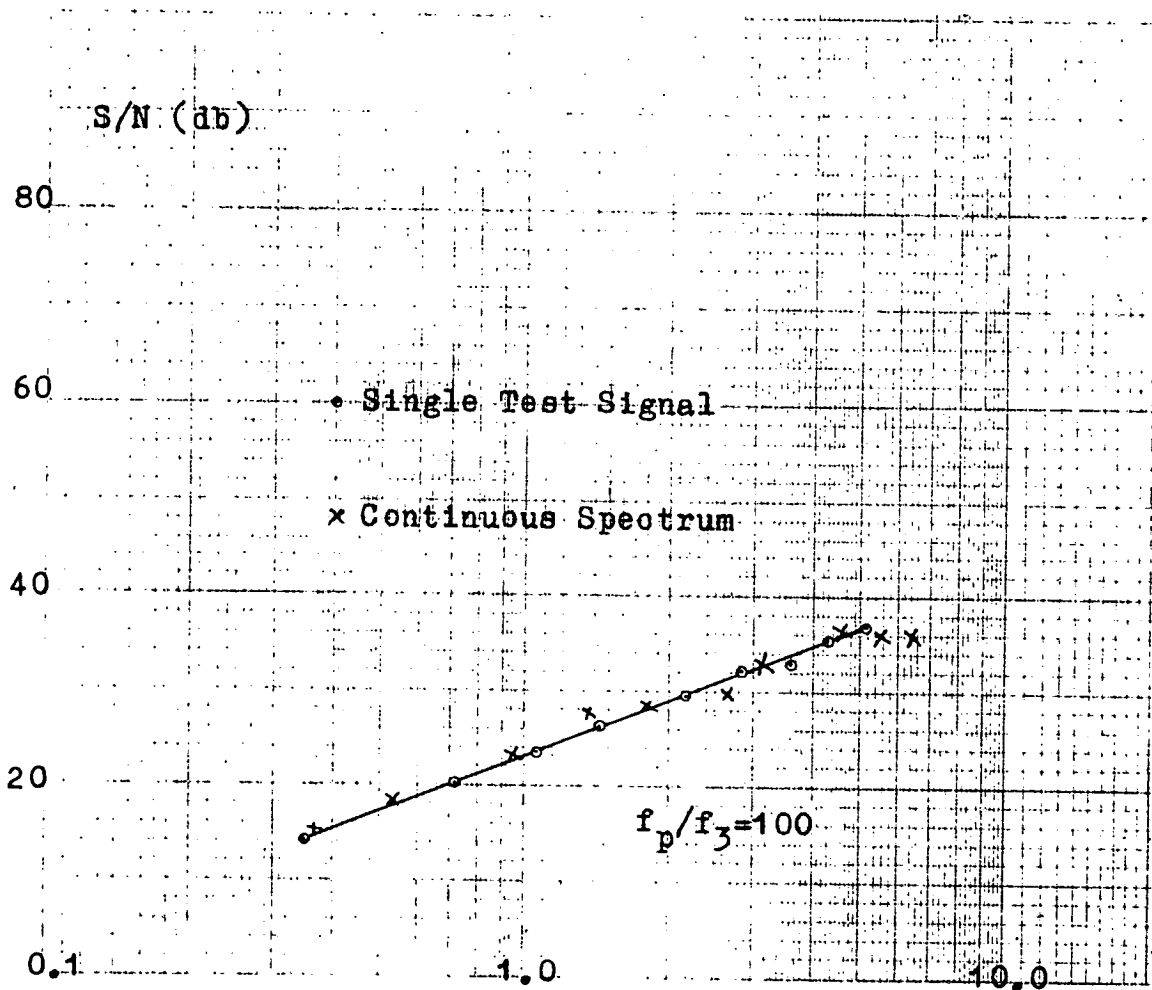


Figure 3.42 S/N VERSUS V_E/V_K (SECOND METHOD)

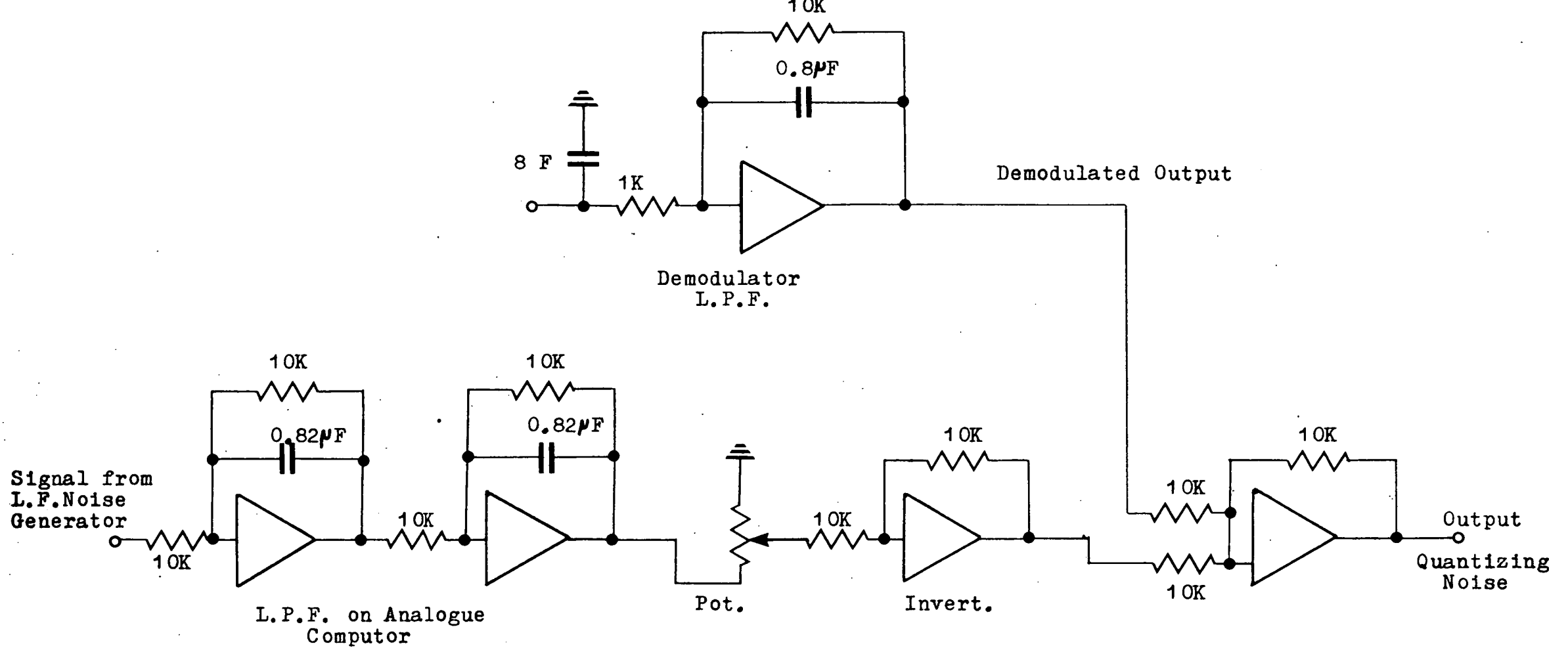


Figure 3.39 ARRANGEMENT FOR MEASURING SIGNAL-TO-NOISE RATIO(SECOND METHOD)

meter. Figure 3.37 shows the high pass filter characteristics and the r.m.s. meter response.

Measurements were taken over the range of operation of the system. The curve of figure 3.38 shows signal-to-noise ratio (db) versus V_E/V_K . The curve is logarithmic up to a value of 3.5 for V_E/V_K , then overloading begins to have effect and the curve turns downwards. At this stage the system saturates.

The quantitative effects of the quantizing noise on static signals must be considered in a different manner. This is done in section 3.7.

3.6.2 Direct Measurement of Signal-to-Noise Ratio

Figure 3.39 shows the second arrangement for measuring signal-to-noise ratio. A low frequency noise generator is used as the signal source. The power spectral density function of the noise generator is shown in figure 3.40. This spectrum is further band-limited by a low pass filter (figure 3.41) to give a power spectrum the same as that in figure 3.35.

In figure 3.39, the two filters on the analogue computer have the same time constants as the RC networks in the demodulator low pass filter. This is done to give the same phase shift to the signal from the generator, as the demodulated signal experiences. By doing this, the two signals can be subtracted to give the quantizing noise remaining. The potentiometer is necessary in order to make the two signals have the same level.

The quantizing noise is measured on the Hewlett Packard 3400A true r.m.s. meter. The output signal must be measured by two separate meters. The HP r.m.s. meter

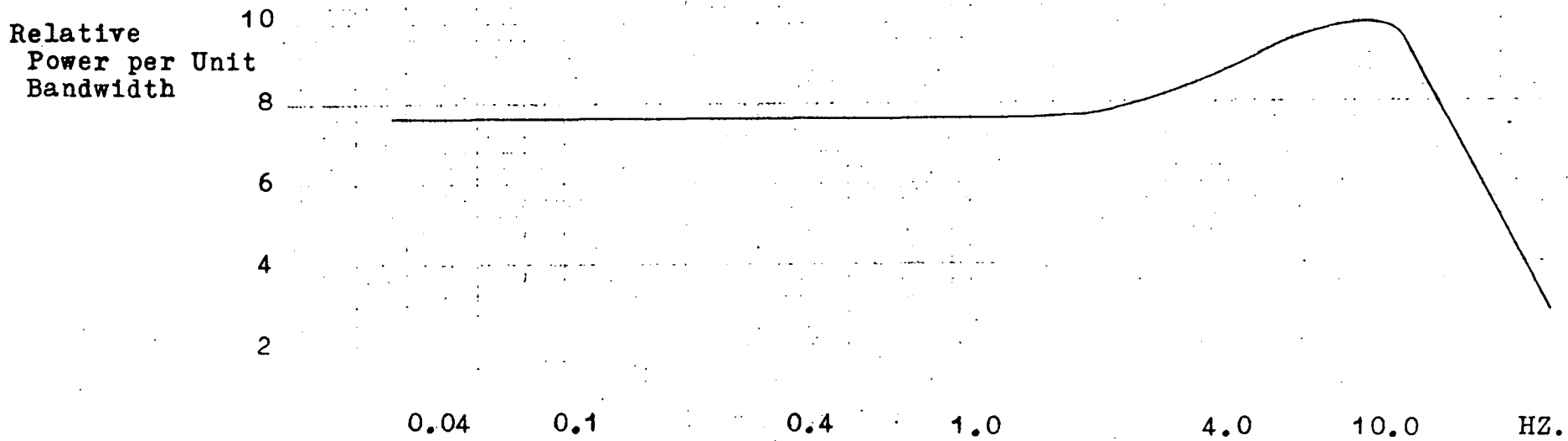


Figure 3.40 POWER SPECTRAL DENSITY FUNCTION L.F. NOISE GENERATOR

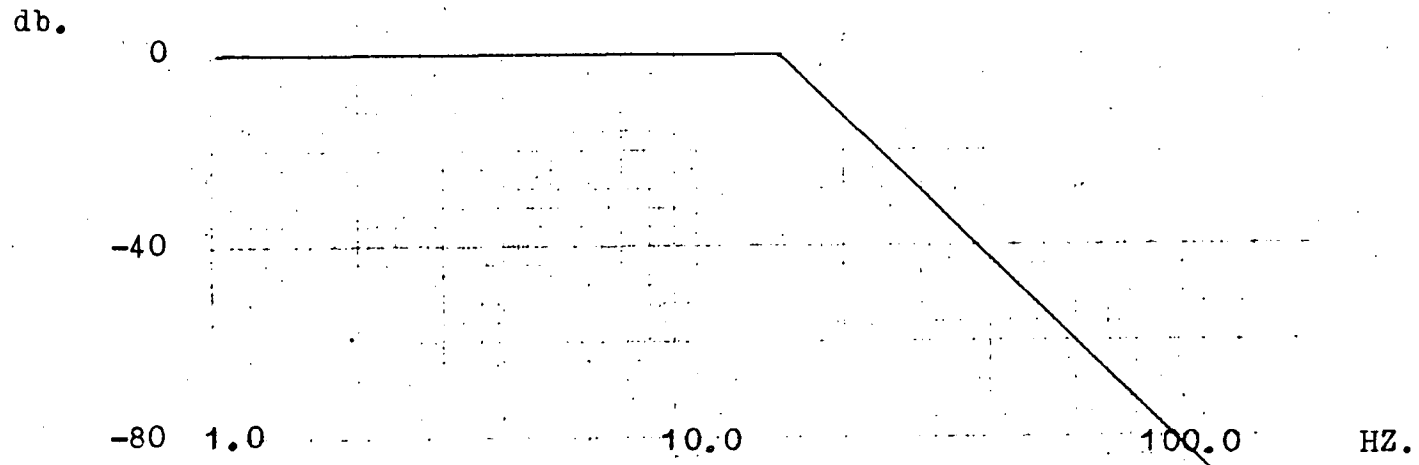


Figure 3.41 FILTER RESPONSE FOR BAND LIMITING L.F. NOISE GENERATOR

is used to give the contribution of the a.c. components of the signal (> 3 cycles per second in this case) and an average reading meter is used to obtain the contribution by the dc components of the signal. In this way the r.m.s. value of the signal can be measured.

$$V_{\text{RMS}} (\text{total}) = \sqrt{V_{\text{dc}}^2 + V_{\text{rms}}^2}$$

Figure 3.42 shows S/N (db) versus V_E/V_K . This curve compares favourably with those obtained for the single test signal.

The measurements for the test signal (15 C/S) were carried out a second time using this second method of measurement. The two curves were found to coincide. (figures 3.38 and 3.42).

Figure 3.42 shows signal-to-noise ratio for the continuous spectrum and the curve for the second single frequency test. These two differ very little. This verifies the fact that deJager's assumptions about the use of f_3 as a representation of the spectrum are valid for delta-sigma modulation.

3.7 QUANTIZING NOISE ON STATIC SIGNAL

In order to quantitatively describe the signal-noise properties for a static signal, the r.m.s. value of the quantizing noise was measured and plotted against the d.c. level received.

On measuring static values at the output of this system, a second filtering occurs, as an average reading meter is essentially a filter. The meter eliminates virtually all the quantizing noise and hence reads the true dc output.

The r.m.s. value of the noise was measured on a Hewlett Packard true r.m.s. voltmeter (model 3400A). The d.c. signal was measured on a Hewlett Packard digital voltmeter, to an accuracy of 0.1 percent.

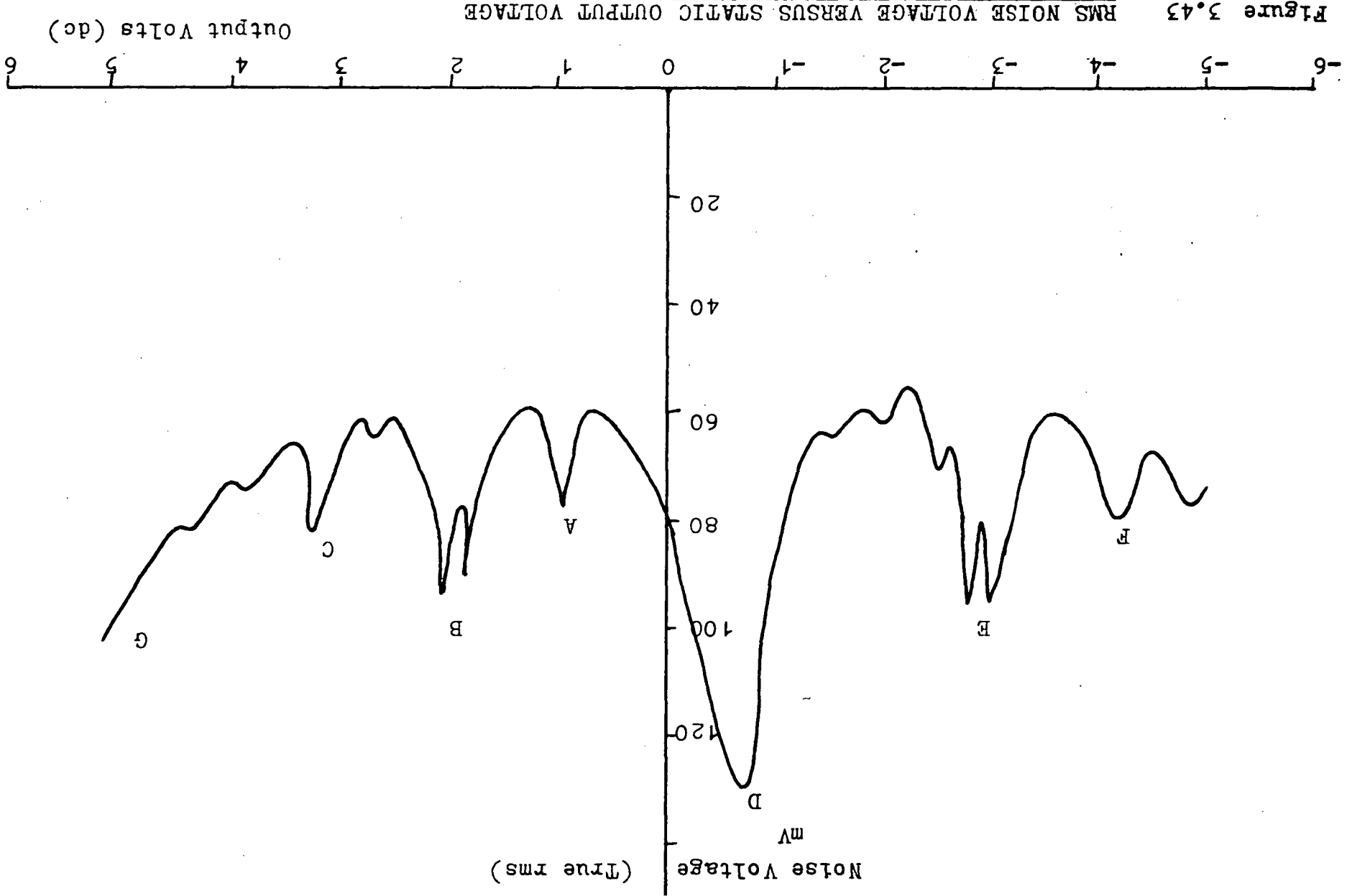


Figure 3.43

If the dc signal transmitted is to be read directly, the reading device will act as a filter, and the accuracy will depend on the meter accuracy. If the signal is to be fed to some other system, where it will be processed or used to regulate some mechanical devices, usually it will still come to a point where it will be filtered, either mechanically or electrically. The quantizing noise is not going to interfere to any great extent with accuracy. It will contribute to the "quality" of the signal only.

Figure 2.43 shows the variation in quantizing noise with dc level. The peaks A, B, C, D, E, F correspond to particular pulse patterns. These patterns were for relatively small periods. (less than six clock pulses). For larger periods the troughs occurred (that is low frequency components dominate).

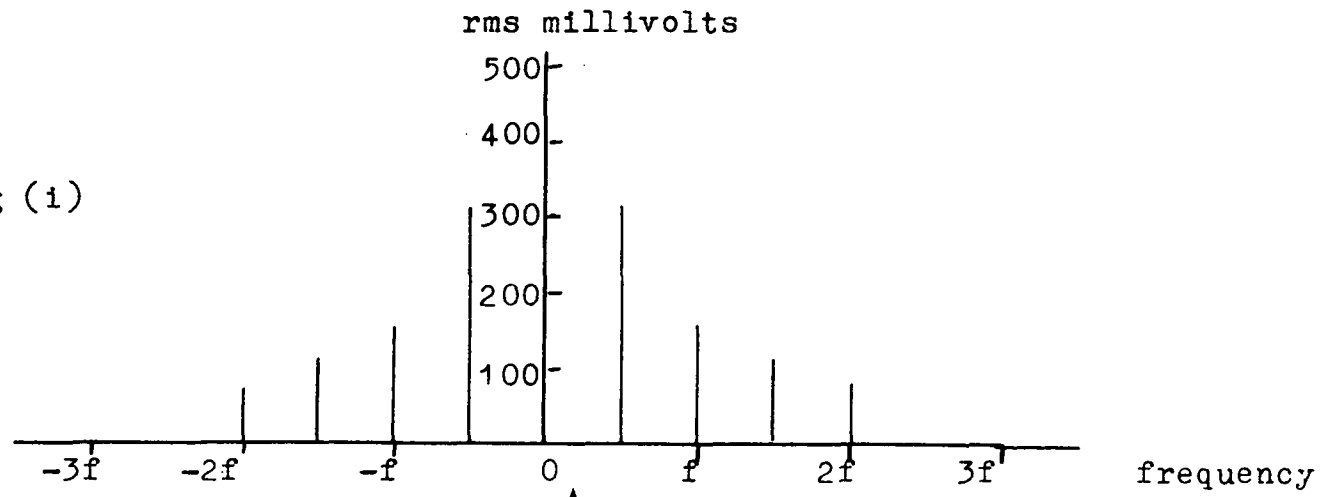
The waveforms of the peaks A, B, C, D, E, F are illustrated in figure 3.44 and the corresponding fourier series given in appendix E. This analysis is done in order to explain the nature of the quantizing noise and show exactly what filtering is required in order to improve the performance (section 4.2).

From the appendix the rms values of the unfiltered waves are tabulated below.

| Peak | A | B | D | E | F |
|--------|--------|-------|--------|--------|--------|
| r.m.s. | 0.706A | 0.74A | 0.564A | 0.497A | 0.366A |

For the unfiltered waves, the r.m.s. value increases with the number of pulses present over a fixed interval of time. In order, the peaks are F, E, D, A, B, C. These waveforms are passed through a low pass filter having the characteristics of figure 3.26.

Before Filtering (i)



After Filtering (ii)

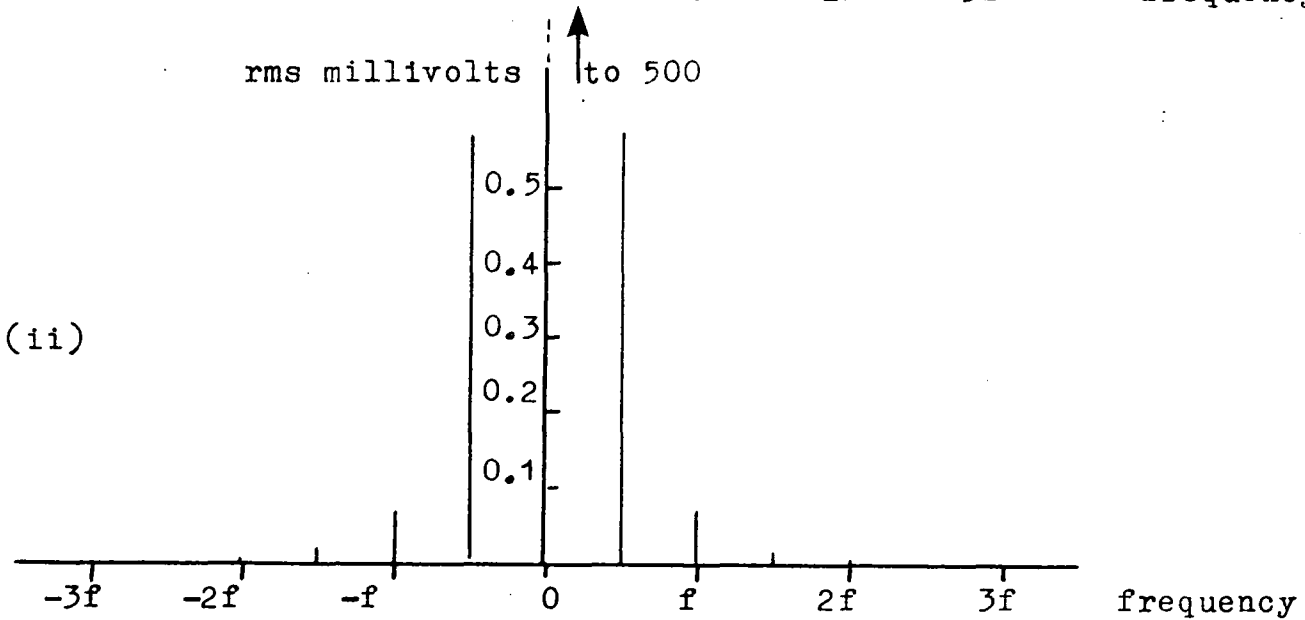
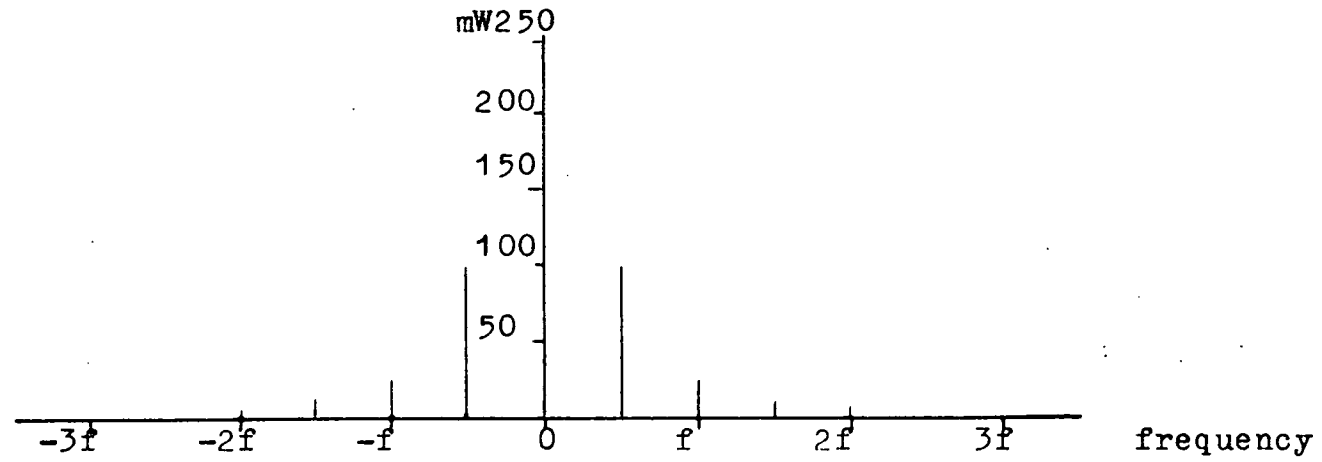


Figure 3.45(i) VOLTAGE SPECTRUM BEFORE AND AFTER FILTERING FOR PEAK D

Before Filtering (i)



After Filtering (ii)

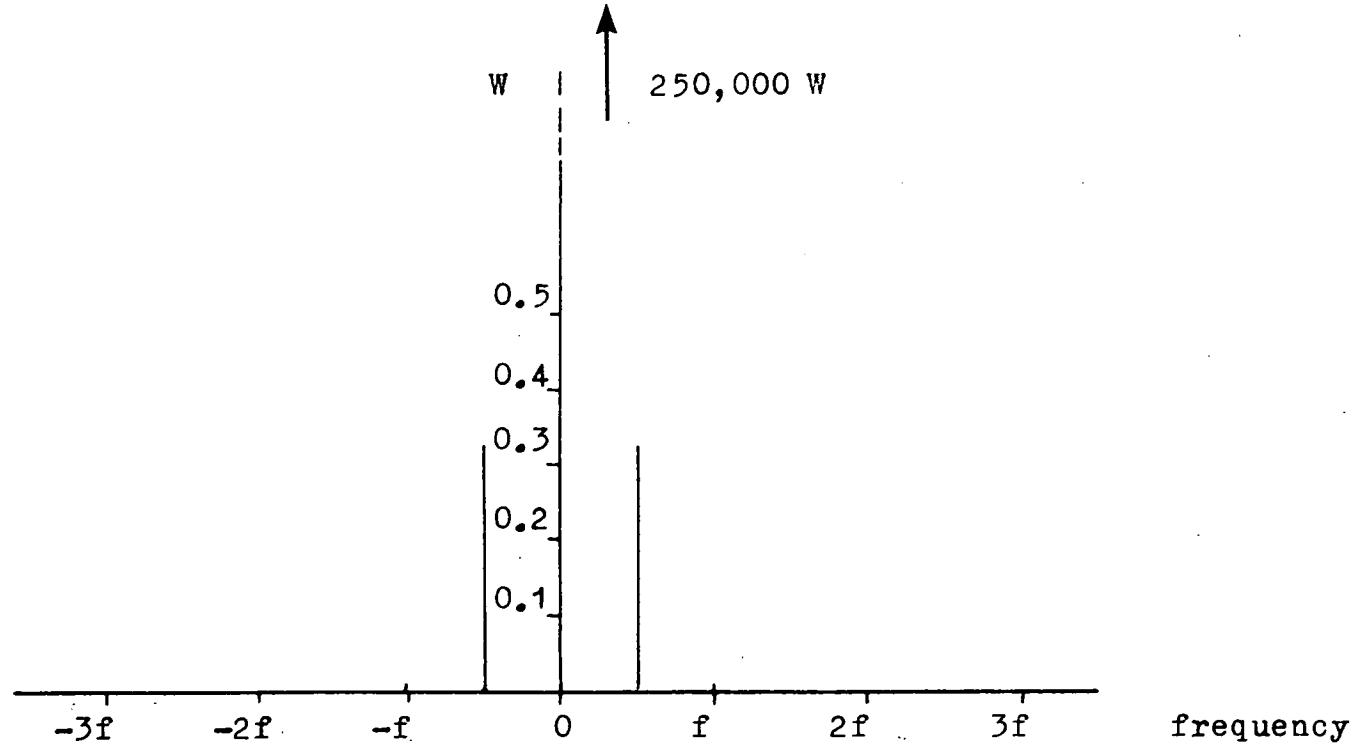


Figure 3.45(i) POWER SPECTRUM BEFORE AND AFTER FILTERING FOR PEAK D

On examining the expression for B and D peaks, it will be noted that a majority of the B components are at a higher harmonic (of the clock pulse fundamental $\frac{2\pi}{T_1}$) than the majority of the harmonics of D. Therefore, on filtering, the rms value of B is reduced proportionally more than the rms of D. It is for this reason that D stands out above the rest of the peaks and that the graph (figure 3.43) has the irregular pattern, rather than a steadily increasing pattern from left to right.

At G, all the clock pulses are present and the maximum r.m.s. value occurs before and after filtering. This is when the system has saturated.

Where-ever this system is used, generally there will be a second filtering stage which will reduce the quantizing noise further. Figure 3.43 of r.m.s. noise volts versus d.c. output is investigated further. The spectrum of D (worst case) is plotted. Figure 3.45(i) and (ii) shows r.m.s. volts and power spectrums before and after filtering.

| f | $\frac{1}{2}f_1$ | f_1 | $1\frac{1}{2}f_1$ | $2f_1$ | 0 |
|------------------------|------------------|-------|-------------------|----------|--------|
| before atten (V) | 0.318 | 0.159 | 0.106 | 0.079 | 0.5 |
| after atten (vM) | 0.57 | 0.071 | 0.0166 | 0.0088 | 500 |
| α | 560 | 2250 | 6400 | 9000 | 1 |
| power before (mW) | 101.0 | 25.4 | 11.2 | 6.2 | 250 |
| power after (μ W) | 0.325 | 0.005 | 0.00028 | 0.000077 | 250 mW |

The figure shows the relative power contained in each harmonic. It is clear that the quality of the signal can be improved by removing the component at half the clock fundamental ($f_p/2 = 500$ Hz).

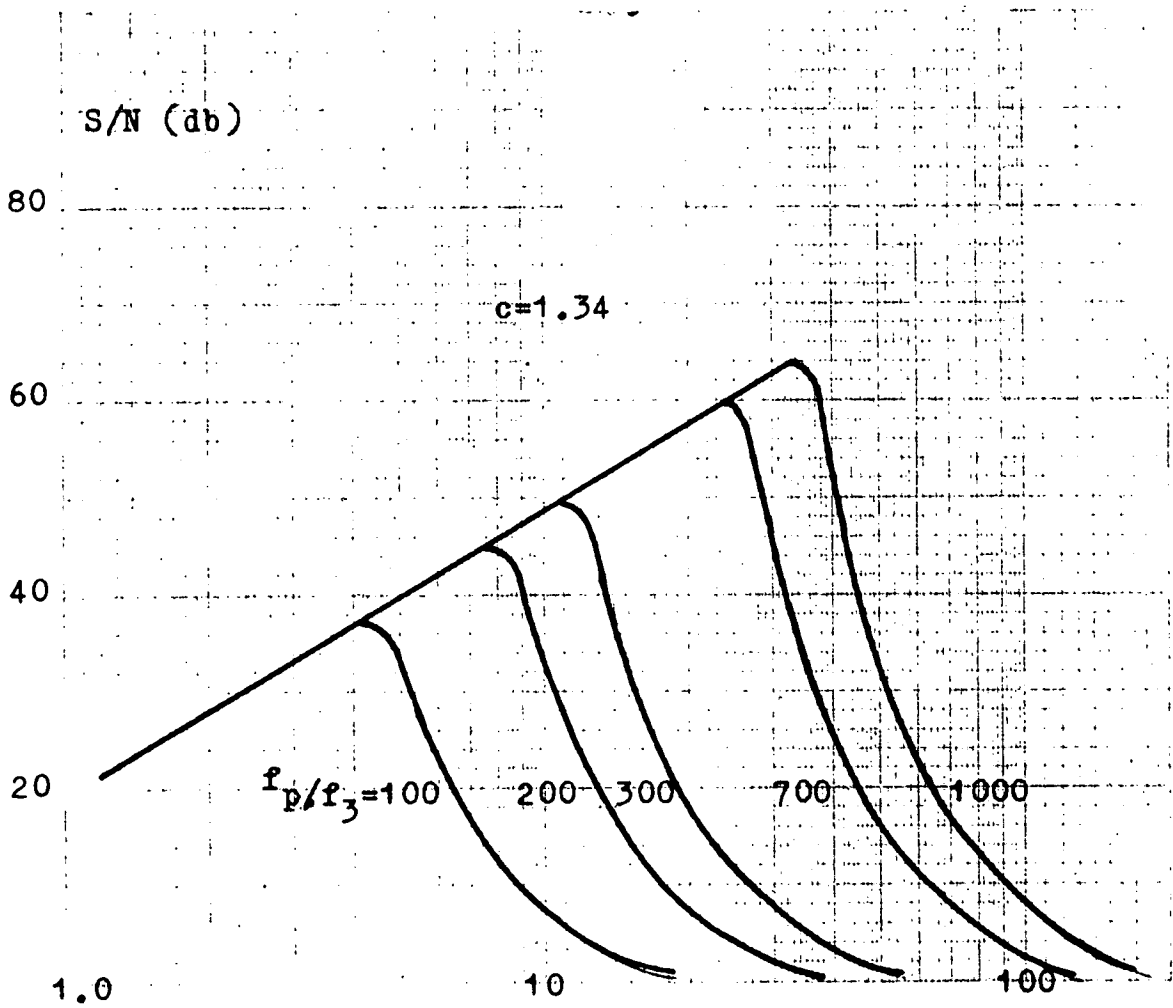


Figure 3.46 S/N VERSUS v_E/v_K FROM THEORY

3.8 COMPARISON OF THEORETICAL AND MEASURED SIGNAL-NOISE PROPERTIES

To compare the measured results of signal-to-noise ratio with theoretically derived values, reference is made to results obtained by Zetterberg⁽⁷⁾. These have already been discussed in section 2.3. Zetterberg obtained the two independent values of quantizing noise power, overloading and granulation respectively.

$$N_o = \frac{\Psi_o}{35 \pi^{3/2}} \frac{A(as_1)}{y^5 c^2} e^{-y^2}$$

$$N_g = \frac{2 \Psi_o K}{(2 \pi)^3} \sqrt{\frac{2}{\pi}} \frac{(f_2 - f_1)}{f_3} \left(\frac{V_K}{V_E} \right)^3, \quad K = \sum_{n=1}^{\infty} \frac{1}{n^3}$$

where Ψ_o , V_E , V_K , y , C , f_1 , f_2 , f_3 , as_1 are as stated previously in chapter II.

If Ψ_o/N_o and Ψ_o/N_g , the signal-to-noise ratios for overloading and granulation respectively, are represented by PSIO, PSIG and the total signal-to-noise ratio in PSIT, then

$$PSIT = \frac{|PSIO| + |PSIG|}{|PSIO| + |PSIG|}$$

Appendix D contains the Elliott 503 program which was used to find PSIT for various power spectral density functions $\Phi(f)$, for different clock frequencies f_p , and for maximum frequency transmitted f_2 .

Figure 3.46 shows the theoretical results for signal-to-noise ratio versus V_E/V_K for different f_p/f_3 . These curves are for a random signal $f(t)$, with power spectral density function $\Phi(f)$ as shown in figure 3.35. In this case, $f_1 = 0$ and the expression for S/N is simplified.

The measured curves of figures 3.38 and 3.42 have the same characteristics as the analytical curve of figure 3.46. Observation of a cathode ray trace of the signal, whilst plotting the experimental curve, revealed when granulation dominated and when it was negligible. These points corresponded to those in theory.

Granulation and overloading noise values are equal very near the peak of the curve in figure 3.46. This occurs when both are small, granulation having nearly disappeared and overloading just beginning with increase in V_E/V_K . The slope of figures 3.38 and 4 2 is slightly different to that of figure 3.46, but the difference is never greater than 3db. The maxima occur within one quarter of a cycle of one another.

3.9 CONCLUSIONS

The delta-sigma modulator described here is a practical telemetering system suitable for time-division-multiplexing.

To multiplex such systems would require high speed sampling of a number of the digital signals (all synchronous) produced by the modulator. In addition synchronizing pulses would be necessary.

It has been shown in a practical case that delta-sigma, and consequently, delta modulation are suitable modulations for the transmission of static and low frequency signals.

CHAPTER FOUR

OTHER CONSIDERATIONS OF DELTA MODULATION

4.1 INTRODUCTION

Chapter III describes a system which will transmit static signals to an accuracy of 0.1 percent or signals up to 20HZ to an accuracy of 1 percent (with a maximum signal-to-noise ratio of 35 db). If greater accuracies and improved signal-to-noise ratio were required, some improvement to the existing system would be necessary. Some methods of doing this are suggested in this chapter.

The improvements to the delta system suggested involve only a small amount of additional circuitry. Any elaborate improvements or drastic changes in principle, involving a considerable amount of additional circuitry, would eliminate the major asset of delta modulation, simplicity.

One of the more elaborate methods of improving the signal-to-noise ratio is the use of "companding". This is discussed for delta modulation in the form of "continuous delta modulation".

Factors which govern the choice of modulation (considering PCM and DM) are given broad consideration in order to convey the relative merits of the two systems.

Mentioned briefly is the use, either locally or remotely, of delta modulation as a analogue-to-digital converter.

4.2 SIMPLE METHODS OF IMPROVING THE PERFORMANCE OF EXISTING SYSTEM

In order to improve the performance of the delta-sigma modulator without making any changes of the principles involved, the following alterations could be made.

- (i) Increased sampling frequency and decreased quantizing step.
- (ii) Improved filtering at the demodulator.
- (iii) Conversion to the "Manchester Code".

By increasing the sampling frequency and reducing the size of the quantizing step, the granulation error is reduced. (section 2.3). This improves the signal-to-noise ratio, but also increases the bandwidth required. Whether the bandwidth can be afforded, depends on the application.

Improved filtering at the demodulator, in the form of rejection filters for frequencies f_p , $f_p/2$, $f_p/3$, would greatly enhance the accuracy of A.C. signals. (It has already been shown that most of the granulation noise is due to these divisions of f_p). The static accuracy would be virtually unaffected, as the reading of the static signals is done with a low pass filter.

The application of the "Manchester Code" to the system simplifies the clock regeneration considerably. There is always an edge of the signal pulses corresponding to the leading edge of the clock pulse.

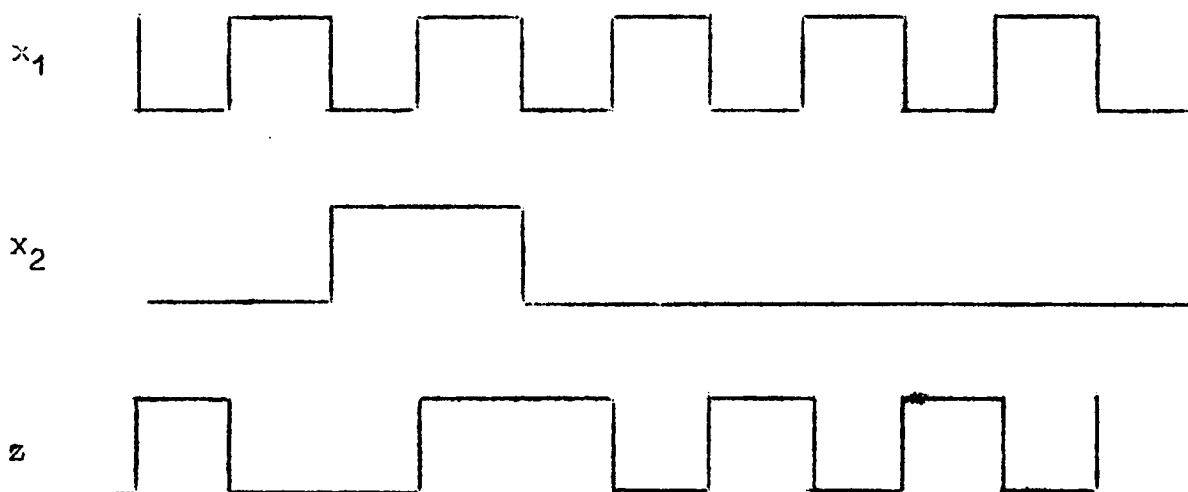


Figure 4.1 MANCHESTER CODE

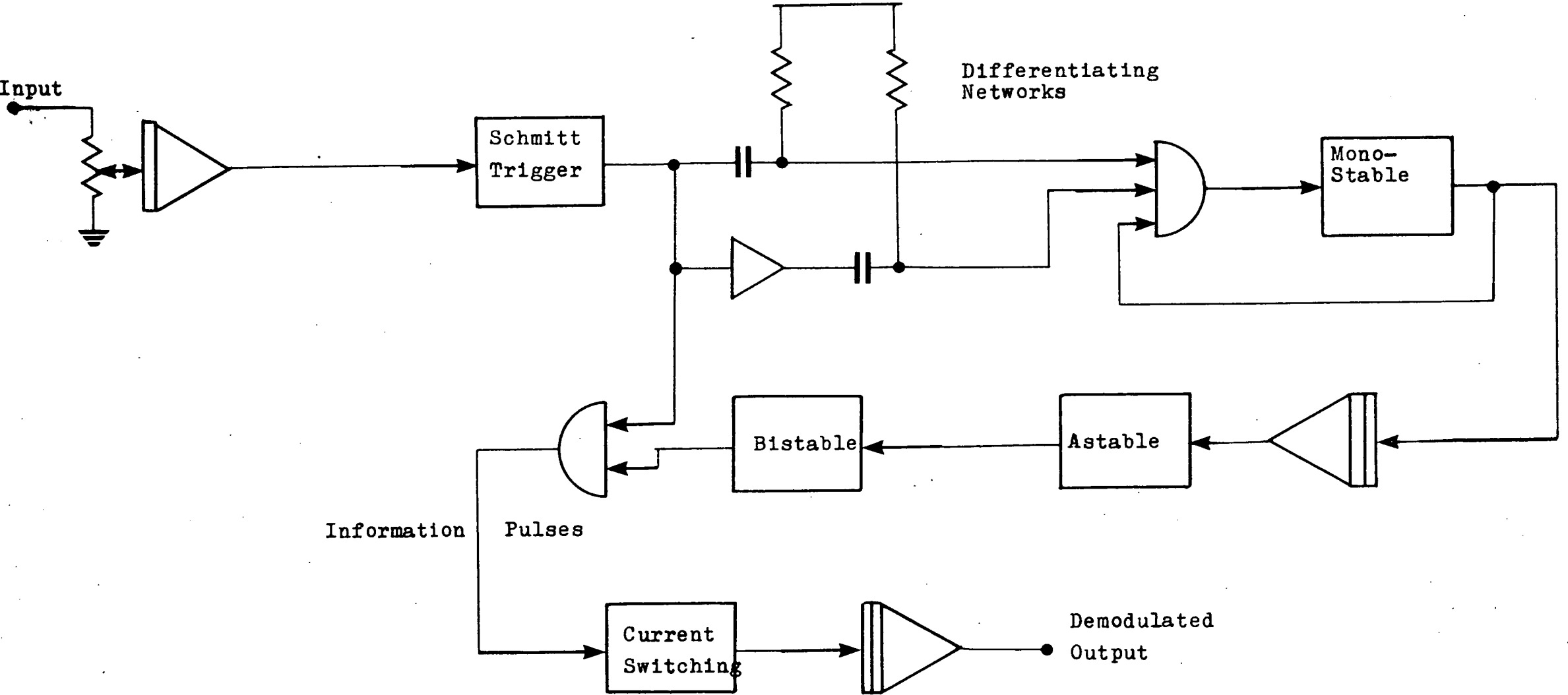


Figure 4.2

BLOCK DIAGRAM OF DEMODULATOR USING MANCHESTER CODE

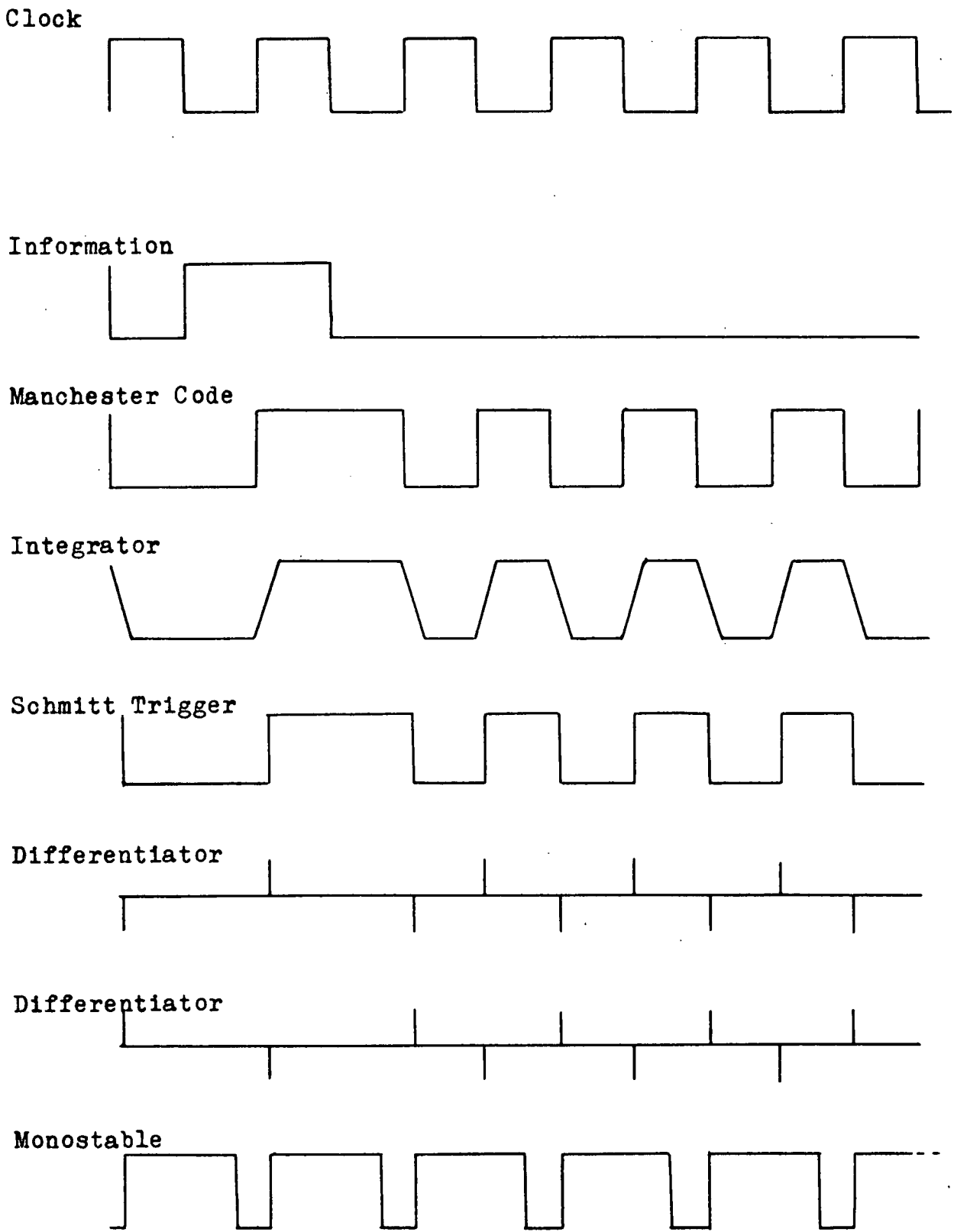


Figure 4.3 WAVEFORMS FOR MANCHESTER CODE

The Manchester Code is best described by figure 4.1.

X_1 is the clock pulse, X_2 the information output from the sequential circuit, and z the Manchester Code output. Appendix G contains the derivation of a sequential circuit which converts X_2 and X_1 to z . This can be done by using an "exclusive OR" gate which is contained in one Fairchild RT μ L 9908 integrated circuit.

Figure 4.2 is a block diagram for a demodulator using the Manchester Code. Figure 4.3 shows the waveforms for block diagram 4.2. The received Manchester Code is integrated to recognize the presence of the pulses. The integrated output operates a schmitt trigger, the output of which is differentiated and inverted then differentiated. These two quantities are fed to an 'OR' gate the output of which operates a monostable-multivibrator. The monostable is fed back to the 'OR' gate to control the differentiating spikes coming through. As figure 4.3 indicates, there is a monostable pulse occurring every leading edge of the clock pulse. This is filtered to give a dc value which controls the clock regenerator in the same manner as described in chapter three.

The new clock is gated with the schmitt trigger output to give information pulses with even mark-space ratio. The remainder of the demodulation operation is as before.

This method of regeneration has the advantage that it is self-synchronizing. If one information pulse is misinterpreted it corrects itself after one more clock pulse.

In the system of chapter III there are three voltage levels which must be identified. By using the Manchester Code there are only two.

4.3 COMPANDED DELTA MODULATION

4.3.1 Companding^(15,16,17)

A compandor performs the function of compression of the signal at, or before modulation, then expansion of the signal after demodulation. Exposure to the noise occurs between the two processes, and an overall noise reduction is achieved.

As stated and shown earlier, weak signals are more susceptible to noise (quantizing). Compression of a signal occurs when the effective gain which is applied to a signal varies as function of the magnitude of the signal, with the effective gain being greater for small signals than for large signals.

Since an instantaneous compandor produces effective gain variations in response to instantaneous values of signal wave, the instantaneous type is well adapted to pulse systems. (As opposed to syllabic companding).

If the noise susceptibility is made less than a linear system over one portion of the range, then it must be greater than that of a linear system in some other portion of the range. Whether an improvement results or not depends entirely on the nature of the signal. Delta modulation, like all other pulse modulations, lends itself to instantaneous companding. This is best done in the form of "continuous delta modulation".

4.3.2 Continuous Delta Modulation

A method of companding to improve the performance of delta modulation has been devised by J.A. Greefkes^(18,19), and F.deJager⁽¹⁹⁾ in their papers on 'continuous delta modulation'.

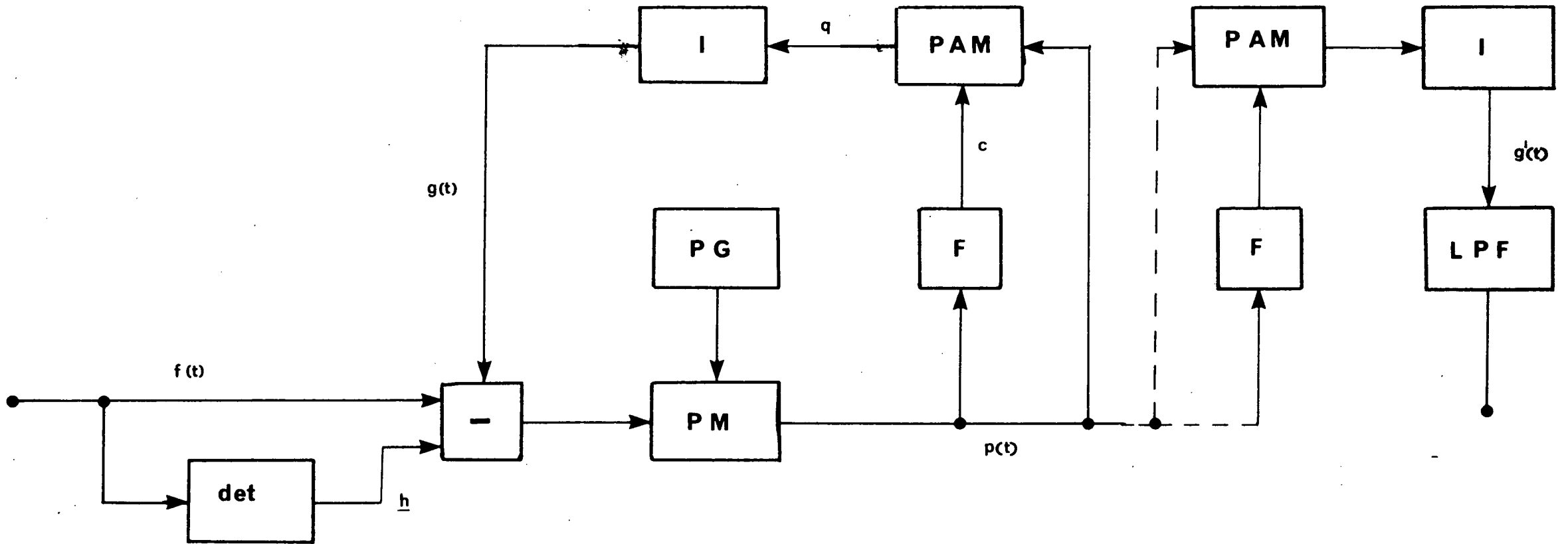


Figure 4.4

CONTINUOUS DELTA MODULATION

In continuous delta modulation the value of the quantizing step is not fixed, but varies as a function of the signal amplitude. Figure 4.4 illustrates the principle of continuous delta modulation.

Information about the height of the quantizing step is transmitted to the receiver by changing the mean number of '1' pulses in the binary pulse pattern.

The two features just mentioned are realized by combining feedback and forward control at the sending end, the height being controlled by the binary pulse pattern.

Figure 4.4, compared with figure 1.1, has a pulse amplitude modulator inserted in the feedback loop. The transmitted pulses p , applied to the integrating network I in the feed-back loop, are controlled in amplitude in the P.A.M. by a control voltage c . This control voltage c is obtained from p by applying it to a low pass filter F . ' c ' represents the mean number of '1' pulses in the pulse pattern.

Detector (det) rectifies and smooths the input signal $f(t)$ to produce a d.c. component \underline{h} which is added to the original input signal. It is assumed that $f(t)$ does not contain very low frequency components. Therefore $f(t)$ and \underline{h} lie in different parts of the spectrum.

As pointed out in section 2.1.1, the system always keeps the difference signal $d(t)$ to a minimum. This applies also to signals in different parts of the spectrum. Thus, as the input signal $f(t)$ is compensated for by the fluctuations in the approximating signal $g(t)$, the d.c. component of \underline{h} is automatically compensated by the d.c. component of $g(t)$. Therefore, over a large range of signal amplitudes the d.c. component of the pulse series q is varied proportionally

with this signal amplitude. It follows that the height of the quantizing step is also varying nearly proportionally with the input signal. In this way, the instantaneous signal-to-noise ratio is kept nearly constant⁽¹⁹⁾.

The receiver is also shown in figure 4.4. It consists of an identical P.A.M. and a low pass filter as in the transmitter. The reconstructed signal $g'(t)$ is essentially the same as $g(t)$. (References 18 and 19 contain detailed description and properties of a continuous delta modulation system).

With this improvement in signal-to-noise ratio, the accuracy of transmission is increased and a very high variation in the input is possible. In his discussion Greefkes compares continuous delta modulation (C.D.M.) and log coded P.C.M. with the same transmission bit rate of 56 KC/S. The quantizing noise for P.C.M., with seven bits linear coding, is 46 db and for C.D.M. 47 db. With the same amount of compression of 26 db, the "idle noise" of PCM log coded is 70 db and for C.D.M. 73 db. The modulation noise, with full modulation for P.C.M. is 32 db., and for C.D.M. 47 db.

The continuous delta modulation system^(18,19) is shown to be a means of transmitting speech at high quality with large dynamic variations. The system has the function of a coder with a digitalized compander per channel. Despite the fact that many functions have to be performed, the number of elements required is small. Greefkes and deJager cite the case of five transistors per transmitter and three or four per receiver.

With a coder per channel, multiplexing can be performed by digital circuits without fear of cross talk. With the decrease in the price of transistors, and the introduction of the integrated circuit a coder per channel could become economical.

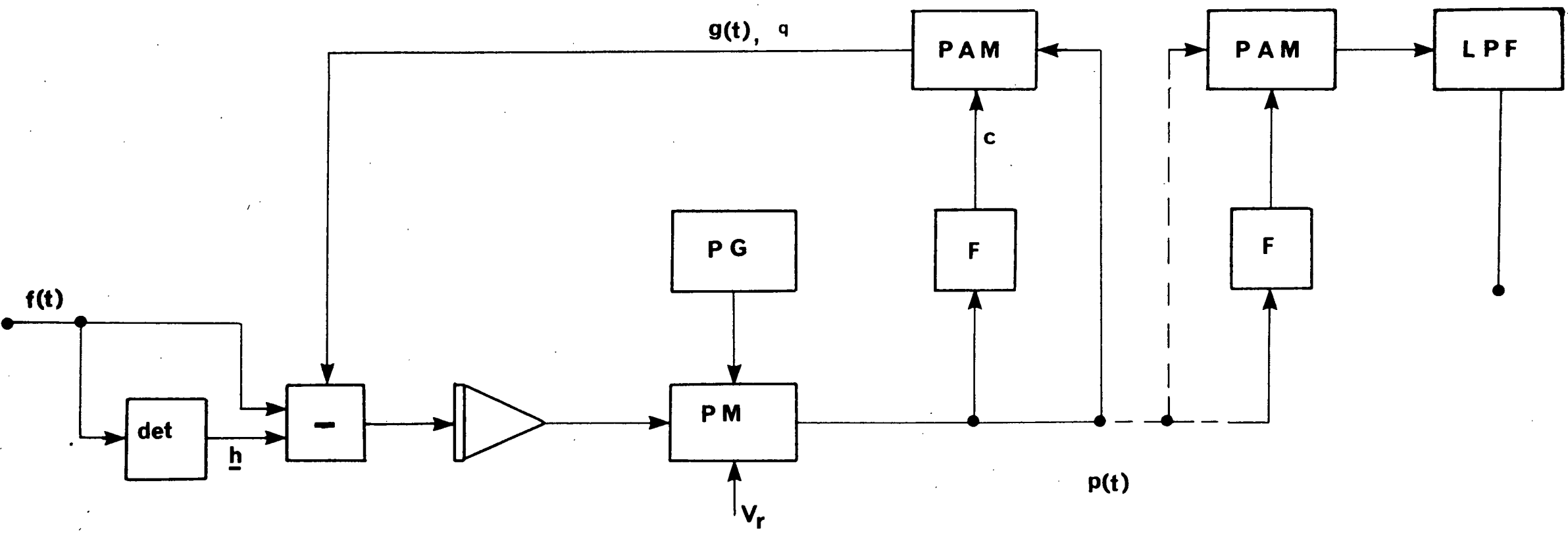


Figure 4.5 CONTINUOUS DELTA-SIGMA MODULATION

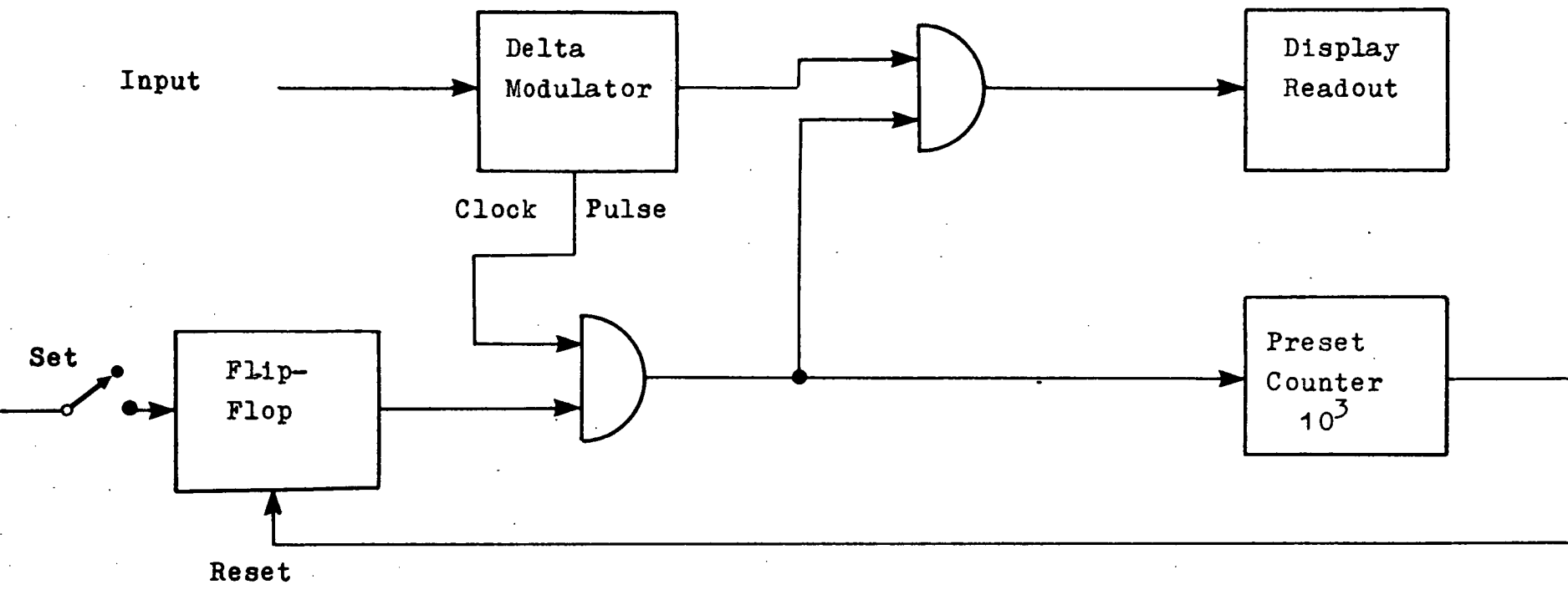


Figure 4.6 DELTA MODULATOR AS AN ANALOGUE TO DIGITAL CONVERTER

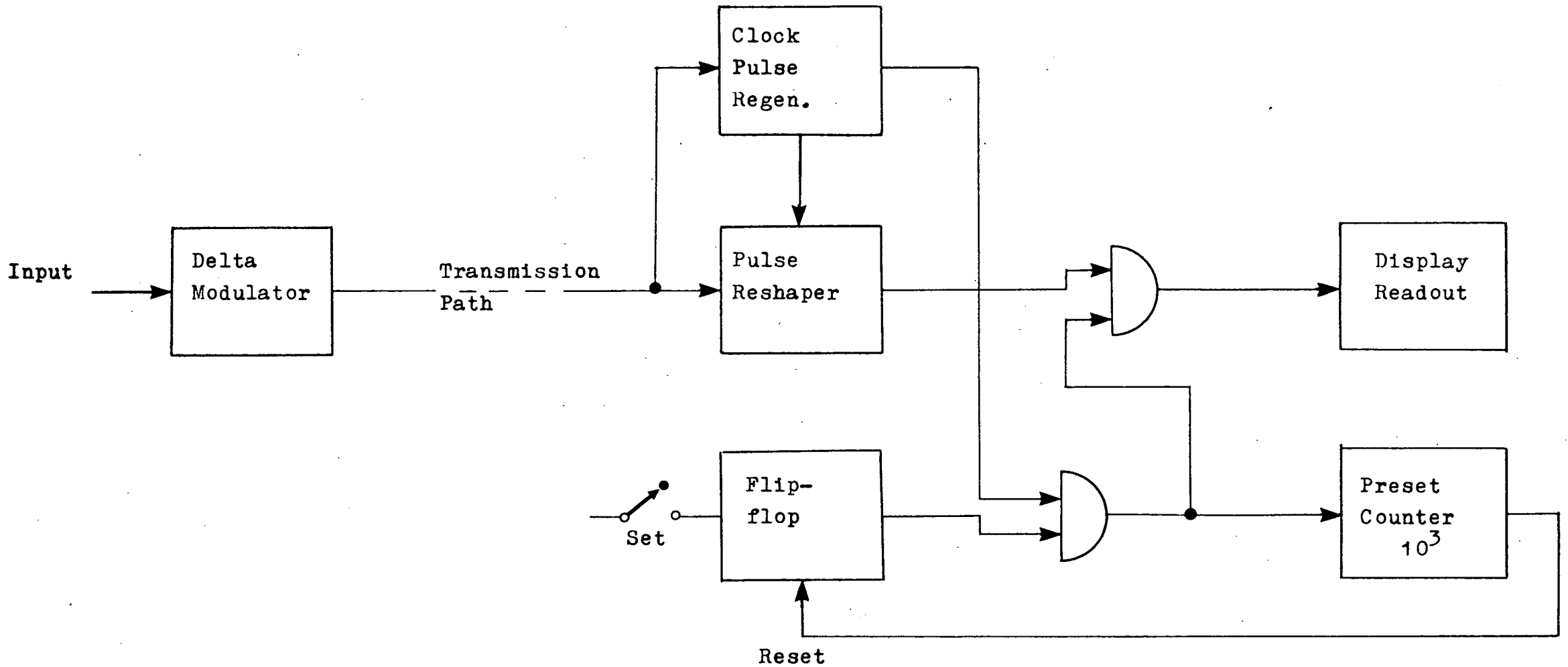


Figure 4.7 DELTA MODULATOR AS A REMOTE ANALOGUE TO DIGITAL CONVERTER

A simple extension of continuous delta modulation will produce continuous delta-sigma modulation. Continuous delta-sigma modulation is illustrated in figure 4.5. The difference between the two is the same in the continuous case as in the ordinary case, in that the signal is first integrated in the delta-sigma modulation. This is another means by which the system of chapter III could be improved.

4.4 ANALOGUE-TO-DIGITAL CONVERTER

The system of chapter III or any delta modulation system can be used either remotely or directly, as an analogue-to-digital converter. This can be done by counting either the positive or negative output pulses in a certain time interval. When the time interval contains N pulses, the reading accuracy is 100/N percent.

Figures 4.6 and 4.7 show direct and remote analogue-to-digital converters, with an accuracy of ± 0.1 percent.

The counting interval is started by setting the flip-flop in the 'one' state. This opens a gate which directs clock pulses to a preset counter (10^3) and then to a second gate which passes pulses coming from the delta modulator (or the pulse reshaper in figure 4.7) to the display readout. After 1000 pulses, the preset counter resets the flip-flop which then closes both gates. The display read-out then contains the number of pulses of the chosen polarity of the modulator. This number is linearly related to the dc level at the input to the modulator.

4.5 CONSIDERATIONS IN CHOOSING DELTA OR PULSE CODE MODULATION

There is little doubt as to the superiority of pulse code modulations when it comes to large signal-to-noise ratio communications. The increase in S/N is obtained at the expense of bandwidth, something which cannot be done in

carrier amplitude modulation. Although these pulse code methods consume bandwidth, other important benefits arise. Besides the advantage, already mentioned, of increased signal-to-noise ratio, there are the technical and economic advantages of time division multiplexing, the merits of which have already been discussed in chapter I.

Delta and delta-sigma modulation have been studied here and P.C.M. discussed in some detail. The two systems are rivals and any decision between them will depend on their quality and their price for a particular application.

Because of the nature of the codes, the delta modulation and demodulation system is far simpler in circuit construction. The P.C.M. must have memory stores or counters at both transmitter and receiver, be it a single channel or a multi-channel system. A delta modulation system needs no memory, as the code consists of one digit only. A transmission line where only one channel is to be propagated is unlikely to have serious bandwidth restrictions. Therefore, a single channel delta modulation system would be the obvious choice.

As so many factors govern the choice of modulation, the discussion here is divided under four main headings. They are:

- (i) bandwidth,
- (ii) circuit simplicity,
- (iii) number of channels,
- (iv) quality of transmission.

There is much interdependence between these divisions, but, broadly speaking, the following sections show how they are considered.

4.5.1 Bandwidth

Bandwidth is a communications commodity which more often than not, is at a premium. If a certain number of channels are required in a given bandwidth with no provision for more, then, provided delta modulation would give the quality and the number, it should be used. However PCM gives $1\frac{1}{2}$ times as many channels per unit bandwidth, so if provision for more channels were required, it would be favoured.

4.5.2 Circuit Simplicity.

Where initial capital cost of installation is important, naturally the cheapest circuits are desired. This depends largely on (ii) and (iii), but is listed separately as, overall, it can be the governing factor of a choice between delta and PCM. Delta modulation also has the advantage in that it consumes only 60 percent of the power of an equivalent PCM system (see section 2.3.2).

4.5.3 Number of Channels

For a one channel system, the cost of a delta coder would be only a fraction of the cost of a PCM system. This arises from the simplicity of the delta system compared with the PCM system. An increase in the number of channels, for a delta system, requires duplication of the delta coder (i.e. a coder per channel). To increase the number of channels of a PCM system requires only the addition of a commutator, a faster clock and synchronizing equipment. Therefore, it could reasonably be expected that there will be a number of channels for which delta and PCM systems are equally priced. Above this number, PCM becomes the more economical in all respects((i), (ii), (iv)).

There are ways of using one coder on a multichannel delta modulation system, but the circuitry ceases to be simple and this important benefit is lost (20).

To carry out a first order estimate of the number of channels at which PCM and delta modulation cost the same, the following assumptions are made:

- (1) Bandwidth is not a prime concern.
- (2) The cost of a single delta modulator is only a fraction $1/M$ of the cost of one PCM modulator.
- (3) The cost of addition of one more channel to an existing PCM system is x times the cost of a one channel system, where $0 < x < 1$.
- (4) The cost of a one channel PCM system is C_p .
- (5) The cost of a one channel delta system is C_d .

If then, N is the number of channels

$$\text{Cost of } N \text{ delta channels } \sum C_d = \frac{N C_p}{M}$$

$$\text{Cost of } N \text{ PCM channels } \sum C_p = C_p + (N-1)x C_p$$

Therefore,

$$\frac{\sum C_d}{\sum C_p} = \frac{N}{M(1+(N-1)x)}$$

$$\sum C_d \geq C_p \text{ if}$$

$$N \geq M + MNx - Mx$$

$$\text{i.e. } N \geq \frac{M(1-x)}{1-Mx}$$

$$\text{As } 0 < x < 1, \quad 1-x > 0$$

For N to be positive

$$Mx \leq 1$$

$$\text{If } x = 0.1 \quad M \leq 10$$

$$\text{For } M = 5, \quad N \geq 9$$

$$M = 8, \quad N \geq 36.$$

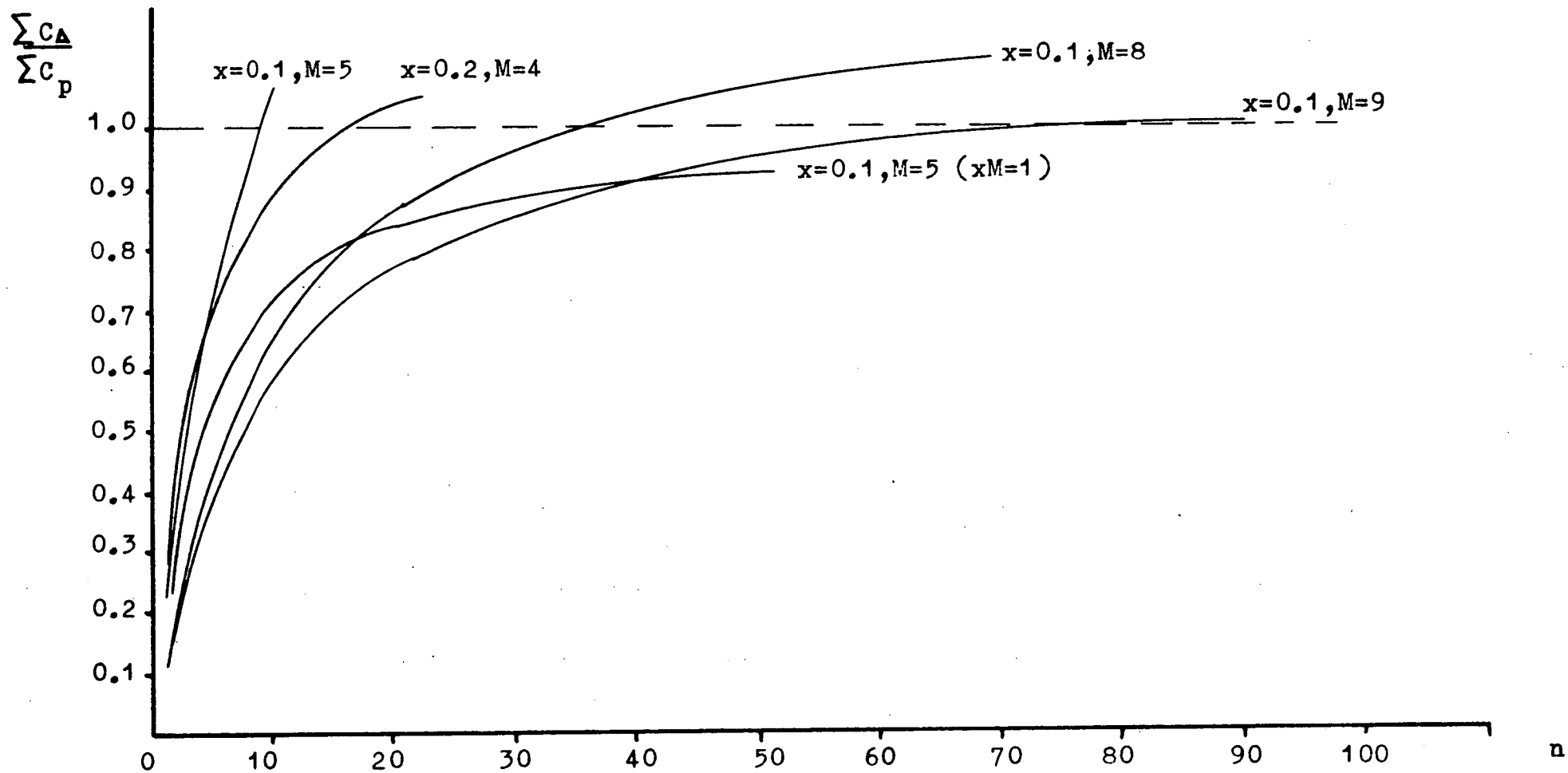
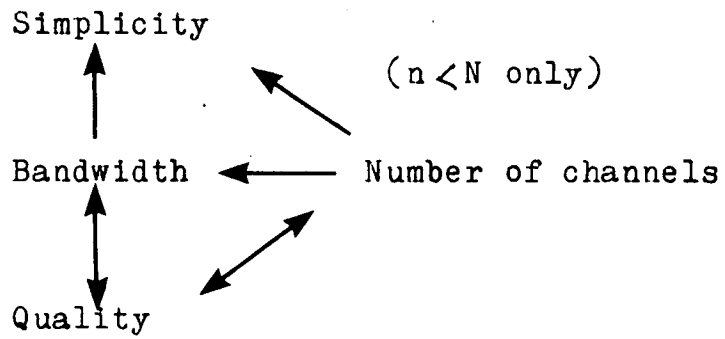
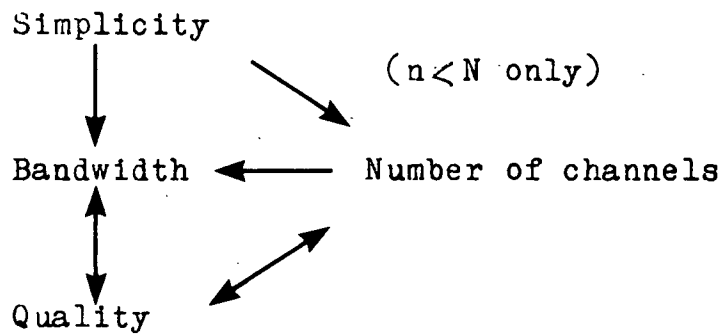


Figure 4.8 RATIO OF COST DELTA MODULATION TO COST PCM VERSUS NUMBER OF CHANNELS

(a) Using DM rather than PCM



(b) Using PCM rather than DM.



N=Number channels for cost DM=cost PCM.
n=Number of channels.

Figure 4.9 "TRADE-OFFS" OF GOVERNING FACTORS

Figure 4.8 shows how $\frac{\sum C_d}{\sum C_p}$ varies with n (the number of channels) for a few values of x and M . The general character of the curves indicate that delta modulation is a more economical proposition for multichannel systems below about 10 to 20 channels. Above 20, the cost of PCM is less than that of delta modulation.

An accurate value of N cannot be given because an estimation of all the cost factors involved is not possible here.

The Australian Post Office is testing out small 20 channel systems in rural areas. The Post Office Authorities have found that delta modulation on a 20 channel system is an economical proposition.

4.5.4 Quality of Transmission

If a system is specified to give a certain signal-to-noise ratio, then, to obtain it, delta modulation requires about $1\frac{1}{2}$ times the P.C.M. bandwidth. For a system with less than N channels, (N as before) the cost of a delta modulation system is less than a PCM system. However, the delta modulation system requires greater bandwidth. The question arises, can the bandwidth be afforded to give the desired quality of transmission? The requirements for quality reflect back on the first three factors mentioned.

Figure 4.9 indicates, basically, how the four points mentioned above can be "traded" for one another.

This discussion and figures 4.8 and 4.9 are by no means a complete picture of the relative advantages and disadvantages of DM and PCM, but they do convey quite a lot of information on a comparative basis. To investigate them more closely would require the consideration of two designs for the one specification.

4.6 CONSIDERATION OF DELTA MODULATION FOR TELEPHONE SYSTEMS

In a discussion on Integrated Switching and transmission systems, H.S. Wragge⁽²¹⁾ looked into the application of electronic switching using time division multiplexing principles. In this t.d.m. switching, the signals would be encoded using a digital rather than an analogue modulation. The signal would then be transmitted and switched while in this digital form.

Wragge discusses the problems involved in introducing Integrated Switching and Transmission Systems (I.S.T.) from several points of view. One such point of view is the effects of the methods of modulation in I.S.T. To date, P.C.M. has been developed to fulfil this kind of role, and it is assumed it would be favoured. However, it appears, from the technical side, that delta modulation may be attractive. Wragge discusses P.C.M. and delta modulation on the following bases:

- (1) Relative properties of the two modulation methods.
- (ii) Switching and signalling equipment aspects.
- (iii) Systems aspects.

His conclusions are, that delta modulation has marginal advantages over P.C.M. provided satisfactory speech quality can be obtained with reasonable bandwidth requirements in relation to P.C.M.

It appears that, because of its development, P.C.M. is more likely to be used for economical reasons, despite the technical advantages of delta modulation, unless development of delta systems is carried out rapidly.

4.7 CONCLUSION

Delta Modulation (and delta-sigma modulation) have a place alongside PCM for the transmission of speech, data, dc signals etc. over modern telecommunications channels.

Delta modulation consumes less power. It is more economical to install when lower qualities of transmission are required. It is more economical when small multichannel systems are required without bandwidth limitations. It is more suitable than PCM when dealing with signals which have spectral densities diminishing for the higher frequencies (as in the case of speech). It compares in the same favourable manner with FM as does PCM.

It has the disadvantage that, at a given bandwidth, the signal-to-noise ratio is not as high as that of PCM. It is no more economical to install than PCM for very large number multichannel systems.

APPENDIX A

IT = 0

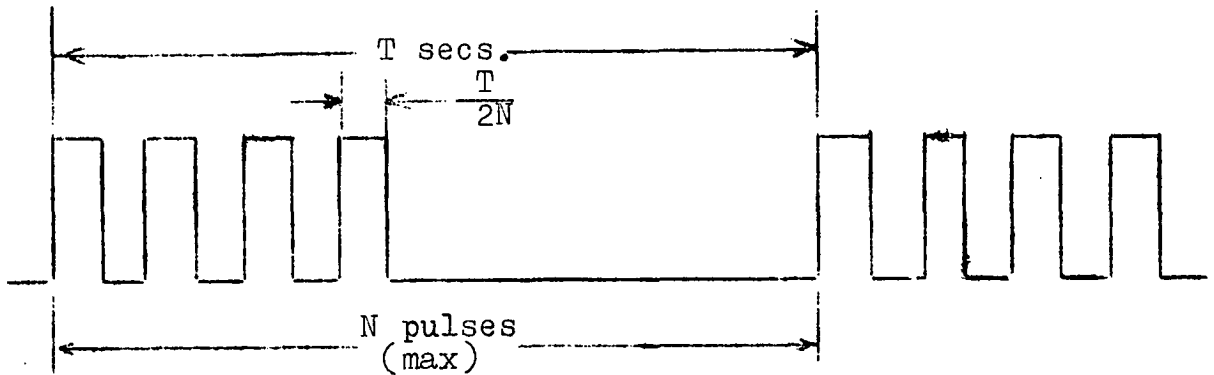


Figure A1 n PULSES OCCURRING IN TIME T

n pulses occur in time T.

The overall IT value is:

$$\begin{aligned} I^* T &= I^- \left(\frac{T}{2N} \times N \right) + I^+ \left(\frac{T}{2N} \cdot n \right) + (N - n) \cdot \frac{T}{2N} I^- \\ &= \frac{T}{2N} \left((2N - n)I^- + nI^+ \right) \end{aligned}$$

On an average over a period of time T, $n = N/2$.

Therefore,

$$I^* T = \frac{T}{2N} \left(\frac{3N}{2} I^- + \frac{N}{2} I^+ \right).$$

For this to have zero value over time T,

$$3I^- = -I^+.$$

Current weighting is then,

$$I^+ = 3I$$

$$I^- = -I.$$

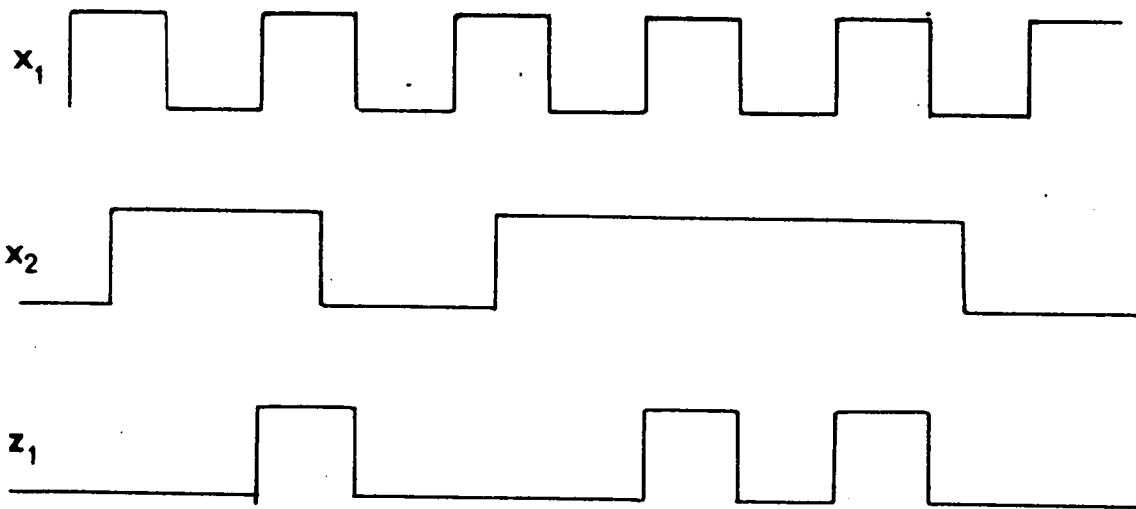


Figure B1 INPUT-OUTPUT WAVEFORMS

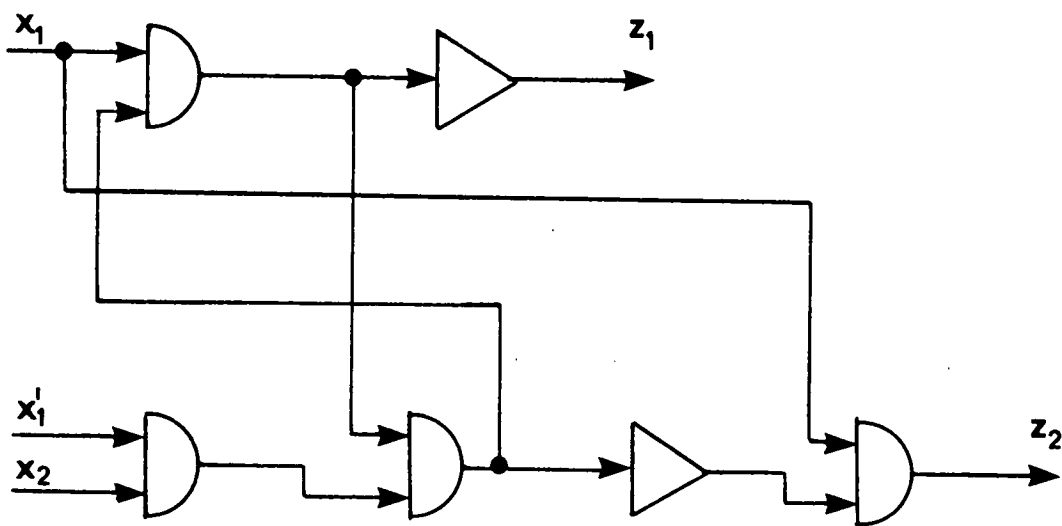


Figure B2 SEQUENTIAL NETWORK REALIZATION

APPENDIX B

TRANSMITTER SEQUENTIAL CIRCUIT DERIVATION⁽¹²⁾

z_1 is to be 'one' if x_1 is 'one' after x_2 in 'one'.

z_1 is to be 'one' if z_1 is 'one' after x_2 is 'zero', after both having been 'one'.

z_1 'zero' if x_1 and x_2 both 'zero' (see figure B1).

FLOWTABLE

| x_1x_2 | x_1x_2 | x_1x_2 | x_1x_2 | z_1 |
|----------|----------|----------|----------|-------|
| 00 | 01 | 11 | 10 | |
| ① | 2 | - | 5 | 0 |
| 1 | ② | 3 | - | 0 |
| - | 2 | ③ | 4 | 1 |
| 1 | - | 3 | ④ | 1 |
| 1 | - | 6 | ⑤ | 0 |
| - | 2 | ⑥ | 5 | 0 |

MERGED TABLE

| | ① | 2 | ⑥ | ⑤ |
|---|----|----|----|----|
| | 1 | ② | ③ | ④ |
| Y | 00 | 01 | 11 | 10 |
| 0 | 0 | 1 | 0 | 0 |
| 1 | 0 | 1 | 1 | 1 |

$$Y = x_1'x_2 + x_1y,$$

This can be written

$$\bar{Y} = (x_1'x_2)' \cdot (x_1y)'$$

A realization of the sequential logic circuit is shown in figure B2.

OUTPUT Z_1

Z table

| | 00 | 01 | 11 | 10 |
|---|----|----|----|----|
| 0 | 0 | 0 | 0 | 0 |
| 1 | 0 | 0 | 1 | 1 |

$$z_1 = x_1 y, \quad z_2 = x_1 y' .$$

These two values $z_1 z_2$, are output from the circuit in figure B2.

APPENDIX C

RECEIVER CIRCUIT SEQUENTIAL NETWORK DERIVATION ⁽¹²⁾

An output from the network is required for the full duration of a clock pulse every time an information pulse appears. As an information pulse always occurs just before a clock pulse, and remains until after the clock pulse has begun, the circuit is relatively simple.

FLOWTABLE

| x_1x_2 | x_1x_2 | x_1x_2 | x_1x_2 | |
|----------|----------|----------|----------|---|
| 00 | 01 | 11 | 10 | z |
| ① | 2 | - | 5 | 0 |
| - | ② | 3 | - | 0 |
| - | - | ③ | 4 | 1 |
| 1 | - | - | ④ | 1 |
| 1 | - | - | ⑤ | 0 |

MERGED TABLE

| Y | 00 | 01 | 11 | 10 |
|---|----|----|----|----|
| 0 | 0 | 0 | 1 | 0 |
| 1 | 0 | 0 | 1 | 1 |

$$Y = x_1(x_1 + y) = (x_1' + (x_2 + y)')'$$

Z TABLE

| | 00 | 01 | 11 | 10 |
|---|----|----|----|----|
| 0 | 0 | 0 | 1 | 0 |
| 1 | 0 | 0 | 1 | 1 |

This gives,

$$z = x_1x_2 + x_1y = y$$

The waveforms and circuit are shown in figures 3.22 and 3.23.

APPENDIX D

ELLIOTT 503 PROGRAM

To apply Zetterberg's⁽⁷⁾ results and find values of S/N for the system of chapter III, calculations were carried out on an Elliott 503 Computer.

Rather than take values of y (hence V_E/V_K) and obtain values of $\int_x^\infty e^{-u^2/2} du$ for different values of x , values of $\int_x^\infty e^{-u^2/2} du$ were tabulated and values of y extracted. Ninety values of $\int_x^\infty e^{-u^2/2} du$ were tabulated on a data tape (see accompanying sheets). The data shows five values of $FRATIO (= f_p/f_3)$ and five sets of C , num 2, den 2.

The second sheet shows the Elliott 503 program used.

1 Data Tape No Two

| | | | | |
|--------|-------|------|-----|------|
| 2 100 | 200 | 300 | 700 | 1000 |
| 3 n=5 | | | | |
| 4 1.34 | 1.0 | 3.0 | | |
| 5 1.38 | 0.192 | 1.0 | | |
| 6 1.30 | 0.365 | 1.0 | | |
| 7 1.96 | 1.0 | 16.0 | | |
| 8 2.56 | 1.0 | 64.0 | | |

9

10

11

12

13

14

15

16

17

18

19

20

21

22

23

24

25

26

27

28

29

30

31

32

33

34

35

36

37

38

39

40

41

42

43

44

45

46

47

48

49

50

51

52

53

54

55

56

57

1

2

3

4

5

6

7

8

9

10

11

12

13

14

15

16

17

18

19

20

21

22

23

24

25

26

27

28

29

30

31

32

33

34

35

36

37

38

39

40

41

42

43

44

45

46

47

48

49

50

51

52

53

54

55

56

57

ELLIOTT 503 PROGRAM

```

1 SIGNAL NOISE RATIO, U1175;
2
3 begin integer i,j,p,n;
4 real x,y,cp,num2,den2,factor,psio,psig,psit,vratio,pi,k,q,K,G,db,g,F,const;
5 array phi[1:90],fratio[1:5];
6 comment The 90 values of the function phi(x) to be read as data correspond
7 to values of x ranging from 0,05 to 4,55 at intervals of 0,05;
8
9 real procedure A(x); value x; real x;
10 begin real x2,P;
11 x2:= x*x;
12 P:= 1,0 + x2*(0,5 + x2*(4,0 - 1,25*x2)/3,0);
13 A:= 1,0 - P/exp(0,5*x2)
14 end A;
15
16 real procedure B(x); value x; real x;
17 begin real x2,x5;
18 x2:= x*x; x5:= x*x2*x2;
19 B:= k*x5*(1,75 + 5,0*x2/12,0)
20 end B;
21
22 sameline; freepoint(4); leadzero(F?);
23 pi:= 3,14159265359; k:= sqrt(0,5*pi);
24 q:= pi*sqrt(8,0); K:= 35,0*k*q/192,0;
25 G:= k*pi3/0,30051422579; db:= 10,0/ln(10,0);
26 for i:= 1 step 1 until 90 do read phi[i];
27 for j:= 1 step 1 until 5 do read fratio[j];
28 read n; for p:= 1 step 1 until n do
29 begin read cp,num2,den2;
30 x:= 0,0; factor:= sqrt(num2/den2);
31 g:= G*factor; const:= 1,5/sqrt(cp*sqrt(2,0));
32 print 'C = ',cp,'FACTOR = ',factor,'VE/VEs5?PSIGDBEs5?PSITDBEs1s2?YEs3?PSIODBEs2?FRATIO = ?';
33 for j:=1 step 1 until 4 do print fratio[j],'; print fratio[5],';
34 for i:=1 step 1 until 90 do
35 begin x:=x+0,05; y:=const*x; F:=q*y;
36 psio:=K*y*exp(y*y)*x4/(A(x)-B(x)*(1,0-phi[i]));
37 print 'y,db*ln(abs(psio));
38 for j:=1 step 1 until 5 do
39 begin vratio:=fratio[j]/F;
40 psig:=g*vratio3;
41 psit:=psio*psig/(abs(psio)+abs(psig));
42 print 'vratio,db*ln(abs(psig)),db*ln(abs(psit))
43 end
44 end row i
45 end group p
46 end program U1175;

```

APPENDIX E

FOURIER REPRESENTATION OF STATIC WAVEFORMS

It can be shown⁽²⁾ that a periodic function (period T) can be represented as a fourier series of the form;

$$f(t) = a_0/2 + \sum_{n=1}^{\infty} (a_n \cos n\omega t + b_n \sin n\omega t)$$

n = a positive integer

$$T = \frac{2\pi}{\omega} = 1/f = \text{period.}$$

$$a_n = \frac{2}{T} \int_{-T/2}^{T/2} f(t) \cos n\omega t dt$$

$$b_n = \frac{2}{T} \int_{-T/2}^{T/2} f(t) \sin n\omega t dt .$$

For the clock-pulse train,

$$\begin{aligned} f(t) &= A, & 0 \leq t \leq T/2 \\ &= 0, & T/2 \leq t \leq T . \end{aligned}$$

$$a_n = \frac{2}{T} \int_0^{T/2} A \cos n\omega t dt$$

$$a_n = \frac{A}{n\pi} \sin n\pi \tag{1}$$

Similarly,

$$b_n = \frac{-A}{n\pi} \cos n\pi$$

$$a_0 = A .$$

Thus,

$$f(t) = A + \frac{A}{\pi} (\sin \omega t - \frac{1}{2} \sin 2\omega t + \frac{1}{3} \sin 3\omega t - \dots)$$

$$\text{The r.m.s. value} = A \cdot \sqrt{1^2 + \frac{1}{4} (\frac{1}{2}^2 + \frac{1}{2.4} + \frac{1}{2.9} + \dots)}$$

$$\text{r.m.s.} \quad A \cdot 1.034$$

Waveform A is represented by:

$$\begin{aligned}
 f(t) &= A, & 0 \leq t \leq T/10 \\
 f(t) &= 0, & T/10 < t \leq T/5 \\
 f(t) &= A, & T/5 < t \leq 3T/10 \\
 f(t) &= 0, & 3T/10 < t \leq 3T/5 \\
 f(t) &= A, & 3T/5 < t \leq 7T/10 \\
 f(t) &= 0, & 7T/10 < t \leq T.
 \end{aligned}$$

For the sake of comparison, the harmonics in the subsequent expressions are given in terms of multiples of the clock pulse fundamental.

Therefore if T_1 is the period of the clock fundamental, similar calculations to those above will give $f_A(t)$ as follows,

$$\begin{aligned}
 f_A(t) &= \frac{3}{5} A + \frac{A}{\pi} (0.93 \cos 1/5 \left(\frac{2\pi}{T_1}\right)t - 0.95 \sin 1/5 \left(\frac{2\pi}{T_1}\right)t - \\
 &\quad - 0.294 \sin 2/5 \left(\frac{2\pi}{T_1}\right)t + 0.41 \cos 2/5 \left(\frac{2\pi}{T_1}\right)t + \\
 &\quad + 0.83 \sin 3/5 \left(\frac{2\pi}{T_1}\right)t + 0.043 \cos 3/5 \left(\frac{2\pi}{T_1}\right)t + \\
 &\quad + 0.237 \sin 4/5 \left(\frac{2\pi}{T_1}\right)t + 0.08 \sin 4/5 \left(\frac{2\pi}{T_1}\right)t + \dots .
 \end{aligned}$$

The others follow similarly;

$$\begin{aligned}
 f_B(t) &= \frac{2}{3} A + \frac{A}{\pi} \left(\frac{\sqrt{3}}{2} \cos \frac{2}{3} \left(\frac{2\pi}{T_1}\right)t - \frac{1}{2} \sin \frac{2}{3} \left(\frac{2\pi}{T_1}\right)t - \sin \left(\frac{2\pi}{T_1}\right)t - \right. \\
 &\quad \left. - \frac{\sqrt{3}}{4} \cos \frac{4}{3} \left(\frac{2\pi}{T_1}\right)t + \frac{1}{4} \sin \frac{4}{3} \left(\frac{2\pi}{T_1}\right)t + \dots \right)
 \end{aligned}$$

$$\begin{aligned}
 f_D(t) &= \frac{A}{2} + \frac{A}{\pi} \left(\cos \frac{1}{2} \left(\frac{2\pi}{T_1}\right)t + \frac{1}{2} \sin \left(\frac{2\pi}{T_1}\right)t - \frac{1}{3} \cos \frac{3}{2} \left(\frac{2\pi}{T_1}\right)t - \right. \\
 &\quad \left. - \frac{1}{4} \sin 2 \left(\frac{2\pi}{T_1}\right)t + \dots \right)
 \end{aligned}$$

$$\begin{aligned}
 f_E(t) &= \frac{A}{3} + \frac{A}{\pi} \left(\frac{\sqrt{3}}{2} \cos \frac{1}{3} \left(\frac{2\pi}{T_1}\right)t - \frac{1}{2} \sin \left(\frac{2\pi}{T_1}\right)t + \frac{\sqrt{3}}{2} \cos \frac{2}{3} \left(\frac{2\pi}{T_1}\right)t + \right. \\
 &\quad \left. + \frac{1}{4} \sin \frac{2}{3} \left(\frac{2\pi}{T_1}\right)t + \frac{1}{3} \sin \left(\frac{2\pi}{T_1}\right)t + \dots \right)
 \end{aligned}$$

$$\begin{aligned}
 f_F(t) &= \frac{A}{4} + \frac{A}{\pi} \left(\frac{1}{\sqrt{2}} \cos \frac{1}{4} \left(\frac{2\pi}{T_1}\right)t - \frac{1}{\sqrt{2}} \sin \frac{1}{4} \left(\frac{2\pi}{T_1}\right)t + \frac{1}{2} \cos \left(\frac{2\pi}{T_1}\right)t + \right. \\
 &\quad + \frac{1}{3\sqrt{2}} \cos \frac{3}{4} \left(\frac{2\pi}{T_1}\right)t - \frac{1}{3\sqrt{2}} \sin \frac{3}{4} \left(\frac{2\pi}{T_1}\right)t + \frac{1}{4} \sin \left(\frac{2\pi}{T_1}\right)t + \\
 &\quad \left. + \dots \right).
 \end{aligned}$$

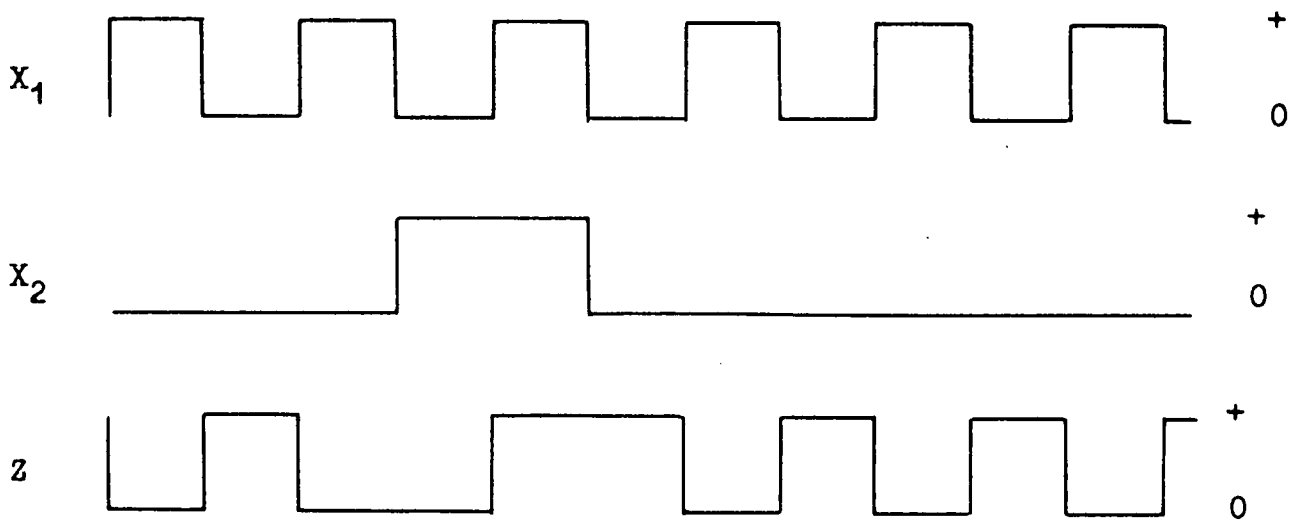


Figure F1 MANCHESTER CODE

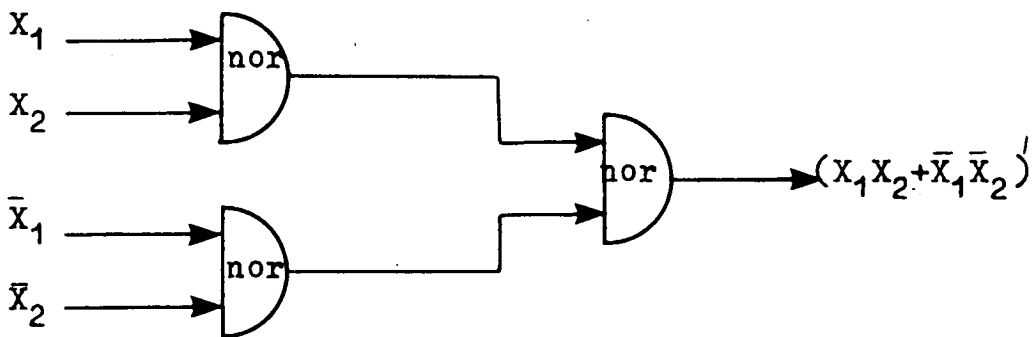


Figure F2 REALIZATION OF CONVERSION TO MANCHESTER CODE

APPENDIX F

MANCHESTER CODE

The circuit used to convert to the Manchester code is designed very simply by Sequential logic methods.⁽¹²⁾

Figure F1 shows the two inputs to the network x_1 and x_2 and the output z as defined in section 4.2.

FLOW TABLE

| x_1x_2 | x_1x_2 | x_1x_2 | x_1x_2 | |
|----------|----------|----------|----------|-----|
| 00 | 01 | 11 | 10 | z |
| ① | - | - | 2 | 1 |
| 1 | 3 | - | ② | 0 |
| - | ③ | 4 | - | 0 |
| 1 | - | ④ | - | 1 |

MERGED TABLE

| | ① | ③ | ④ | ② |
|---|----|----|----|----|
| | 00 | 01 | 11 | 10 |
| 0 | 0 | 0 | 0 | 0 |
| 1 | - | - | - | - |

$$y = \bar{x}_1\bar{x}_2 + x_1x_2$$

and

$$z = \bar{x}_1\bar{x}_2 + x_1x_2$$

Figure F2 shows the realization of the logic network to produce the output z .

BIBLIOGRAPHY

References cited in text

1. Hancock, J.C.: An Introduction to the Principles of Communications Theory. McGraw-Hill, 1961.
2. Lathi, B.P.: Signals, Systems and Communications. John Wiley, 1965.
3. Shannon, C.E.: Communications in the Presence of Noise. Proc. I.R.E. Vol. 37, Number 10, 1949.
4. de Jager, F.: Delta Modulation, A Method of P.C.M. Transmission using the 1-Unit Code. Philips Research Reports, Vol. 7, 1952.
5. Inose, H., Yasuda, Y., Murkami, J.: A Telemetering System by Code Modulation - Δ - Σ Modulation. IEEE Trans. Space Electronics and Telemetry, Set 8, 1962.
6. Bennett, W.R.: Spectra of Quantized Signals. Bell Systems Tech. Journal, Vol. 27, 1948.
7. Zetterberg, L.H.: A Comparison Between Delta and Pulse Code Modulation. Ericsson Technics, Vol. 2, 1955.
8. Oliver, Pierce, Shannon,: The Philosophy of P.C.M. Proc. IRE, Volume 36, 1948.
9. Shannon, C.E.: Mathematical theory of Communications. Bell Systems Technical Journal, Vol. 27, 1948.
10. Libois, L.J.: Un nouveau procédé de modulation codée "la modulation en delta". L'Onde Electrique, vol. 32, page 26, 1952.
11. Balder, J.C., Kramer, C.: Analogue to Digital Conversion by Means of Delta Modulation. IEEE Trans. Space Electronics and Telemetry.
12. Gray, H.J.: Digital Computer Engineering. Prentice-Hall Inc. 1963.
13. Fairchild Semi-Conductor Linear Integrated Circuits Applications Handbook. Edited by J.N. Giles.
14. Fairchild RTL Composite Data Sheet Industrial Micrologic Integrated Circuits.
15. Reiling, P.A.: Companding in P.C.M. Bell Labs. Record, V. 26, December 1948.
16. Mallinckrodt, C.O.: Instantaneous Compandors. Bell Systems Tech. Journal. Vol. 30, 1951.
17. Smith: Instantaneous Companding of Quantized Signals. Bell Systems Technical Journal. Vol. 36, 1957.
18. Greefkes, J.A.: Continuous Delta Modulation. Colloque de Commutation Electronique. (from an extract - date unknown)

19. Greefkes, J., de Jager, F.: Continuous Delta Modulation. Philips Research Reports. Vol. 23, April, 1968.
20. Bavers, F.K.: What Use is Delta Modulation to the Transmission Engineer? AIEE Trans. Vol. 76, Part 1, 1957.
21. Wragge, H.S.: On the Method of Modulation for Use in a Metropolitan Integrated Switching and Transmission System. A.P.O. Research Laboratory Report, Number 6142, 1966.
22. Deutsch, R.: Non linear transformations of Random Processes. Prentice Hall 1962.
23. Middleton, D.: An Introduction to Statistical Communication Theory. McGraw-Hill, 1960.
24. Lewis, D.J.H.: Noise in Non linear Systems. Honours Thesis, unpublished.
25. Lee, Y.W.: Statistical Theory of Communications. John Wiley, 1960.
26. Elliott Facts.
27. Handbook on 503 Algol.
28. Schaeffler, G.F.: A Course in Algol Programming. Macmillan, 1966.

BIBLIOGRAPHY

References Consulted but not cited in Text

- Schouten, de Jager, Greefkes. Delta Modulation, A New Modulation System for Telecommunications. Philips Technical Review, March 1952.
- Goldman, S.: Information Theory. Prentice-Hall, 1953.
- Fine, T.: Properties of an Optimum Digital System and Applications. IEEE Trans on Information Theory, Vol. IT-10, Oct. 1964.
- Hohn, F.E.: Applied Bodean Algebra. Macmillan 1966.
- Bennett, W.R.: Methods of Solving Noise Problems. Proc. IRE, 1959.
- Halijak, C.A., Tripp, J.S.: A deterministic Study of Delta Modulation. IEEE Trans. Automatic Control, 1963.
- Winkler, M.R.: High Information Delta-Modulation. IEEE Trans. Automatic Control, 1963.
- Van der Weg, H.: Noise of a Single Integration Delta Modulation System with an N-digit Code. Philips Research Reports, Vol. 8, 1953.
- Cherry, C.: On Human Communications. John Wiley, 1957.
- Feldman, Bennett: Bandwidth and Transmission Performance. Bell Systems Technical Journal Vol. 28, 1949.
- Horton, Vaughan; Transmission of Digital Information over Telephone Circuits. Bell Systems Technical Journal, Vol. 34, 1955.
- Meacham, L., Peterson, E.: Multichannel Modulation Systems. Bell Systems Technical Journal, Vol. 27, 1948.
- Bennett, W.R.: Statistics of Regenerative Transmission. Bell Systems Technical Journal, Vol. 38, 1958.
- Bennett, W.R.: Time-Division Multiplexed Systems. Bell Systems Technical Journal. Volume 20, 1941.
- Steele, R.: Two Transistor Delta Modulators. Electronic Engineering, Sept. 1963.
- Black, H.S.: Modulation Theory. Van Nostrand 1953.
- Lender, A., Kozuch, M.: Single-bit Delta Modulating Systems. Electronics, Vol. 34, November 1961.
- Tibbs, C.E.: Frequency Modulation Engineering. Chapman and Hall, 1947.
- Bell, D.A.: Information Theory and its Engineering Applications. Pitman, 1953.
- Stewart, J.L.: Circuit Theory and Design. John Wiley, 1956.